AN INTERFERENCE ANALYSIS FRAMEWORK (IAF) FOR SPECTRUM SHARING FEASIBILITY AND COEXISTENCE DETERMINATION

A Dissertation

Presented to
The Academic Faculty
By

Mark Lofquist

University of Colorado, Boulder

Virginia Polytechnic Institute and State University

M.S. Electrical Engineering December 1999

B.S. Electrical Engineering May 1999

J. Sargeants Reynolds Community College

A.S. Engineering 1997

A thesis submitted to the
Faculty of the Graduate School of the University of Colorado in partial fulfillment
of the requirements for the degree of
Doctor of Philosophy
Technology, Cybersecurity, and Policy Program 2019

This thesis entitled:

AN INTERFERENCE ANALYSIS FRAMEWORK (IAF) FOR SPECTRUM SHARING FEASIBILITY AND COEXISTENCE DETERMINATION

written by Mark Lofquist
has been approved for the Department of Engineering

_____
Kevin Gifford, PH.D

_____
David Reed, Ph.D

Date,_____

The final copy of this thesis has been examined by the signatories, and we find that both the content and the form meet acceptable presentation standards of scholarly work in the above mentioned discipline.
(This statement must be included on the signature page)

ABSTRACT

Due to recent increases in mobile broadband services by consumers, the Federal Communications Commission (FCC) is compelled to make more spectrum available for commercial use. The FCC spectrum-service rulemaking process does not formally assess risk of interference, apply statistical distributions, or recommend coexistence testing. The methodology developed in this dissertation proposes a framework that applies risk, statistics, and coexistence testing and demonstrates how spectrum regulatory decision-making processes would benefit from using a more technically defensible approach. Allowing new systems into a spectrum band can cause interference to the operating incumbent users but preventing new commercial spectrum systems can have negative economic and technological repercussions. Therefore, carefully assessing the effects of a more heavily used spectrum by treating analytical spectrum coexistence testing metrics as distributions can lead to more information-based, data-driven decision making.

When using risk assessments, regulators' decisions will improve to include results from well-engineered and transparent spectrum coexistence testing accounting for measurement uncertainties with translations to real-world deployments by accounting for all applicable variabilities.

ACKNOWLEDGMENTS

Many thanks for the support from family and friends who stood by throughout this adventurous endeavor.

Thanks for the support from the Ph.D. committee, to Dale Hatfield for his formative discussions in the initial phase of this dissertation. Also, a special thanks for the support and advice from Dr. David Reed and Dr. Kevin Gifford throughout the completion of this dissertation.

Professionally, thanks to the MITRE Corporation for making its resources available. Particular thanks to Ms. Darcy Swain Walsh, Dr. Michael Sheehan, Dr. Keith Hartley, and Dr. William Young for their guidance. Thanks also for the support from my professional sponsors, the National Institute of Standards and Technology (NIST) (Dr. Duncan McGillivray), the Department of Defense (DoD) Test Range Management Center (Mr. Thomas O'Brien), and the DoD Chief Information Office (Mr. Tom Taylor) for your inspiration to succeed.

TABLE OF CONTENTS

LIST OF TABLES

LIST OF FIGURES

ACRONYMS AND ALPHANYMS

3GPP	3rd Generation Partnership Project
5G	Fifth-generation mobile networks
ABC	Adjacent band compatibility
AIRWAVES	Advancing Innovation and Reinvigorating Widespread Access to Viable Electromagnetic Spectrum
AMT	Aeronautical mobile telemetry
AMT	Aeronautical mobile telemetry
ANSI	American National Standards Institute
ARNS	Aeronautical Radio Navigation Service
ARTM	Advanced range telemetry
ATC	Ancillary terrestrial component
AWS-1	The first advanced wireless services band
AWS-3	The third advanced wireless services band
B-C	Benefits cost ratio
BER	Bit error rate
C/I	Carrier-to-interfering signal power ratio
CCDF	Complementary cumulative distribution functions
CDF	Cumulative distribution function
CCDF	Complementary cumulative distribution function
CINR	Carrier to interference plus noise ratio
CMRS	Commercial mobile broadband service
COST	Coopération européenne dans le domaine de la recherche Scientifique et Technique
CSMAC	Commerce Spectrum Management Advisory Committee
dB	Decibel
dBm	Decibel referenced to 1 milli-watt
dBW	Decibels reference to 1 Watt
DoD	Department of Defense
DoT	Department of Transportation
Dr.	Doctor (title)
eB/N0	Energy per bit / thermal noise
eHata	Extended Hata
EIIP	Effective isotropic incident power
EIRP	Effective isotropic radiated powers

EIRP	Effective isotropic radiated power
eNB	Enhanced node B
EVM	Error vector magnitude
F-C	Frequency-consequence
FAA	Federal Aviation Administration
FCC	Federal Communications Commission
FSPL	Free space path loss
GLN	General location and navigation
GNSS	Global Navigation Satellite Service
GPS	Global Positioning System
GPSDO	GPS disciplined oscillator devices
HPP	High precision positioning
Hz	Hertz, cycles per second
IAF	Interference analysis framework
IEEE	Institute of Electrical and Electronics Engineers
INR	Interference to noise ratio
IPC	Interference protection criteria
IRAC	Interdepartment Radio Advisory Committee
ITS	NTIA Institute for Telecommunications Sciences
ITU	International Telecommunication Union
K	Kelvin
kHz	kilohertz
km	kilometer
KPI	Key performance indicator
LNA	Low noise amplifier
LTE	Long-Term Evolution
MATLAB	Matrix laboratory
MC	Monte Carlo
MetSat	Meteorological satellite
MHz	Mega Hertz (1e6 Hz)
MOBILE NOW	Making Opportunities for Broadband Investment and Limiting Excessive and Needless Obstacles to Wireless Act
MSS	Mobile Satellite Service
MU	Measurement uncertainty
mW	Milliwatt
NASCTN	National Advanced Spectrum and Communications Test Network

NBS	National Bureau of Standards
NF	Noise figure
NGSO	Non-geostationary satellite orbit
NIST	National Institute of Standards and Technology
NPEF	National space-based positioning navigation and timing systems engineering forum
NPRM	Notice of proposed rulemaking
NTIA	National Telecommunications and Information Administration
OoB	Out of band
OTA	Over the air
Ph.D.	Doctor of Philosophy
PL	Path loss
PRF	Pulse repetition frequency
PUE	EIRP output power of a UE
R&O	Report and order
RCC IRIG	Range Commanders' Council Inter-Range Instrumentation Group
RF	Radio frequency
RIIA	Risk-informed interference assessment
RNSS	Radio Navigation-Satellite Service
RSRP	Reference signal received power
RTK	Real-time kinematics
SINR	Signal to interference ratio
SNR	Signal to noise ratio
SUI	Stanford University interim model
SWG	Sub working group
TAC	FCC Technological Advisory Council
TV	Television
U.S.	United States
UE	User equipment
UTC	Coordinated Universal Time
UWB	Ultra-wide band
W	Watt
Wi-Fi	Wireless Fidelity (referring to IEEE 802.11x)

1. INTRODUCTION

This paper's contribution to improving current spectrum decision-making methods is a set of recommendations to enhance the quality of information supporting risk informed interference assessment (RIIA) analyses. In the past, spectrum regulatory decisions considered only the worst-case scenarios involving the worst performing devices. This practice is insufficient in maximizing spectrum use because ignoring the likelihood of harmful interference results in overly conservative results. A repeatable and scientifically-based analysis framework presents the regulatory decision makers with the continuum of effects across varying and uncertain conditions across devices, as well as quantifies the implications of those uncertainties. Rigorous test methods, consideration of uncertainties, and the application of risk informed methods will provide improved accuracy and context for interpretation of testing results (i.e. translating test results to real world deployment implications).

This dissertation describes the development and application of an interdisciplinary framework that includes science-based spectrum coexistence testing methods to ascertain technically-sound inputs for conducting an interference risk assessment. The interdisciplinary aspect includes bringing the fields of measurement science (metrology), statistics, and radio frequency (RF) engineering together to better inform policy in the spectrum coexistence subject matter expertise.

1.1. Growth of Wireless Services

4G mobile broadband subscriptions are growing at an approximate annual rate of 25%, and by 2021 mobile devices will account for more than 63% of total internet proxy (IP) traffic [1]. The growth of wireless is linked to the nation's gross domestic product (GDP), and on average, a 10% increase in the Mobile Broadband adoption ratio causes a 0.8% increase in the U.S. GDP [1]. According to FCC Commissioner Brendan Carr, the build-out of fifth-generation mobile networks could mean 3 million new jobs, $275 billion in private sector network investment, and $500 billion added to the U.S. gross domestic product [1].

In recognition of the value of spectrum and related devices, a 2010 Presidential Memorandum directs the Department of Commerce, working with the FCC, to make spectrum available during the next ten years for expanded wireless broadband use. The Presidential Memorandum states:

"This new era in global technology leadership will only happen if there is adequate spectrum available to support the forthcoming myriad of wireless devices, networks, and applications that can drive the new economy. To do so, we can use our American ingenuity to wring abundance from scarcity, by finding ways to use spectrum more efficiently. We can also unlock the value of otherwise underutilized spectrum and open new avenues for spectrum users to derive value through the development of advanced, situation-aware spectrum-sharing technologies." [2]

Consequently, acts such as the Spectrum Pipeline [3], MOBILE NOW [4], and AIRWAVES [5] have elicited an expansion in commercial spectrum availability. With a commercial desire to expand the amount of available spectrum for allocation, regulators would benefit from a repeatable, defensible, and valid approach to make informed decisions involving new spectrum allocations. This approach must consider service rules, sharing methods, auction details, legacy user relocation, system adaptation, and technology evolution. A regulator's ability to make dispassionate spectrum management regulatory decisions is key to expanding services such as mobile broadband in a fair, well-reasoned manner. Using more comprehensive spectrum measurement data would add necessary rigor for repurposing spectrum to meet market demands and maximize spectrum use. *Making uninformed spectrum management regulatory decisions could inadvertently stifle the growth of mobile broadband and harm critical Federal missions and objectives.*

Creating reasonable guard bands in the frequency space and reasonable protection zones in geospatial space would help maximize spectrum use, quoting FCC Commissioner Michael O'Rielly at the Wi-Fi Alliance in June 2019, "*We no longer have the luxury of over-protecting incumbents via technical rules, enormous guard bands, or super-sized protection zones. The goal is to use every megahertz as efficiently as possible"* [6]. O'Rielly's quote is evidence that the Commission wishes to continue the momentum of economic growth from mobile broadband and is motivated to use spectrum more efficiently.

1.2. Applying the Scientific Rigor to Spectrum Coexistence Testing

Spectrum coexistence tests predict the effects of a spectrum service rule change or a new entrant to the spectrum. Testing through active experimentation with necessary

control can establish a causal or physical relationship between observed (measured) phenomena and active agents (causes) [7].

Interference testing of a spectrum-dependent system entails increasing the output power of a potential interferer (i.e. a candidate new entrant to the spectrum) while measuring the effects to the incumbent's spectrum-dependent system. In contrast, coexistence testing is the measurement of two spectrum dependent systems' ability to complete their intended operations simultaneously. This dissertation will refer to measures of interference, harmful-interference, spectrum cohabitation, etc. as *spectrum coexistence testing*.

Conducting a spectrum coexistence test involves procuring available technically-ready versions of the spectrum dependent systems equipment in question, emulating their operational environments (or control factors), and measuring the effects on various response variables.

1.3. Dissertation Purpose

In the past, spectrum regulatory decisions considered only the worst-case scenarios involving the worst performing devices. This practice is insufficient in maximizing spectrum use because ignoring the likelihood of harmful interference results in overly conservative results. A repeatable and scientifically-based analysis technique presents regulatory decision makers with a continuum of effects across varying and uncertain conditions across devices, as well as provide the opportunity to quantify the implications of those uncertainties. Rigorous test methods, consideration of uncertainties, and the application of risk informed methods will provide improved accuracy and context for

interpretation of testing results (i.e. translating test results to real world deployment implications).

This dissertation describes the development and application of an interdisciplinary framework for analysis based on standards-based testing and the treatment of spectrum-related measurands as statistical distributions. Distributions of measurement uncertainty, path loss (PL) variabilities, and deployment details will serve as valuable inputs to risk assessments and benefit spectrum regulators by providing values with confidence levels. Since many recent spectrum coexistence tests involve Long Term Evolution (LTE), a variant of commercial mobile broadband service, this dissertation also describes and implements a technique for predicting commercial mobile broadband LTE uplink and downlink emissions. These techniques will help inform incumbent spectrum users of the impacts of LTE deployments near their spectrum operations. Estimates that describe interference likelihoods should be provided as statistical distributions instead of simple single declaratory values. Single values present a misleading illusion of operational precision.

A spectrum allocation or service rule change request proposed by or to the FCC will benefit from a well-defined framework that ensures the appropriate information is provided in a risk assessment.

1.4. Research Statement and Methodology

This dissertation describes methods of improving the quality of inputs to RIIAs. The research will:

- Review spectrum coexistence test methods where spectrum interference analyses or tests to identify and/or propose improvements to the inputs of these methods.
- Provide examples and a use case to demonstrate potential benefits of using control factors and response variables as statistical distributions instead of single *declarative* values.
- Provide examples of how field collected spectrum measurement data benefits spectrum coexistence determinations.

This dissertation's contribution to improving current spectrum decision-making methods is a set of recommendations to enhance the quality of information supporting RIIA analyses including techniques of how to predict LTE deployments, uplink and downlink emissions. These supplementary practices include using standards-based spectrum coexistence testing methods that include measurement uncertainty (MU), key performance indicators (KPIs) that describe performance, and field measurements to augment PL predictions.

Also, this dissertation describes the proposed methods for improving risk assessment inputs in the form of a framework which is then applied to a use case. The framework will guide regulators in identifying and analyzing KPIs that describe harmful interference and the performance objectives of the systems in question. Response variables are defined as recordable changes in measurands that vary from baseline conditions.

Finally, this dissertation proposes the use of field collection methods to better predict RF propagation and interference effects. In the examples and use case herein, LTE waveforms will be used because LTE is the current dominant mobile broadband technology. These LTE field collections will be applied to an interference analysis framework that is based on scientific coexistence testing, and the application of MUs with

results described as statistical distributions to demonstrate likelihoods of interference effects. The methodology is as follows:

- Consider interference effects in evaluating the implications between uncoordinated spectrum-dependent systems operating co-channel or in the adjacent band(s).
- Using standardized testing and statistical methods from the literature, develop an interference assessment framework for improving the inputs to the FCC RIIA.
- For the chosen interference use case, LTE network deployments are studied using cell tower location databases and smartphone measurements of LTE downlink power to predict the interference levels that LTE would offer.
- Framework application to a use case detailing interference effects to a relevant and current spectrum regulatory issue, using the IAF to analyze the Ligado Network's proposal to deploy a nationwide mobile broadband network in the ancillary terrestrial component spectrum.

Two papers that inspired this research is an IEEE study which investigated baseline Global Positioning Service (GPS) operations [8] and the effects of various interference types adjacent to GPS operations [9]. These papers (further reviewed in subsection 2.6) found baseline carrier-to-noise ratios (CNRs) vary approximately 20 dB over a few hours of normal GPS operations and interference power levels that affect GPS is a function of signal type (e.g. coherent carrier wave, amplitude modulation, frequency modulation, white gaussian noise each affect GPS at different power levels). These papers' findings raise the questions: (i) should spectrum coexistence tests consider baseline variations, and (ii) should they test against the actual signal types experienced in the field?

1.5. Outline of the Dissertation

Following this introductory chapter, Chapter 2 contains a literature review of spectrum management regulatory bodies' spectrum rule change procedures, spectrum interference risk assessments, LTE as a commercial entrant to the spectrum, coexistence

testing standards, measurement uncertainty, descriptions of KPIs and spectrum propagation variabilities. These topics will be used in a proposed interference analysis framework (IAF) designed to guide the collection of the pertinent data for spectrum interference assessments. In Chapter 3, the IAF is described as a way to provide technically defensible inputs to a RIIA. Chapter 4 contains methods and approaches for completing the steps of the IAF, such as predicting LTE uplink and downlink emissive behaviors, methods for applying MU principals to spectrum test beds and propagation variabilities to coexistence determinations. Chapter 5 presents the tables and plots of the results and analyses of the proposed methods. Chapter 6 exercises the IAF in a matter of spectrum coexistence testing currently being considered by the FCC. Chapter 7 summarizes the information and identifies areas of future research.

2. LITERATURE REVIEW

This chapter reviews current regulatory decision-making methods and describes current U.S. spectrum policy processes, the RIIA, LTE history, standards-based spectrum coexistence testing, and best practices in metrology. This background information provides context for how improvements can be made in spectrum risk assessments by first requiring scientifically-based coexistence testing to produce trusted results. When translating these results to deployment details and determining stand-off distances, it is necessary to account for variabilities in RF propagations channels. As these variabilities in RF received powers are presented as statistical distributions with varying confidence intervals, translating spectrum coexistence test results into operational details further requires describing RF operational behaviors as statistical distributions instead of single values. Modeling RF behavior is only helpful if there is a connection to realistic and observable behavior. True RF propagation behavior includes transmitter and receiver hardware (including antenna effects) and the RF channel under consideration.

2.1. Spectrum Regulators in the U.S.

The United States (U.S.) is unique among the Member Nations of the International Telecommunication Union (ITU) in that spectrum management is regulated through a bifurcated system separated by the Federal government and non-Federal (commercial) spectrum. Separate spectrum regulatory bodies create the potential for checks and balances between the two managers that can, in theory, ensure meeting the legitimate interests of both commercial entities and government to the highest degree possible [10].

The two organizations that are assigned responsibility for spectrum management are (1) the Federal Communications Commission (FCC), which handles commercial spectrum and (2) the National Telecommunications and Information Administration (NTIA), responsible for government spectrum.

The Communications Act of 1934 established the FCC as an independent agency that reports to Congress, while NTIA, an agency within the Commerce Department was formed in 1978 as a successor to the Office of Telecommunications Policy staffed by the White House. Each of these organizations operates under a different set of procedures and policies. The rules governing the FCC are in Title 47: Telecommunications of the Code of Federal Regulations. NTIA publishes its rules in the Manual of Regulations and Procedures for Radio Frequency Spectrum Management.

The two regulatory bodies have fundamentally different approaches to their mission. The FCC makes decisions that may profoundly affect a business or the public interest, and their working environment is often highly political. As a result, the FCC is transparent, holding public proceedings. Debating aspects of a decision occurs in an open forum, and rulemaking depends upon inputs from competing proponents. In contrast, the NTIA is analytical in its approach to spectrum management by publicly sharing measurement campaign results while the Interdepartmental Radio Advisory Committee (IRAC) discusses spectrum actions in meetings that are not open to the public.

These regulatory bodies collaborate to make decisions regarding spectrum sharing. The FCC has a liaison representative on the IRAC and serves as a member of the IRAC's Frequency Assignment Subcommittee. The NTIA reviews FCC actions, and submits comments along with those from the public. Neither U.S. regulator defines a transparent,

science-based decision-making process. The current decision-making process is a multivariant process involving different priorities, such as financially based needs of the commercial and national security sectors or mission-based needs of Federal wireless systems.

Neither of the two spectrum regulatory bodies in the U.S. use a decision-making process that requires performing coexistence tests or reporting values as distributions. The following subsection will describe the current methods used by the FCC and NTIA.

2.1.1. **The Federal Communications Commission (FCC)**

The policies made by the FCC is well defined in their website. The FCC's process contains open comment periods where stakeholders can describe evidence for their case using measurement or modeling data. Evidence, however, is not required in making spectrum licensing or service rule decisions. Table 1 shows FCC's four-step process for spectrum-related decisions. The notice of inquiry is a call for information, and the notice of proposed rulemaking (NPRM) is a call for comments from stakeholders (including the public). The decision to amend or reject the proposed rule change is recorded in a report and order (R&O). Finally, the petition for reconsideration is a mechanism to address specific issues identified in the R&O by the stakeholders. The process is transparent as all of the comments and responses are entered into a publicly viewable Federal Register Notice.

The call for comments during the NPRM period allows for a submission of a risk analysis and/or test data to the decision-making process. This four-step process is adaptive because it is guided by the comments received.

Table 1. FCC rulemaking procedure

Stage in FCC Process	Description
I. A. Notice of Inquiry (NOI)	• Designed primarily for fact gathering. Serves to seek information about a broad subject or generate ideas. • This document will generally ask questions and provide few conclusions. • Describes where and when comments may be submitted and reviewed, and responses. • Comment review.
I. B. Notice of Proposed Rulemaking (NPRM)	• An NPRM is issued to detail proposed changes to FCC rules and to seek public comment. • The NPRM describes where and when comments may be submitted, where and when comments and responses can be reviewed. • After comments review, the FCC may choose to issue a "Further NPRM" to provide an opportunity for the public to comment further.
I. C. Report & Order (R&O)	• The R&O amends the rules or decides not to do so. • Summaries of the R&O are published in the Federal Register.
II. A. Petition for Reconsideration	• If people feel that certain issues were not well defined or resolved, a Petition for Reconsideration may be filed within 30 days. • The FCC may issue a Memorandum Opinion and Order or an Order of Reconsideration amending the rules or stating that the rules will not be changed.

The FCC rulemaking procedure, as published on the FCC website [6], offers multiple comment periods to solicit input from stakeholders. Comments can vary widely—from opinions of concerned citizens worried about antenna towers in their backyards, to lengthy test reports demonstrating harmful interference hazards to an incumbent user of

the spectrum. FCC spectrum regulators sift through these inputs and make decisions they deem appropriate.

The FCC rule-making procedure does not formally assess risk, recommend coexistence testing or field-collected data. However, the FCC's Office of Engineering and Technology's (OET) conducts spectrum coexistence testing to provide evidence for spectrum regulations written by the FCC.

The FCC OET's mission includes creating new opportunities for competitive wireless services to coexist in the spectrum [11]. One method of identifying new commercial spectrum services and deployments is through coexistence testing of systems. The FCC.gov website hosts technical memoranda, measurement procedures, and reports written by the OET [12]. An example spectrum coexistence test performed by the OET from 2014 is the Digital TV (DTV) and LTE interference study [13]. This coexistence test was performed in the 600 MHz band where LTE systems would soon be deployed in adjacent frequency bands to the existing broadcast television frequency bands. The results of this test could affect decisions allowing LTE into this frequency band. The coexistence test report describes varying the level of LTE power and recording the effect on DTV signal performance. The methods described do not:

- Prescribe using statistical methods of the measurement data or offer confidence intervals in the reported measurement values
- Consider test bed measurement uncertainties
- Provide results as distributions

- Use actual TV signals with TV transmitter antenna effects and RF propagation channel effects (instead a TV generator in a piece of Rhode Swartz test equipment was used)
- Use actual LTE signals (instead white gaussian noise was used as a surrogate)

This OET test report states that the LTE surrogate signals do not consider the different modulation schemes found in LTE[1] or include the temporal behavior found in actual LTE emissions [13, pg. 8]. The test methods used in this example are missing realistic operational considerations such as RF propagation stochastic channel effects and real-world signals from the devices under test.

2.1.2. **The National Telecommunications and Information Agency (NTIA)**

Similarly, the NTIA does not use or prescribe a framework that analyzes coexistence potential. Unlike the FCC, the NTIA does not use a publicly facing rule-making procedure because they manage bands for one entity, the Federal government. TheNTIA conducts spectrum sharing feasibility and interference prediction studies for Federal-on-Federal or commercial-on-Federal spectrum systems. Recently, with the widespread adoption of commercial mobile broadband services, many of these studies quantify the effects of mobile broadband on Federal systems. The Department of Defense

[1] For example, LTE emissions change modulation based on user path losses and data throughput requirements. These different modulations can impact other spectrum users differently.

(DoD) uses large swaths of spectrum to complete missions such as radar, radionavigation, communications, telemetry, and satellite links [14]. Two of NTIA's offices: The Office of Spectrum Management (OSM) and the Institute for Telecommunications Sciences (ITS) create inputs for spectrum regulatory decisions. ITS performs much of the spectrum coexistence effects through testing[2] while OSM makes the spectrum use decisions (and enforcement) for Federal agencies. In the spectrum sharing test reports released by the ITS, there is a paucity of literature that includes measurement uncertainties. In some example test reports in this chapter, the NTIA reports stand-off distance recommendations using free space path loss (FSPL) propagation models. In measurements taken in Chapter 5 of this paper the FSPL model will be compared to other PL models and field collected data. Examples of NTIA spectrum coexistence studies are provided in the context of interference-to-GPS receivers in Appendix A of this dissertation.

The NTIA manages the Commerce Spectrum Management Advisory Committee (CSMAC) which conducts spectrum sharing studies and plans. The CSMAC makes recommendations regarding spectrum service rule changes by balancing the needs of commerce and Federal government operations. This dissertation reinvestigates portions of the 2012 CSMAC report describing the feasibility (and effects) of repurposing 500 MHz of spectrum from Federal to commercial use [15]. To study the feasibility of converting Federal spectrum to commercial mobile broadband (or LTE), the CSMAC created five sub-working groups (Sub WGs) in 2012 to investigate the effects of new LTE systems

[2] For simplicity of terminology, throughout this dissertation the term "spectrum coexistence testing" or "coexistence testing" will be used to also mean interference effects testing as the goal is for coexistence.

operating near Federal spectrum bands. The WG studying meteorological satellite services [16] and aeronautical mobile telemetry (AMT) [17] is referenced in this dissertation. The 2012 WGs relied on assuming LTE cell tower deployment densities, and user devices' behaviors. To support the use case in Chapter 6, Chapters 4 and 5 of this paper reexamines the CSMAC assumptions, such as cell tower deployment details and demonstrates methods for predicting LTE uplink and downlink powers.

CSMAC also addressed the translating of interference measurements to deployment distances and found that not considering losses due to clutter can produce conservative errors by as much as 40 dB [17, Appendix 7-6]. To support the use case in Chapter 6 of this dissertation, methods and results of LTE signal field measurements are analyzed to demonstrate how such measurements can be applied to interference predictions. Field measurement data collections require a large number of samples to demonstrate statistical significance. Considering risk of interference measurement and PL values as statistical distributions provides more insight thus improving interference assessments.

2.2. Risk in Spectrum Regulatory Decision-Making

An evaluation of risk in a decision-making process considers likelihood versus consequence. A spectrum interference *risk assessment* is the identification and quantification of the hazards in a specific spectrum access use case. This dissertation is concerned with spectrum interference hazards, hereafter referred to as *harmful interference* [18]. Risk management in spectrum policy decision making accounts for the actions taken to quantify and reduce risks described in a risk assessment. Spectrum regulators make decisions about spectrum service rule changes (for example) with *reduction of interference*

risk as a guiding principle. Those regulators need a broad interdisciplinary suite of information to make well-informed decisions.

When making decisions on wireless spectrum use, the presence of *uncertainty* is a necessary consideration to ascertain the associated risks or impacts to other spectrum users. Impacts to other spectrum users can be identified by subjecting wireless systems (such as radios or radars) to coexistence testing—a quantification of harmful interference is a measure of the performance degrading levels. These harmful interference levels may be converted to operational deployment scenarios (conversions from power levels to distances) explaining the effects in their intended deployments. Operational risks are multidimensional and require consideration of more than just simple risk aversion. Some risks can have potentially significant consequences, such as interference that prevents the U.S. Missile Defense Agency from detecting incoming missiles or a radar's ability to help navigate a plane on to an aircraft carrier's deck. Some risks are inevitable and need to be tolerated, such as rain fading to a millimeter wave link or building clutter attenuating a signal in an urban environment. When raining, any systems using millimeter waves are designed around the risk (or hazard) of rain fading. Some hazards caused by harmful interference occur so seldomly that they are imperceptible to the user.[3] In general, spectrum policy cannot feasibly seek to eliminate all risk but will instead pursue reasonable reductions. In 1959, the Nobel prize winning economist, Ronald Coase explained the roles of the FCC:

[3] For example, opening a microwave oven before the timer has expired can interfere with a Wi-Fi link for the few milliseconds it takes for the microwave's magnetron to power down.

"It is sometimes implied that the aim of regulation in the radio industry should be to minimize interference. But this would be wrong. The aim should be to maximize output" [19].

Coase's words were prescient; the recently reported increases in spectrum value[4] suggest spectrum availability is crucial [20]. There are opportunity costs associated with frequency bands that show little activity and there are benefits to repurposing underutilized spectrum to more in-demand services. For example, the broadcast TV auction was intended to clear broadcast TV spectrum by offering broadcasters a monetary incentive to abandon the broadcast TV market or retune their stations to a lower band. The FCC offered the "cleared" TV spectrum to bidders interested in deploying mobile broadband services. This incentive auction repurposed 84 MHz of spectrum and netted $7 billion to the U.S. treasury [21]. To maximize use, all spectrum stakeholders should not be too conservative in claims of harmful interference.

2.3. Incorporating a Risk-Informed Process for Spectrum Regulators

This section explores an example of a risk assessment for harm to GPS receivers from outside sources of interference. This risk matrix uses a five-point scale for likelihood and consequence axes to describe different hazards. The ratings shown in Figure 1 are qualitative, relative, and opinion-based comparisons. Items of acceptable risk are in the green and yellow regions.

[4] "We estimate that the economic value of the 645.5 MHz of licensed spectrum is almost $500 billion [23]."

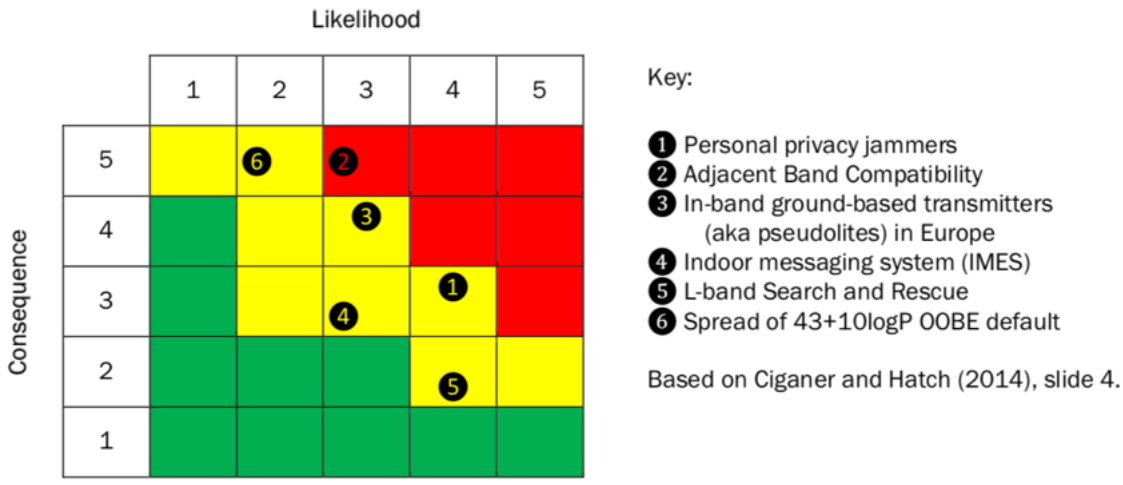

Figure 1. Perceived spectrum risks to GPS [22]

Item 2 from the Key of Figure 1, "Adjacent Band Compatibility", is in the red region with a consequence rating of 5 (or grave consequence) and a likelihood rating of 3 (represented as 5:3). Figure 1 can be interpreted to indicate that GPS is not tolerant to adjacent band systems. Although not shown, an additional risk factor in this graphic could demonstrate that GPS receivers are vulnerable to any condition that blocks the sky, not working indoors or under heavy foliage. GPS receivers are collecting signals that are space-based and therefore have vulnerabilities even without adjacent band interference.

The analysis of spectrum coexistence involves testing processes, operational (such as deployment) statistics, and accepted definitions of *harm*. Stakeholders must come to consensus on these definitions of harm and deployment details for spectrum coexistence testing to continue. Defining interference in terms of generalized power levels or tracing values to the noise floor will not stand the test of technical scrutiny. Risk-informed analysis with quantifiable measures is an improvement over the "worst-case" analysis which

provides little value as just one data point on a continuum of likelihoods. A spectrum incumbent is less likely to support changes to entrants or service rule changes than maintain the status quo. However, in cases where the goal is to maximize spectrum use, it is required to accommodate these changes.

2.4. The Federal Communications Commission's Technological Advisory Council Risk-Informed Interference Assessment

The FCC's adoption of risk assessment methods is a notable example of a spectrum regulatory body adopting a risk management technique. On December 1, 2017, in Public Notice DA 17-1165 [23], the FCC announced the adoption of TAC's RIIA and statistical-based service rules. In the parlance of the National Institute of Standards and Technology (NIST) Cybersecurity Framework, the FCC decision-making process now enters a new evaluation criteria for risk management mitigation techniques called "*Risk Informed" as defined by the NIST cybersecurity standard,* [24]. The Public Notice states that the FCC requires an interference assessment with a quantitative analysis of interactions between spectrum services before making decisions regarding levels of interference protection. The RIIA was chosen because it would offer a *quantitative assessment* (intended to be an improvement over the qualitative assessments as shown in Figure 1) to inform spectrum regulatory decisions. If the inputs to the RIIA are defensible, the assessments it produces will help regulators make their decisions. The Quick Intro to the RIIA released in 2015 [25] considers the likelihood versus consequence combinations for multiple hazard (interference) scenarios and provides more information than a worst-case analysis. Worst-case scenarios consider only the significance of worst hazard without considering its possibility or plausibility, potentially leading to false positives in hazard claims. The RIIA

method is a systematic, quantitative analysis of interference hazards caused by collocated spectrum dependent systems. RIIA uses a four-step process, shown in Figure 2.

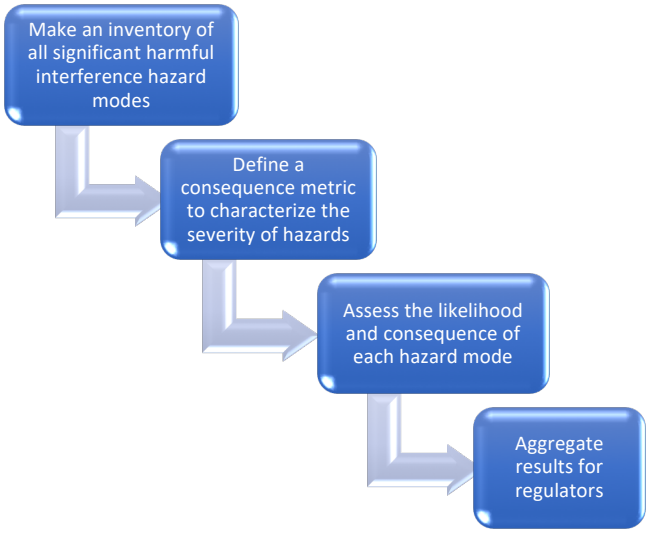

Figure 2. Risk Informed Interference Assessment four-step process [25]

Since the release of "A Quick Intro to RIIA" [25], case studies have been performed to exercise the framework, including coexistence between meteorological satellite (MetSat) and LTE mobile communications [26], multiple operating non-geostationary satellite orbit (NGSO) systems [27], and dedicated short-range communications and Wi-Fi. The following three subsections will review RIIA as applied to those case studies. A defined assessment process increases repeatability, and regulators of spectrum can enter what the NIST Cybersecurity Risk Management Framework labels as Tier 3: *Repeatable* [24]. *Repeatability* means if the decision-making process were repeated, the same outcome would occur.

2.5. Example of an RIIA in the Literature

An example case study using RIIA assessing the coexistence among non-geostationary-satellite orbit (NGSO) systems was performed by the FCC TAC in 2017 [27]. This case study is more complex than the previous case study's satellite coexistence scenarios because NGSO contains thousands of satellites, with a larger number of altitudes, and moving rapidly across the field of view. This RIIA begins with an analysis of baseline hazards (those that occur in the absence of added interference) as well as co-channel and adjacent channel interference hazards between NGSO systems. The effects of adding NGSO cluster coexistence was studied after quantifying baseline system performance. Studying non-interference cases are important because service outages and stressed links occur during normal operations.

2.5.1. **RIIA Step 1: Inventory Hazards**

The first element of the NGSO RIIA was gathering hazard or harm data. As an improvement to the previously performed MetSat/LTE case study, the NGSO study investigated baseline hazards that degrade performance, such as atmosphere, rain/cloud conditions, beam divergence, misconfiguration, and elevation. Even with no interference present, RIIA used "10% degradation in data throughput" as a definition of harmful interference. Interference hazards included both co-channel and adjacent channel interference. NGSO-on-NGSO interference is mitigated by improved coordination of orbits and/or band segmentation techniques. NGSO operators can use sensing or coordination to reduce interfering events [27].

2.5.2. **RIIA Step 2: Define Consequence Metrics**

The second element of the NGSO RIIA defines the consequence metrics: (a) corporate metrics (for example, the ability to complete a mission or loss of revenue or profit); (b) service metrics (data throughput degradation, time period or time percentage of outage, and link quality); and (c) RF metrics (observable quantities such as bit error rate (BER) or interference-to-noise ratio (INR)). To better measure the number of users exposed to the degraded performance, the RIIA also considered population density as a metric. This is an important caveat: just as interference happens in a receiver, degraded performance happens when there is a user to experience it.

2.5.3. **RIIA Step 3: Assess the Likelihood of Each Hazard Mode**

The third element of the RIIA is the likelihood-consequence values, which are measurements of service degradation (not interference) expressed as percent degradation in the interference metric using complementary cumulative distribution functions (CCDFs). A Monte Carlo technique produced the CCDFs (used as frequency-consequence (F-C) curves) predicting throughput degradation across many trials of use case scenarios. Figure 3 shows a sample of the F-C curves. Figure 3a shows an increase in percent degradation in throughput when two systems operate at the same time while not coordinating their access to the spectrum. Note the lone system has a baseline degradation in throughput due to the inherent operating conditions that come from normal operations, such as rain fading and RF PL components (such as clutter and terrain). Figure 3b shows the improvement in percent throughput degradation when the two NGSO systems coordinate with each other. The shift to the left in Figure 3b shows improvement of reducing risk of throughput degradation by enabling coordination among satellites.

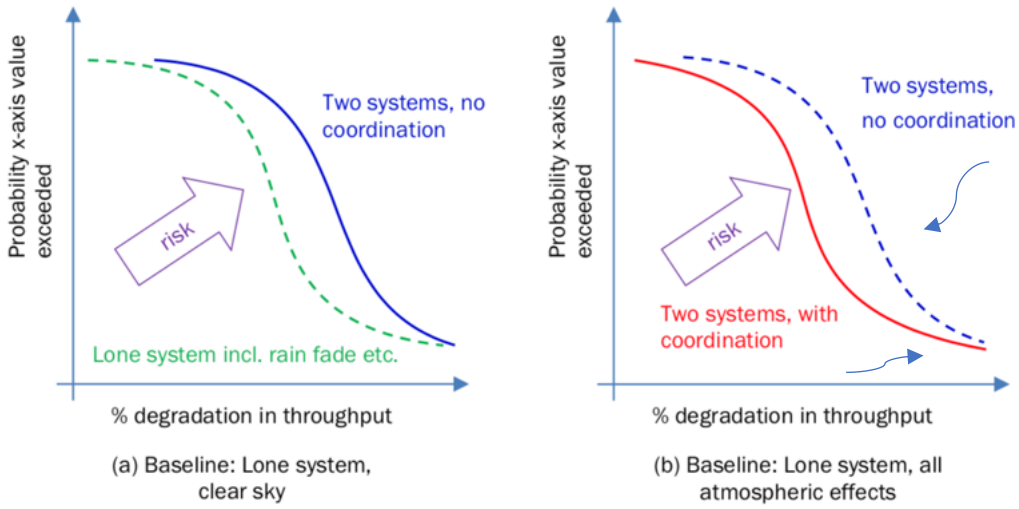

Figure 3. NGSO-NGSO sample F-C results curve [27]

2.5.4. **RIIA Step 4: Aggregate the Results**

The fourth element of the RIIA is the aggregation of results. Results are delivered in the form of risk charts showing the most hazardous scenarios, in this example, showing coordination effectiveness. Because this RIIA paper was a proof of concept, final quantitative risk CCDF curves were not available in the NGSO report; its conclusion was that RIIA could be applied to this problem, but actual quantitative results were not delivered. The report suggested 3 mitigation strategies [27]:

- Corporate: ability to complete a mission (for Federal users); and increased capital expenditure, loss of revenue, or loss of profit (for the private sector)
- Service: link availability and service quality (BER for data services, spectral efficiency in bit/s per Hz, etc.)
- RF: quantities observable in the radio frequency environment, such as changes in INR, signal-to-interference and/or carrier-to-interference plus noise ratios (SINR, C/(N+I)), absolute interfering signal level, receiver noise floor degradation, etc.

A useful output of this NGSO study over previous RIIA efforts was the addition of baseline conditions and mitigation strategies to the analysis. The two examples of RIIA

implementation by TAC produced results through computer modeling of scenarios [27]. Models can be controlled (removing the random externalities that affect real-world radio propagation) and execute thousands of trials at the expense of processing power and time, but measurements of actual hardware could add much needed realism to measured results and conclusions. Modeling communication systems leaves many uncertainties unaddressed. For example, PL models and position and beam shape uncertainties can yield false positive results in interference calculations. Applying a standards-based coexistence test to feed an RIIA could increase confidence in results and their applications to actual deployments of the systems under consideration.

2.5.5. **Gaps in the Application of RIIA**

There are statistical tools available to study spectrum interference effects, such as the Spectrum Engineering Advanced Monte Carlo Analysis Tool (SEAMCAT) [28] provided and managed by the European Communications Office of the European Conference of Postal and Telecommunications Administrations. SEAMCAT through its Monte Carlo utility will produce statistical results by cycling through loops of possible placements of mobile spectrum users, varying RF channel parameters, and other likelihoods of interfering factors. In the end however, tools like SEAMCAT rely on an interference protection criteria (IPC) such as an INR. For example, if a value of INR is chosen that does not rely describe harmful interference then such tools can deliver misleading results.

The examples of RIIA in the literature treat the IPC as a fixed measure. In other words, when a hazard is defined as -6 dB INR, at no point in the RIIA is this value questioned or treated as a random process. An INR that is arbitrarily assigned, overly conservative, or simply inaccurate will make the interference assessment incomplete and

possibly misleading. Therefore, the (hazard) inputs to a RIIA must be transparent, defensible, and include statistical bounds of uncertainty.

2.6. Variations in Interference Levels

A motivator of this research is to address the attempts spectrum regulatory bodies have made to generalize interference protection criteria. Generalizations can lead to overly conservative spectrum management decisions keeping technology-advancing services from being deployed. For example, in the radionavigation satellite services (RNSS) band, allowing a 1-dB decrease in carrier to noise ratio due to the aggregate interference from all non-RNSS sources equates to limiting the aggregate interfering signal power to 6 dB below the noise level of the GPS receiver. In an attempt to generalize interference protection, this IPC has been applied to other radio services outside of radionavigation. Not only has this measure been widely used in RNSS ITU Radio Recommendations, it is used for radar, fixed and mobile services, and radio altimeters. The use of an INR of -6 dB criterion has gained widespread acceptance in the ITU Radio Study Groups as an IPC for numerous radio services. This is recommended as a general rule, regardless of interference energy type.

However, in an analysis of various RF-interference effects in GPS receivers using different interference signal types (specifically, coherent continuous wave (CW), non-coherent CW, swept CW, amplitude modulated (AM), frequency modulated (FM), and gaussian noise) show different effects on GPS at the same power levels [9]. The interference level was held constant and interference minimum power was defined as the level of interfering power that made a detrimental change to the GPS receiver's reported carrier to noise ratio (C/N_0, a measurement of signal quality). Across these interference

types, the signal power level that causes a degradation varied by 25 dB (a difference of almost 400 times the power). Interference testing needs to include the actual signal types of potentially interfering waveforms to obtain accurate power levels. Therefore, testing to find an IPC using a CW tone is not an applicable surrogate to make decisions regarding an LTE waveform. The results of these interference powers is shown in Table 2

In spectrum coexistence testing and spectrum management decisions, using appropriate signal types is imperative to quantify interference effects because different types of interferers affects incumbent systems at different power levels. Also, of importance is demonstrating how a C/N_0 level harms systems performance and can therefore be labeled *harmful interference*. Lastly, tracing these interfering power levels for determining stand-off distances requires an understanding of the RF propagating environment where these intended deployments are located.

Table 2, Results of GPS receiver interference signals, results reprinted from [9].

Type of Interference	Interference power level as a change to C/N_0 in dBm
Gaussian noise	-103
Coherent CW	-88
Non-coherent CW	-85
Swept CW	-84
AM	-78
FM	-96

Many recent spectrum service rule changes and auctions are based on the deployment of LTE services. Having a greater understanding of LTE deployment details, uplink and downlink emissive behaviors will give spectrum regulatory bodies a better understanding of these variable system parameters.

2.7. Long Term Evolution (LTE) as a Commercial Mobile Radio Service

Since the "Unleashing the Wireless Broadband Revolution" Presidential memorandum [2] many recent spectrum coexistence tests include entering commercial mobile broadband systems. The LTE communication standard has come to dominate the market share of mobile broadband services and its emissive behavior is of concern to incumbent spectrum users. This standard was shaped by the previous cellular standard to use time and frequency sharing with orthogonal frequency division multiple access. LTE is adaptable to varying conditions, such as in reducing coding and modulation schemes to accommodate users that have poor link conditions to its base stations. An understanding of LTE's history and design details aid in quantifying its ability to operate adjacent or co-channel to incumbent spectrum users. An understanding of LTE's history and design details aid in quantifying its ability to operate adjacent or co-channel to incumbent spectrum users as considered in the use case described in Chapter 6.

2.7.1. LTE History

The LTE communication standard was created to provide ultra-mobile broadband access to a variety of mobile devices (smartphones, tablets, Internet of Things (IoT)). LTE came from the International Telecommunications Union (ITU) Fourth Generation (4G)

directives for International Mobile Telecommunications (IMT) Advanced. The ITU specified an all-IP packet switched network where even voice over LTE (VoLTE) is IP packet based. LTE was advertised with peak data rates of up to 100 Mbps for high-mobility mobile access and up to 1 Gbps for low-mobility access. Adaptive modulation schemes allow users to stay connected at a lower order modulation when signal to noise ratio (SNRs) were compromised due to signal degradation (i.e. measured as a lower SNR). Frequency division within their allocated channel into 180 kHz resource blocks made up of 15 kHz resource elements. LTE divides up time by 1 millisecond transmission time intervals (TTIs). LTE methods of sharing frequency and time resources is done dynamically by the base stations (enhanced node Bs, or eNBs) which divides up resource blocks based on a users' needs for data.

These networks offer smooth handovers[5] across eNBs and heterogeneous networks, (including across different LTE bands, 2G and 3G networks, small cells such as picocells, femtocells, and relays, and WLANs). Many of the eNBs' decisions are based on a user equipment's (UE's) assessment of the downlink signal received from the eNB. In other words, if the UE receives a downlink signal at a very low level, the UE will amplify its transmission to satisfy the SNR needed at the eNB's receive antenna. Conversely, if a UE receives a downlink signal at a high level, the UE can transmit at a much lower level saving battery life while still satisfying the eNB's requirement that the UEs' signal levels are incident at the eNB antenna at the same power.

[5] Handovers here means passing the users' signal from one eNB to another based on signal strength.

2.7.2. **LTE Design**

LTE UEs collect downlink power levels using the received signal reference power (RSRP) that can be used to estimate PL[6] from eNB (downlink) to user equipment (UE). RSRP is measured in dBm at the UE and is used by the UE to calculate its output (uplink) power needed to satisfy the eNB's receive strength. RSRP is measured across one LTE resource element or 15 kHz (note, there are 600 resource elements in a 10 MHz LTE channel). The eNB uses power control for all attached UEs, the setting an eNB uses for UE received power is the P_0. When open-loop power control (OLPC) is used, the UE output power (in dBm) is shown in equation (1) in terms of P_0 and PL, where $\propto$ is a scaling factor. Equation (2) expands the PL term in terms of output eNB power (P_{eNB}) and RSRP. Equation (3) shows output power of a UE in terms of P_{eNB} and RSRP [29]. This expression is the OLPC equation, which will be used in this paper to predict P_{UE}. Informed predictions of P_{UE} will be used to predict potential interference effects to other spectrum users.

$$P_{UE} = P_0 + \propto \cdot PL \quad (1)$$

$$PL = P_{eNB} - RSRP \quad (2)$$

$$P_{UE} = P_0 + \propto \cdot (P_{eNB} - 10 \cdot log_{10}(600\ resource\ elements) - RSRP) \quad (3)$$

[6] The uncertainty of the calculated PL is subject to the measurement uncertainty of the UE RSRP reporting.

2.7.3. **LTE Interference Predictions Studies**

As LTE grows in popularity, many interference/coexistence cases and studies have been executed to gain an understanding of the technology and operational deployments. In 2012 [30], the commerce spectrum management advisory committee (CSMAC) was tasked to study the effects of nationwide LTE deployments in the 1755 MHz to 1780 MHz uplink and 2155 MHz to 2180 MHz downlink [31]. Since many Federal (specifically DoD) systems operate in or near these bands, degradation in their systems' performances could be of great concern for national security or other Federal missions. CSMAC convened five working groups (WGs) to study FCC Auction 97 effects. These CSMAC WGs were largely concerned with LTE uplink powers and the powers of UEs aggregated together.

Table 3, Titles of the five CSMAC working groups

WG	Title	Description
WG 1	1695-1710 MHz Meteorological-Satellite	Improved modeling of commercial wireless network and possible reduction of exclusion zones.
WG 2	1755-1850 MHz Law Enforcement Surveillance, Explosive Ordnance Disposal, and other short distance links	Correlation of agency city by city transition plans with industry implementation priorities, prioritizing vacating the 1755-1780 MHz portion
WG 3	1755-1850 MHz Satellite Control and Electronic Warfare	Definition and specification (including any interference acceptance rules) of zones around satellite sites. Coordination path and rules for electronic warfare development and training
WG 4	1755-1850 MHz Tactical Radio Relay and Fixed Microwave	Definition and specification (including any interference acceptance rules) of zones around DoD sites that require access. Relocation process of fixed microwave links starting from the 1755-1780 MHz
WG 5	1755-1850 MHz Airborne Operations (Air Combat Trainings System, Unmanned Aerial Vehicles, Precision-Guided Munitions, Aeronautical Telemetry)	Determination of protection requirements for Federal operations. Understanding of periodic nature and the impact to commercial wireless of government airborne operations.

Table 3 lists the five CSMAC WGs tasked with determining feasibility and impacts of holding the AWS-3 Auction 97. Each of the WGs used the same LTE network deployment details to predict potential interference effects to the incumbent spectrum users once the Auction 97 was complete and the mobile broadband carriers deployed their LTE systems. To study the feasibility of the Auction 97, each WG was required to understand the details of the Federal incumbent user and LTE.

2.7.4. **CSMAC LTE Network Assumptions**

CSMAC predicted UE power output distributions by making LTE network assumptions such as cell radii, UE traffic types, eNB settings. The following LTE network assumptions determined P_{UE} distributions.

- LTE Frequency Division Duplex system with 10 MHz LTE bandwidth
- 100% system loading at LTE Base Station (eNodeB)
- All Physical Resource Blocks are occupied at all times
- 100% outdoor UE distribution
- P_0 = –90 dBm and alpha = 0.8 for uplink (UL) Power Control (urban/suburban/rural)
- Proportional fair algorithm for LTE Scheduler
- Full-buffer traffic model (i.e., all UEs are sending constant streams of data)

The CSMAC LTE predictions were approximately five years ago, and their methods of producing P_{UE} distributions are not described in a fashion for readers to reproduce or update. Through the IAF, this dissertation will demonstrate transparent methods (including drive testing to capture legacy LTE network parameters) and results to predict eNB deployment and P_{UE} distributions, and apply those distributions to spectrum coexistence analyses. After these CSMAC analyses, the FCC went forward with the auction to distribute licenses for commercial broadband use of the AWS-3 band.

2.7.5. **The spectrum and FCC Auction 97**

In 2015, the FCC held Auction 97 for commercial broadband spectrum bands. After the Auction, mobile broadband LTE systems entered the spectrum previously used exclusively by Federal missions. The auction changed the service rules of the bands described in Table 4. The AWS-3 band includes paired (separate uplink and downlink) and unpaired (spectrum for just uplink) for commercial LTE networks. Band types and

frequencies of the AWS-3 licenses are shown in Table 4. Blocks G through J are uplink bands that will be occupied by smartphones and other LTE devices that subscribers use for broadband mobile communications. Band edges like 1780 MHz will be a border between Federal and non-Federal systems with no guard bands in place.

Table 4. Auction 97 license types and corresponding frequency bands

Block	Frequencies	Bandwidth	Pairing
A1	1695 MHz to 1700 MHz	5 MHz	Unpaired
B1	1700 MHz to 1710 MHz	10 MHz	Unpaired
G	1755 MHz to 1760 MHz & 2155 MHz to 2160 MHz	10 MHz	2 x 5 MHz
H	1760 MHz to 1765 & 2160 MHz to 2165 MHz	10 MHz	2 x 5 MHz
I	1765 MHz to 1770 MHz & 2165 MHz to 2170 MHz	10 MHz	2 x 5 MHz
J	1770 MHz to 1780 MHz & 2170 MHz to 2180 MHz	20 MHz	2 x 10 MHz

The auction grossed more than $40 billion for the U.S. treasury [6] and portions of that revenue was spent in relocating Federal spectrum systems to vacate the new LTE bands.

2.7.6. **Summary**

To predict effects of auctioning off spectrum for mobile broadband, the CSMAC WGs made predictions about effects of LTE on incumbent Federal spectrum-dependent systems. Since the methods of the CSMAC LTE estimations and analyses are not described

in a manner that is transparent or repeatable, this dissertation will reexamine many of the CSMAC WG LTE assumptions and methods. Documenting and reproducing the CSMAC methods will allow modifications that represent LTE growth in services and deployment densities. Therefore, the following Chapters demonstrate alternative methods of predicting LTE cell radii, uplink and downlink powers using LTE deployment databases. Also, methods will be shown to collect LTE downlink powers to improve the CSMAC WGs LTE deployment details and apply measurements to a use case. The following section describes two spectrum coexistence testing examples performed by the NTIA ITS, and how

2.8. Spectrum Coexistence Testing Examples

Applicable coexistence testing can only be performed once equipment is available (i.e. past a technical readiness level allowing for testing) only then can test houses, test networks (specifically the National Advanced Spectrum and Communications Test Network (NASCTN), and regulators (specifically NTIA ITS) conduct measurement campaigns (***hereafter referred to as spectrum coexistence tests***). The following two subsections describe two spectrum coexistence test examples for LTE operating in an adjacent band to GPS and AMT.

2.8.1. GPS Coexistence Testing

Space-based GPS was initially designed and operated as a satellite navigation system for the DoD in the 1970s. Although GPS was intended to function as a positioning system for the DoD, other applications for the system emerged in the commercial sector [32]. For example, civilians found uses for the positioning and timing features provided by

the satellite cluster to help with mapping and directions. Because GPS is a broadcast system,[7] there is no limit to the number of users able to access the signals.

The original GPS design used two frequencies: one centered at 1575.42 MHz, called L1, and a second centered at 1227.60 MHz, called L2. Other bands were added later, such as L5, used for instrumentation aviation and safety of life [32]. This paper focuses on the L1 legacy civilian band of GPS that is widely used in consumer and industrial products.[8]

For years, GPS had few spectrum neighbors. Then, a new product idea called ultra-wide band (UWB) was proposed to operate in the same band as any system without causing harmful interference [68]. The ITS of NTIA tested these claims, connecting UWB and GPS systems together to measure the effects [33]. NTIA also tested GPS operations in the presence of adjacent band mobile satellite services (MSS) including its ancillary terrestrial component (ATC)[9]. In each of these tests, the definitions of IPC for the GPS changed from break-lock (complete loss of synchronization to GPS satellites) to a 1 dB degradation of the GPS receiver's C/N_0 [34]. The reason for the difference between these different IPCs is not explained in any available literature. The different test methods and definitions of interference protection led to confusion of what constitutes harmful interference to GPS and how it translates to standoff distances. This dissertation recommends using KPIs that describe system performance (e.g. timing or position errors) to mitigate these types of issues.

[7] To use its services, GPS users require only a receiver the transmitters are space-based built, operated, and maintained by the United States Air Force. GPS services also use ground-based augmentation emitters, these augmentation services are not discussed in this dissertation as testing of their services are not available in the literature.

[8] L1 is closest to the Commercial Mobile Radio Services band(s) identified in the Introduction of this paper.

[9] The ATC is a land-based augmentation system that improves the operation of MSS

2.8.2. **Effects of Adjacent Band LTE on AMT**

In similar application to the GPS example, AMT operations and the impacts of new LTE entrants adjacent were described in the CSMAC Working Group 5 [17]. The IPC for AMT was taken from ITU Radio Recommendation M.1459 [35]. This recommendation did not account for LTE signal types therefore its applicability would need further research because if signal types were not accounted for, the interference predictions would not necessarily apply to LTE. CSMAC produced protection distances from LTE uplink and downlink to the AMT receivers as shown in Table 5. These distances were predicted through analysis with no testing of the effects of LTE powers levels to the operations of AMT. For example, the distance of 80 km corresponds to a power level of LTE and there is no evidence that power level cause harm to the AMT performance. These stand-off distances were calculated based on an INR, where LTE power is a fraction of thermal noise already present at the AMT receiver antenna. NTIA used its irregular terrain propagation model (ITM) to translate these LTE power values to distances. The ITM accounts for terrain model by using the United States Geological Service (USGS) database but no clutter data was considered. The CSMA WG5 reported "a proposal to compare measured data of aggregation of power from LTE to the airborne systems with the model currently being used for the analysis to understand the difference in loss, understanding that such measurements must be based on the ground truth of what an actual LTE network deployment for the band would be and the actual airborne systems that operate in the band" [17, page 7], but that process was never concluded. Adding measured propagation data to these analyses, or considerations of clutter was not applied to the AMT LTE study.

Table 5, Stand-off distance between predicted AWS-3 LTE deployments and AMT receiver sites

AMT Site	Distance form LTE UE	Distance form LTE eNB Minimum	Distance form LTE eNB Maximum
Atlantic test range	80 km	100 km	560 km
Point Mugu	140 km	100 km	560 km
Eglin Air Force Base	75 km	100 km	560 km

The subject of coexistence was revisited in more detail by the Defense Department at Edwards Air Force Base in a paper titled "An Initial Look at Adjacent Band Interference Between Aeronautical Mobile Telemetry and Long-Term Evolution Wireless Service" [36]. The adjacent band effects of LTE on AMT are the subject of an ongoing test executed at the Boulder Labs by the NASCTN[10]. The test plan for the NASCTN coexistence test is found on their website [37]. The test plan is based off the methods described in the ANSI Spectrum Coexistence test standard C63.27 [38]. In the NASCTN test, actual LTE uplink recordings from the field will be injected into the testbed where effects to AMT will be recorded.

In WG5, the CSMAC did not consider clutter losses, measured propagation data, harmful effects, or verified LTE deployment details when predicting LTE effects on AMT operations. The methods and results in this paper will reinvestigate LTE uplink and

[10] More information about the NASCTN is found at their website: https://www.nist.gov/communications-technology-laboratory/nasctn

downlink behavior, record LTE downlink emissions over distances and use these results to demonstrate how to improve LTE interference predictions. Spectrum coexistence testing using standards-based methods can better ascertain the actual harmful effects to AMT receivers. Since LTE deployments equate to billions of dollars to the U.S. GDP, investing in improvements to these methods is warranted.

2.9. Standards for Spectrum Coexistence Testing

When predicting effects of LTE deployments to AMT operations, CSMAC relied on an "accepted interference level". If spectrum coexistence test data is used to support a spectrum service rule change, then methods and confidence in results should also be reported. Using standards-based methods will offer transparent methods that can be repeated by anyone who would question or contest the results. The literature reveals two spectrum coexistence standards that describe best practices and methods for making repeatable, science-based tests in this space. The following subsections describe the Institute of Electrical and Electronics Engineers (IEEE) 1900.2.2008 [39] and the American National Standards Institute (ANSI) C63.27 [38] standard for spectrum coexistence testing.

2.9.1. **The IEEE 1900.2**

In 2008, the IEEE standards coordinating committee on dynamic spectrum access networks sought to define standards for defining both interference and coexistence between radio systems [39].

The IEEE defined coexistence as two or more spectrum-dependent devices or networks operating without harmful interference. The IEEE process for determining coexistence (its test process) is shown in Figure 4.

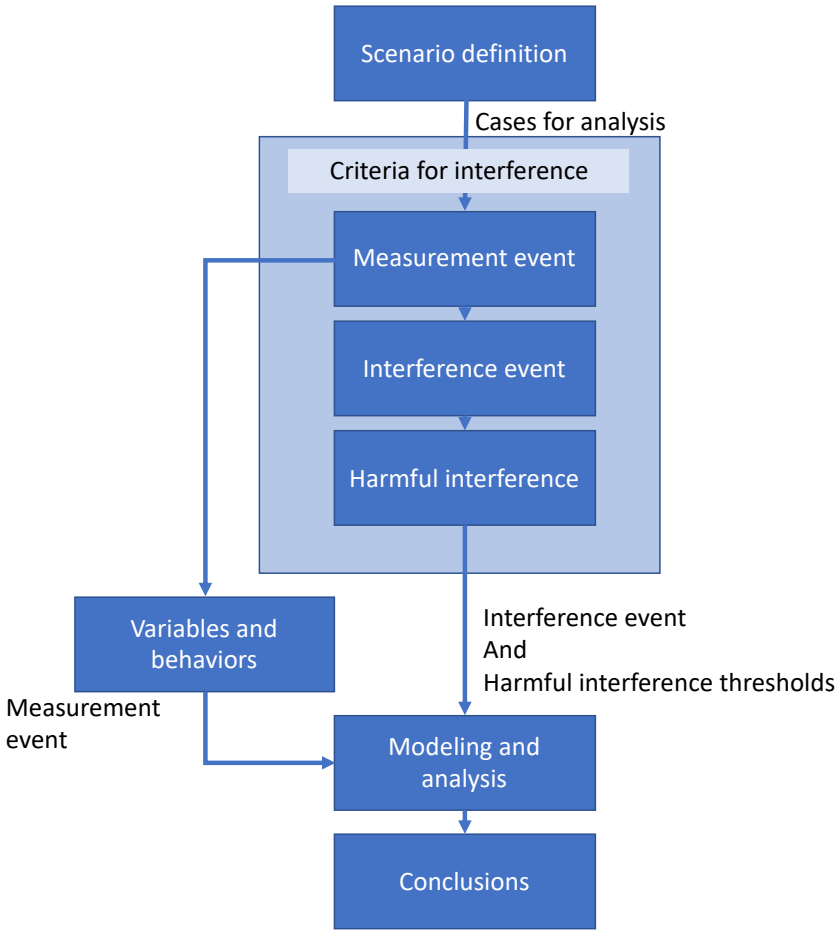

Figure 4. IEEE 1900.2 coexistence analysis process (reprinted from [39])

The flowchart in Figure 4 shows the IEEE 1900.2 recommended steps of spectrum coexistence (or interference determination) testing. The first step is to define the scenario, which refers to the operational characteristics as described in this paper. Defining the criteria for interference includes identifying interfering events—for example, a KPI is degraded to the point where harmful interference has been identified. The "criteria for

interference" box in the Figure is the *threshold* of a KPI as defined in this paper, is harmful interference. Because the threshold may change over time or be redefined with the introduction of new evidence,[11] it is important to report more than just the events that happen at the thresholds. The 1900.2 was published in 2008 without further updates; much of the material could be considered outdated (because communication systems evolve over time) and the methods are not present in all recent spectrum coexistence test events. For example, the 1900.2 section on MU states "analyses and measurements have an associated uncertainty" [39].

Including MU in a spectrum coexistence test translates to confidence in testing results by making the bounds of uncertainty in the test transparent. An example to the contrary, in 2011, the National Space-Based Positioning Navigation and Timing Systems Engineering Forum (NPEF) conducted tests of LTE in bands surrounding GPS but did not include any uncertainty analyses of measures in its report [40]. The output of the NPEF test was designed to measure a 1 dB rise in the noise floor of several GPS receivers, without mentioning the bounds of uncertainty in the measurement test setup.

2.9.2. **The ANSI C63.27**

In 2016, in an effort to define and standardize spectrum coexistence testing methods, ANSI formed an accredited standards committee. The group, called C63, created standard C63.27 [38]. The 1900.2 has not been updated in more than six years and the C63

[11] Such as Canada changing its definition of GPS interference protection (–70 dBW/MHz versus –100 dBW/MHz). Another example is when a spectrum-dependent system adopts an error correction mechanism increasing robustness to interference tolerating more energy in an adjacent band.

gives only a few spectrum dependent systems as examples, such as medical devices. Even though the C63 may not use many examples, the methods therein are science-based and relevant to all spectrum dependent systems. This standard was created as an:

> *"evaluation process and supporting test methods are provided in this standard to quantify the ability of a wireless device to coexist with other wireless services in its intended radio frequency (RF) environments"* [38]

As with the IEEE 1900.2, a tester following the C63.27 standardized test methods must define the intended spectrum test environment, KPIs (with thresholds of performance), and technical details of the equipment under test. The testing environments may differ from the intended operational environments; for example, a mobile broadband system that is intended to operate outdoors at walking or driving speeds is tested in a controlled laboratory setting. This coexistence test standard describes four methods of equipment interconnection, shown in Table 6, each increasing in realism and complexity. The first method is modeling; for example, using tools like MathWorks MATLAB®[6] LTE and Propagation Toolbox, which can provide PL predictions using Mathworks MATLAB® Propagation Toolbox Version 12. Modeling and simulations have the advantage of simplicity in executing multiple trials (as compared with field testing); many experiments can be made with the only expense being computer processing power.[13] Simulations are only as accurate as the number of realistic inputs entered. For example, simulating RF PL should include all RF blockages or clutter that will be experienced by an

12 MATLAB is a product sold by MathWorks, the academic version is available for students and is taught in the curriculum of many engineering schools.

13 There are certainly test cases that can require very costly computational power exceeding the costs of physical testing. But historically, field testing is quite expensive and offloading those costs to automation and computational resources might make financial sense in some cases.

RF signal in the real world with multipath, clutter, and other externalities likely to affect RF wireless conditions. Realistic variations and uncertainties must be included in a simulation.

Table 6. Methods for evaluating spectrum coexistence

Methods for evaluating spectrum coexistence	Description	Pros	Cons
Modeling	Executable from a computer	Only option when equipment not available for testing	Lacking operational realism / model accuracy
Over cables	Connecting samples of equipment	Well-controlled environment, reproducible outlying conditions	Lack antenna and propagation effects
Hybrid	Some equipment cabled, some in chambers	Same as cabled, addition of some antenna effect	Same as over cables
OTA	Equipment emits over air in operational environment	Matches operational conditions	Unquantifiable uncontrolled factors

Testing systems over cables requires procuring actual hardware of sufficient technical readiness for testing, or hardware emulation capabilities. In spectrum coexistence testing, some systems may not be available for testing and surrogates or "like" systems need to be inserted in their stead. Surrogate waveforms can be produced using software defined radios, or synthetic waveforms can be emitted using test equipment (like a vector signal generator).

The methods of spectrum coexistence testing are a trade-off of complexity and uncontrolled factors versus confidence in the results. For example, a fully controlled OTA test would be ideal, however, repeating data collection may require many flights of an airplane which could be time and cost prohibitive. By contrast, many trials of an experiment can be modeled on a computer for much less expense, however, propagation models that account for all clutter and terrain effects is not available. By contrast, testing exclusively over cables is convenient and allows for controlled and predictable propagation effects. A hybrid of systems over cables and systems propagating introduces the antenna effects of the systems being tested adding testing realism. Hybrid or over the air (OTA) testing is necessary to include antenna effects of systems that use high gain antennas, beamforming, antenna shaping, multiple in/multiple out, etc.

Spectrum coexistence testing with standards-based methods will yield the needed evidence for claims about IPC and claims of harmful interference. The values from the C63 methods will include MU and confidence bounds lending insight into likelihoods of interference and providing trust in the reported measurands.

2.9.3. **Key performance Indicators for Determining Interference Effects**

The CSMAC WG1 used a -10 dB INR IPC for weather satellites but states in Appendix 5-1 that analyses must be performed to confirm this IPC is appropriate. WG1 did not verify this IPC yet, the stand-off distances where LTE is allowed to operate was based off this metric. A spectrum coexistence test using a weather satellite receiver's metric of performance such as BER, or signal to noise ratio would give evidence usable to determine LTE stand-off distances. These measures of system performance and harm from interference are the system's KPIs.

The standards for spectrum coexistence testing describe using KPIs as measures of interference effects. Protection from interference from adjacent band (on in-band which is known as “co-channel”) emitters requires measuring wireless systems performances with and without the presence of other signals. Performance criteria are the KPIs of that system. More specifically, they are a system’s response variables that are deemed descriptive of system performance. Some response variables are more valuable to end users and adding weights to those criteria aids in describing impacts during a spectrum coexistence test. Weighting KPIs is also an effective way to differentiate service priorities across a variety of stakeholders. Some wireless services, such as voice services, or gaming systems would weigh the degradation in latency performance as catastrophic failures while other services would weight BER as a KPI.

In a spectrum coexistence test, the variables changed during test are labelled as control factors. Examples of control factors that can be changed during a coexistence test are output power, modulation and coding schemes, and separation distances. Spectrum dependent systems under test have several response variables, the most important of which are labeled as KPIs. Another example, KPIs for a Defense Department Aeronautical Mobile Telemetry (AMT) systems are defined as those variables crucial for meeting their operational mission objectives [41]. For testing AMT, KPIs are evaluated as response variables to indicate if potentially interfering emissions (in this example from LTE) are impacting AMT operations. A sample list of KPIs evaluated as response variables for this test are bit synchronization, BER distributions (from the perspective of the AMT receiver) and received signal strength indicator (RSSI).

Other AMT operating conditions (or control factors) also are included in the test considerations of [41], which provides an example set of considerations including AMT at a variety of signal strengths and modulation types and variety of LTE conditions to arrive at various combinations of carrier to interferer ratios (C/I).

In the literature, many methods of defining interference protection have been applied to GPS testing (shown in Appendix A), but one such metric was defined in the Department of Transportation (DoT) Adjacent Band Compatibility (ABC) test where the definition of harm was a 1-dB degradation in carrier to noise ratio (C/N_0). However, this protection criterion is not directly a measure in performance degradation. A user would not notice this degradation an impact to the service. To measure a 1 dB change in value the test bed must have an uncertainty resolution less than 1 dB. MU is a concept used in measurement science that gives confidence bounds to reported values. The C63 test standard requires that a spectrum coexistence test bed quantifies and applies the testbed MU when reporting results.

2.10. Measurement Uncertainty

Measurements are a comparison of observed values to a standard. The study of these quantitative values obtained through measurement is the field of measurement science, or metrology [50]. When comparing observed values to a standard there is an inherent value of error which cannot be mitigated. MU is the attempt to quantify the size of that error and reporting that size as a range of uncertainty better describes measurements. To define confidence in results, the C63 spectrum coexistence test standard advocates using principals of quantifying measurement uncertainty in the reported results.

2.10.1. The Two Types of MU

MUs that are determined through repeated measurements are referred to as type-A uncertainties. MU values that are taken from equipment data sheets, engineering intuition, or other sources are type-B uncertainties. Type-B uncertainties are non-statistical information that can be used to estimate unknown distributional parameters, including:

- scientific judgment
- manufacturer specifications
- other indirectly related or incompletely specified information

Type-A and type-B MUs are treated differently, as illustrated in the following sections of this chapter. Although type-B errors are less well defined (they are sometimes opinions-based), including these errors provides more descriptive results than omitting error predictions. Chapters 4 and 5 describe MU calculation methods with examples as related to a spectrum coexistence testbed and propagation variabilities.

2.11. Variations in RF Power

Just as MU is standard practice for metrologists, their practices can be applied to spectrum variabilities to translate spectrum coexistence test data to stand-off distances. In spectrum coexistence testing, an attempt is made at describing relative and absolute RF power levels, frequencies, and times. Making spectrum coexistence policy decisions requires an understanding of spectrum coexistence test measurements including what variabilities are expected in field deployments. For policy makers, general statements are made from measurements taken in laboratory and field test environments. Frequently, these power levels are taken from test equipment after the signals travel through RF communication equipment, cables, and antennas, and/or over the air. Test equipment that

is traceable to a standard can have associated uncertainties; for example, cables, connectors, and RF components can offer uncertainties to the measurements taken in a lab. Likewise, field measurements are typically performed through complex propagation channels that offer variability to measurement results, such as clutter losses, time varying conditions, and multipath. OTA measurement values have variabilities and the test equipment have unintended MUs. Spectrum regulators should trust measurement values and these values must include their associated uncertainties and variabilities. A standards-based treatment of uncertainties is presented in measurement uncertainty guides, documents such as Guide to the Expression of Uncertainty in Measurement (known as the GUM) process [50], and those treatments will be used in the descriptions and examples in this dissertation. In Chapter 6 of this dissertation, the Joint Committee for Guides in Metrology's (JCGM) techniques of MU will be applied. The JCGM authored, maintains, and promotes the use of the GUM. Furthermore, this dissertation applies MU principals to the highly variable PL conditions experienced by spectrum dependent systems in the field. As an example of how variabilities in an OTA RF channel (also known as a propagation channel) manifest themselves in the same way that uncertainties occur in a test bed, radar emissions captured from a fixed site is used in Figure 6.

To make improved PL predictions, the IAF prescribes a technique to apply the principles and calculation methods of MU to PL variability. Figure 5 shows an example, reprinted from [42]. The data points in Figure 5 are measurements of RF energy versus distance in 6 urban sites. Although there is a trend showing PL is directly proportional to distance, there are many values (in dB) of PL in a given distance. For example, the PL value for d = 2 km, ranges from approximately -80 to -140 dB, a range of 60 dB (or

100,000 times in absolute values). The conclusion drawn from the measured data in Figure 5, was that in the equation $distance^{-n}$, n = 2.7. This value of n creates a monotonic fit that cuts through the centroid of the measured data with a standard deviation of 11.8 dB. A MU with 95 % confidence is approximately two times the stand deviation, or +/- 24 dB (24 dB is approximately 400 times the power at a given distance).

OTA testing results show that an average PL value for a given distance is insufficient in describing the continuum of PL possibilities, including standard deviation lends more insight to the PL distribution.

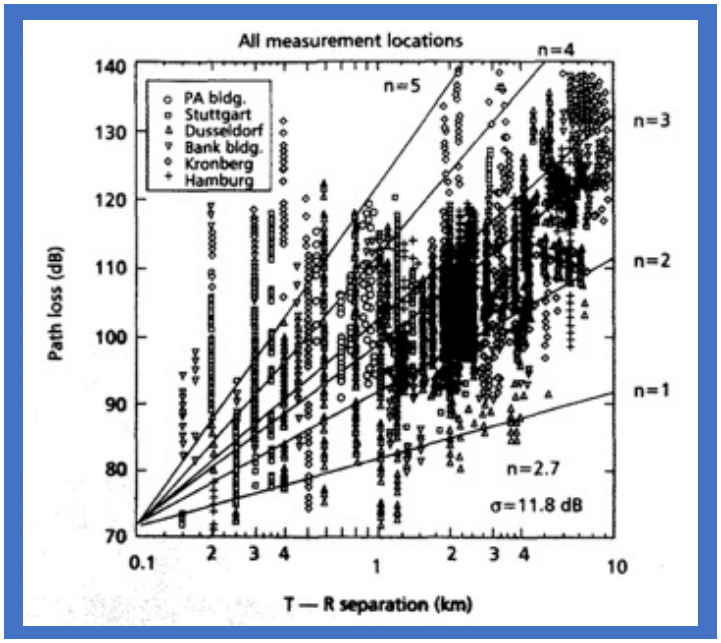

Figure 5, Path loss measurements performed across six urban sites in Europe, reprinted from [42].

Predicting interference using PL models that do not include clutter or terrain losses can under predict received powers and lead to conservative assessments. For example, in operational conditions ground-to-ground PL measurements are much higher than predicted

by PL models, because the models do not include building and terrain clutter values. For example, a spectrum compatibility assessment performed by the NTIA titled *Ultrawideband and Global Positioning System* specifically suggests using FSPL models when determining mandatory keep-away distances [68]. FSPL models do not consider clutter from vegetation, fabricated structures, or terrain and clutter losses alter PL measurements by many dB. Propagation models that account for clutter are available, but area-specific clutter can be ascertained through *observational studies* – using measurements in the field.

Observational studies (also referred to as spectrum monitoring) show that even as conditions are held constant, measurements of spectrum-dependent systems can reveal variations that need to be considered when evaluating interference likelihoods. As an example, in NIST Technical Note 1954 [43], radar emissions were collected for 60 second periods as shown in Figure 6. The test conditions included a stationary spectrum monitoring receiver located on a rooftop collecting radar pulses from a relatively stationary ship. Some of the 60-second collections showed little temporal signal fading, while other collections showed significant fading. Figure 6a shows a variation in received signal power by approximately 32 dB, while Figure 6b shows an observational spectrum capture with no observable variation in the received RF power. It is not known if these signal variations were due to measurement error or externalities such as radar equipment or RF propagation channel conditions. This example shows there are variations in signals that need to be considered, and values such as “received radar power” need to be treated as distributions that must be described with statistical values such as median, standard deviation, and percentile.

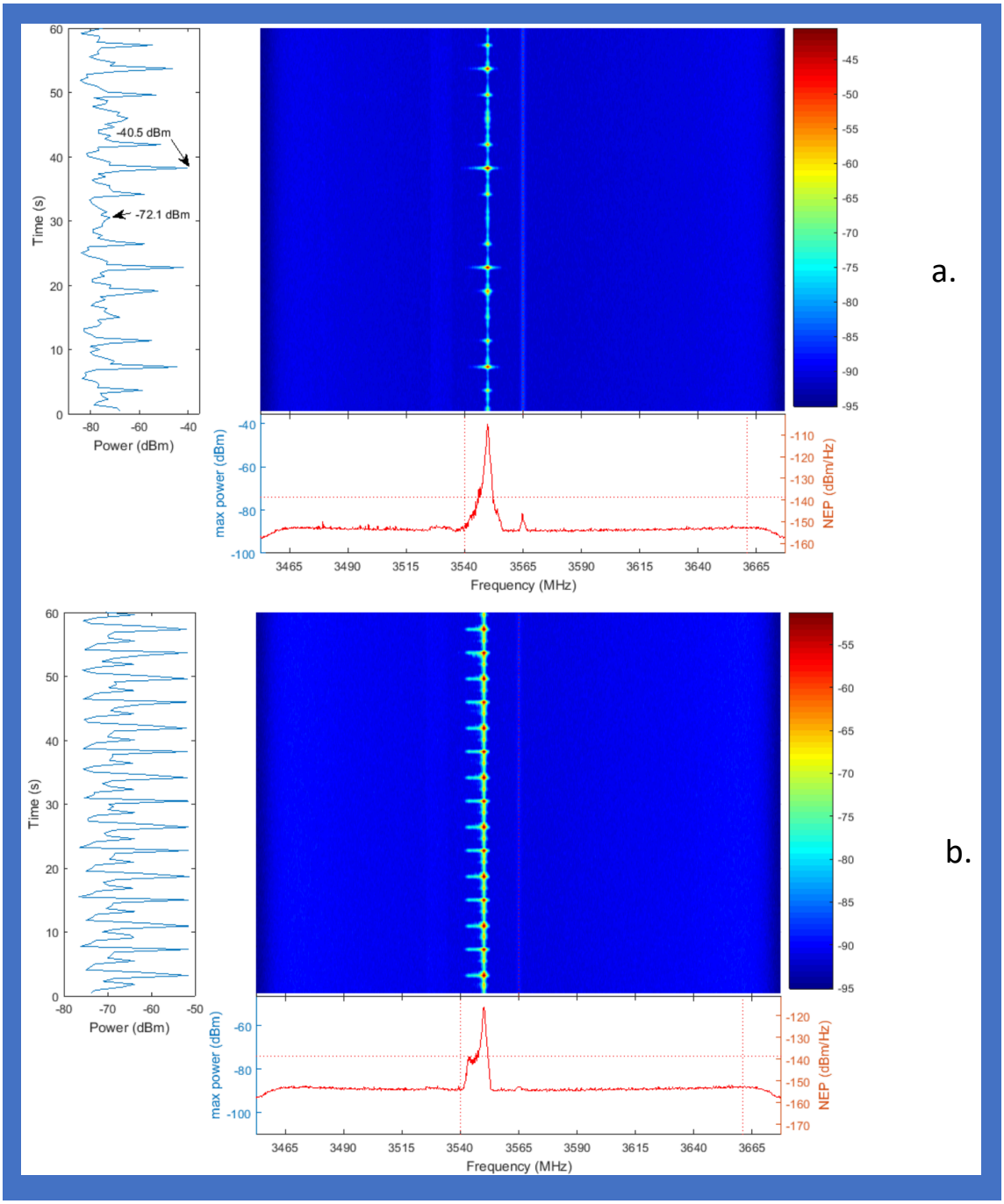

Figure 6. Two 60-second observational captures of a 1-Megawatt shipborne radar emitting while at sea. The receiving antenna was stationary, near the coast, recording in-phase and quadrature energy through an antenna, front end, and recorded using a vector signal transceiver : a. shows a variation of –32 dB and b. shows no observable variability [43].

The received radar power example from Figure 6 is one demonstration of how, in spectrum policy, decisions about "where to operate" are derived from the conversion from RF powers to distances. RF power values come with great variability and when translating powers to distances the results should also be expressed as statistical distributions.

An example of using a simple FSPL model to convert interference power levels to stand-off distances is in the DoT ABC test results, where LTE downlink power are projected on to a two-dimensional map to demonstrate GPS receiver stand-off distance to avoid a 1 dB drop in C/N_0 performance. An example is shown in Figure 7, a conversion from LTE power (in dBW) to stand-off distances (in meters) using a FSPL model shows a signal from 14,000 km causes a 1 dB degradation in C/N_0. This dissertation will demonstrate methods that will test the measurement of this IPC and the conversion of powers to stand-off distances. The risk of using inappropriate spectrum models when translating powers to distances can lead to overly conservative coexistence determinations.

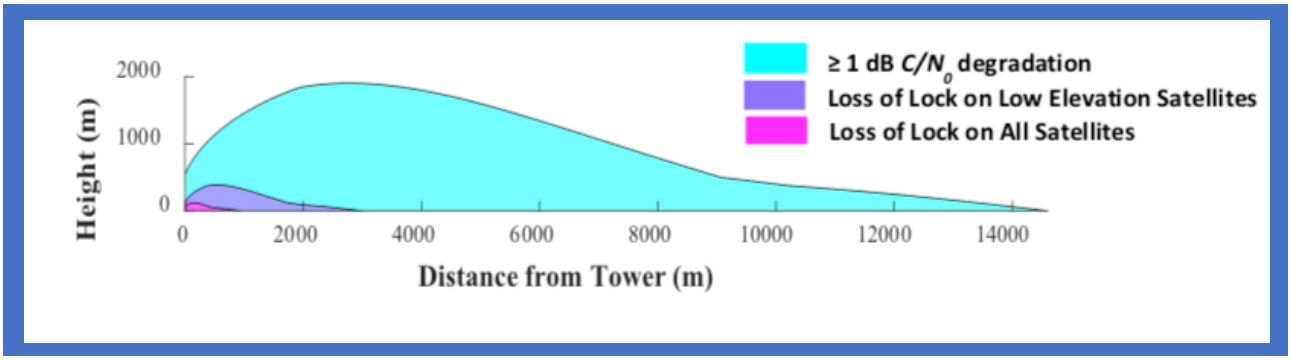

Figure 7, Impact of a 29 dBW Cellular Base Station Transmitting at 1530 MHz on a High Precision GPS/GNSS Receiver [76].

The following chapter will address gaps in current spectrum regulatory processes adding spectrum coexistence testing to the inputs of the FCC's RIIA. Testing done in this manner will provide trusted results that spectrum regulators can use to make better band allocation and service rule change decisions. These recommendations will be provided in the form of the IAF.

3. AN EXTENDED FRAMEWORK FOR SPECTRUM COEXISTENCE DETERMINATIONS

To improve the quality and consistency of information spectrum policymakers use to make interference assessments, this paper proposes the IAF. This framework is intended to help improve the inputs to RIIA by guiding the assessor through the steps needed to ensure the quality of interference protection criteria.

This chapter describes the IAF, a framework guiding spectrum coexistence testing using standards-based testing methods with an emphasis on treating values as distributions as opposed to single declarative values.

3.1. A Framework for Spectrum Coexistence Testing

Spectrum coexistence testing attempts to describe relative and absolute RF power levels, frequencies, and times. Making informed spectrum coexistence policy decisions requires an understanding of spectrum coexistence test measurements and the translation of those measurements to deployed distances. Policymakers formulate generalized statements from measurements taken in laboratory and field test environments. Frequently, these power levels are taken from test equipment after the signals travel through RF communication equipment, cables, and antennas, and over the air. Test equipment, even when traceable to a standard, have associated uncertainties; for example, cables, connectors, and RF components can offer uncertainties to the measurements taken in a lab. Field measurements that propagate through complex RF channels offer variability to measurement results. Variations in received signal power are due to clutter losses, time-varying conditions, and multipath. Each reported measurement value has an associated

variability and unintended MU. Spectrum regulatory decisions require measurement values that are trusted, repeatable, and verifiable. Therefore, values must be reported along with their associated uncertainties. A standards-based treatment of uncertainties is presented in the GUM standard in documents such as [44], [50]. Those treatments will be used in the descriptions and examples in this chapter.

Based on gaps identified in the literature review, the IAF, shown in Figure 8, consists of system descriptions, deployment specifics, KPI determination, coexistence testing with MUs, and variabilities incorporated into a RIIA. The components and this framework produce a rigorous, repeatable, science-supported suite of information that regulators can use to make informed decisions.

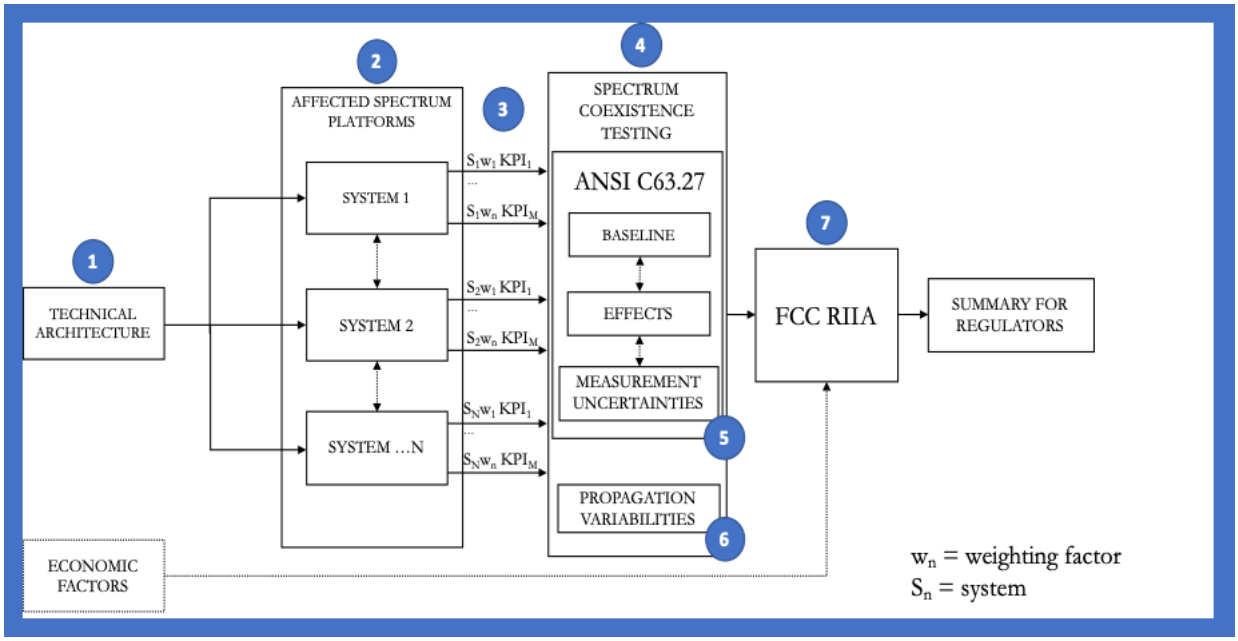

Figure 8. Proposed interference analysis framework, IAF for coexistence determination with labels for the major components discussed in the text of this chapter.

The output IAF provides appropriate measurands into the RIIA before presenting them to spectrum regulators. The framework ensures the inputs to the RIIA are based on standards-based methods, causality is ensured, and variabilities and uncertainties are quantified. This section serves to describe the blocks in Figure 8, and the following chapters will apply the framework to current spectrum service rule changes.

3.1.1. **Technical Architecture, (1)**

This item of the framework describes the detailed technical and operational uses of the spectrum. This item is a high-level description of historical and proposed (forward-looking) details of the spectrum landscape in terms of geographical, frequency, and power dimensions. For example, (hypothetical) broadcasters have used a band of spectrum for years; now, a proposed system will operate nationwide in the adjacent band on small area networks.

3.1.2. **Affected System Platforms, (2)**

This item of the framework is for descriptions and details of the spectrum-dependent systems. This item includes details on incumbent systems with location and operational details, including baseline performance metrics. New entrants to the spectrum (or systems seeking service rule changes) must provide detailed operational and deployment details. Continuing the hypothetical example from above: broadcasters have 1-megawatt transmitters, and the new entrant will have 100-milliwatt fixed systems operating indoors, and the adjacent band emissions may cause harm to set-top boxes in homes.

3.1.3. **KPIs, (3)**

Protection from interference from in-band and/or adjacent band emitters requires measuring system performance with and without the presence of other signals. KPIs are a system's response variables that are deemed descriptive of system performance. Some response variables are more valuable to end users (for example latency may be more critical than throughput), therefore, adding weights to those criteria aids in describing impacts during a spectrum coexistence test. Weighting KPIs is outside of the scope of this dissertation, but it is an effective way to differentiate service priorities across a variety of stakeholders.

3.1.4. **Spectrum Coexistence Testing, (4), (5), (6)**

When equipment is of a sufficient technical readiness level for testing, spectrum-dependent systems tested in conditions that emulate operational details is a necessary part of spectrum coexistence testing. When conducting such tests, there is a balance between the low controllability of field testing versus the high controllability of laboratory testing. Laboratory testing has increased flexibility at a lower cost to create varied and applicable spectrum conditions. Because of the externalities that exist in an outdoor RF propagation environment, measurements in the field are typically observational measurements from which causal inferences are difficult to make. By contrast, a well-designed laboratory coexistence test allows for exercising many more control factors in a repeatable (even automatable) way. MU is a metrology technique that quantifies a coexistence test bed's confidence in measuring small perturbations of measure. A high MU equates to a low confidence in values less than or equal to the testbed uncertainty. Best practice in measurement science is to identify MUs and seek to reduce them wherever feasible (e.g.

metrology grade connectors, cables, and test equipment). Variabilities are uncontrollable variations such as the changes in PL based on terrain and clutter.

This dissertation posits that a hybrid method of spectrum coexistence testing, which includes the insertion (when practicable) of field-collected phenomena into laboratory coexistence testing adds a realism otherwise challenging to obtain in a laboratory environment. The IAF recommends using the C63 with the addition of treating variabilities in the same manner as MUs. Regulators should support the ANSI C63 and contribute to the literature with use cases and lessons learned with the ANSI for improving both future sharing studies and the standard. Chapter 6 of this dissertation applies the IAF to a use case whose spectrum coexistence test results are taken from a test report that applied the C63 standard. These results include MU and actual system performance KPIs that are descriptive of the devices' performance metrics.

3.1.5. **Risk Informed Interference Assessment, (7)**

RIIA, is a useful way to assess, summarize, and communicate technical results to regulators. Overlaying results of likelihood of interference in a CCDF curve with areas of harmful interference is intuitive to the qualified expert working in the field of spectrum coexistence management. The IAF improves the inputs to the RIIA and recommends using the RIIA as it exists in the literature.

3.2. Methods

The IAF architecture developed for this dissertation came from identifying gaps in the literature from the definitions of harmful interference and interference measurements. Definitions of harmful interference should come from measurements that determine causal

performance degrading effects from another spectrum user. The information collected at the end of exercising the IAF (which includes the RIIA) provides a comprehensive suite of information useful to spectrum regulators for making informed decisions.

3.2.1. **Harmful Interference**

In this paper "interference" is used to describe causal and measurable effects[14] to a wireless system from another user of the spectrum. Interference is "harmful" when it causes a degradation in performance to other users of the spectrum. The ITU Radio Regulations define harmful interference as:

> *"[RF energy] which endangers the functioning of a radionavigation service or of other safety services or seriously degrades, obstructs, or repeatedly interrupts a radiocommunication service operating in accordance with [the ITU] Radio Regulations" [45].*

Wireless systems are subject to many externalities[15] that affect system performance outside of interference from others. For example, many factors affect propagation channels including weather, the radiation environment multipath, atmospherics, the specific use case. It is critical to identify and quantify the inherent effects on the wireless system in a baseline performance measurement. Only by understanding baseline performance and the variability in that performance can operators understand degraded system performance due to interference from neighboring or co-channel wireless systems (caused by man-made wireless systems) or parse out other unaccounted anomalous effects (other causal factors that affect wireless system performance).

[14] Measurable externalities quantifiable by a repeatable means using transparent, well-described methods.
[15] Examples include RF channel effects (e.g., clutter, multipath, doppler, satellite orbits).

3.2.2. **Interference Protection Criteria**

IPC act as a mechanism to protect licensed spectrum users. IPC serves as a definition of thresholds of values that cause harm to system performance objectives. The NTIA defines IPC as a relative or absolute interfering signal level defined at the receiver input, under specified conditions, such that the allowable performance degradation is not exceeded [76]. Communication systems that take advantage of spread spectrum technologies can operate with their intended signal below the thermal noise floor. Therefore, interference levels can be expressed relative to the intended signal or relative to the system's noise level. For example, given an absolute interference power level I, there exists an INR, or carrier-to-interfering signal power ratio (C/I). When including thermal noise (which is solely a function of temperature) and interference levels, the IPC figure of merit used is carrier to interference plus noise ratio, (CINR). A well-executed spectrum coexistence test reveals the effects of KPIs over a range of CINR measurements. IPCs are formulated and informed in ways, such as test and evaluation, simulation, historical works, or a combination of these. The IAF aims to present IPC based on scientific rigor through standards-based testing on performance-descriptive KPIs that consider MUs and confidence intervals.

3.2.3. **Variability and Uncertainty**

An MU is a quantity that limits the minimum measurable quantity and should be minimized in a coexistence test. Variability is the consideration of the ranges of a variable's possible values. Factors that affect the performance of a communication system are random processes and treating these values as single points is misleading. Much of the literature gives IPC in terms of one number, such as "INR > -6 dB", does not reveal INR is

probabilistic and is a continuum of values. Also, the inference signal type affects INR levels that causes harmful interference, a CW tone is different than a white gaussian noise (and LTE has many waveforms contained in its signaling). An example of variability is the range of SNR values measured by a satellite receiver, the signal level will vary because of a satellite's distance changing as it arcs across the sky and when emitting through ground clutter at low Earth angles. The IAF and C63 standard require reporting values with their associated variabilities and uncertainties. The IAF also demonstrates treating spectrum coexistence measures as distributions.

As noted in section 2.10, the two major types of uncertainty are type A and type B. Type A uncertainty is taken from measurements statistically analyzed and presented in a probability density function. Type B uncertainty is derived from an assumed distribution based on assumed information, or engineering judgment. Whether using engineering intuition or exhaustive measurements, it is important to consider some bounds of uncertainty to demonstrate confidence in data. Stating, for example, baseline conditions are $C/N_0 = (42 \pm 7)$ dB is more valuable to a decision maker than simply noting 42 dB. In this example, the "$\pm$7 dB" is the 95 % confidence range around the measurand, 42 dB. With this margin of uncertainty, the differences between 42 and 43 are within the noise of the uncertainty error and cannot be confidently stated. A measurand outside that uncertainty, such as 50 dB is confidently different than the 42 dB measurand.

In applying the IAF, this dissertation reveals how data-driven decisions improve when employing standards-based testing methods including variabilities and uncertainties associated with the measurands. The following two chapters demonstrate the effectiveness of the IAF by describing methods and results for gathering technical details of LTE,

applying MU to testbeds, and quantifying RF propagation variabilities. The IAF is then applied to a use case to demonstrate how the previous interference predictions could benefit from coexistence testing. The IAF will then be applied to a use case; outputting distributions of measurands needed by spectrum regulators; using standards-based test methods, the quantities presented are technically defensible.

4. METHODOLOGIES TO IMPROVE SPECTRUM COEXISTENCE DETERMINATIONS

In applying the IAF, to guide the inputs to a RIIA, the first component is defining the technical architectures and affected system platforms. The first three sections of this Chapter describe the details of the LTE system platform, item two from the IAF. The LTE methods are applied to the use case in Chapter 6. The ubiquitous commercial mobile broadband service waveform, LTE, has become the dominant 4G mobile broadband technology. This chapter also describes methods and the background of MU (item 5 of the IAF) and application examples of GUM techniques applied to predicting spectrum coexistence. Since LTE is a common spectrum dependent system in recent spectrum coexistence tests and feasibility studies, an understanding of its uplink and downlink behavior is required for technical background. The following methods will be used to describe those behaviors:

- Reproducing CSMAC P_{UE} curves
- Using eNB deployment details of existing LTE networks to predict cell coverage areas (cell radii).
    - Using PL models from the literature these eNB deployments can be converted to received power at a UE placed randomly in a coverage area.
    - Applying the received power at a test UE and LTE network parameters settings the UE output power (P_{UE}) can be predicted.

With an understanding of LTE UE uplink output powers, interference assessors have the information needed to better predict potential interference effects. The UE received power, RSRP is in an AWS-1 band and the resulting P_{UE} can be applied to comparable frequency bands with minimal error.

The first approach is to use eNB location datasets to determine distributions of cell site coverage, referred to as *cell radii*. With an understanding of cell radii distributions, an

approach is developed to calculate the PL to the edge using eHata propagation models. Finally, distributions predict the output power of UEs located at the edge needed to close the RF link using the LTE OLPC equation. These techniques are then plotted in CDFs to reproduce and update the CSMAC UE EIRP CDF curves from the literature.

The ANSI C63.27 spectrum coexistence testing standard requires the application of MU (items 4 and 5 of the IAF). This chapter describes MU as applied by metrologists and includes a Monte Carlo method for quantifying MU. This chapter then applies these MU methods to quantifying variabilities of PL values (item 6 of the IAF). Mapping the uncertainties and variabilities of RF powers and propagation distances will give spectrum regulators and stakeholders more insight into a RIIA.

4.1. Methods to Analyze of LTE Network Cell Tower (eNB) Deployments

LTE is the subject of many spectrum coexistence studies in the recent literature. As spectrum allocations and services of mobile broadband grows, LTE deployments are of increasing concern to incumbent spectrum users. For example, the DoD has had access to relatively large bandwidths of spectrum with few spectrum neighbors. Those times have passed; for example, after the AWS-3 auction, the DoD has spectrum commercial mobile broadband neighbors (with no guard band between the 1755 MHz to 1780 MHz LTE uplink and the 1780 MHz to 1850 MHz) at 1780 MHz. Understanding the effects of adjacent band LTE uplink to Defense Department assets requires LTE deployments and emissions details. This section proposes a method of using eNB location datasets and PL models to predict LTE downlink pathloss. Then assuming reciprocity of uplink versus downlink and LTE network settings the EIRP of a UE can be predicted. The results of the methods described

in this section are shown in section 5.1 of this paper. The methods for calculating eNB spacing and therefore cell radii are described in [46].

4.1.1. **eNB Location Datasets**

In [46], two eNB location datasets were used (i) data provided by a nation-wide mobile broadband service provider (referred to as provider data), (ii) the CSMAC *randomized real* cell tower database [17]. Provider dataset includes cell tower latitude versus longitude, antenna heights, for planned AWS-3 LTE macrocell deployments. For the purposes of developing the cell radii predictions and subsequent analyses, this section uses the coordinates (latitude and longitude) of current and future macro-cell eNB deployments and their anticipated or deployed antenna heights.

The eNB location data from the commercial carrier covers approximately 14 000 cell tower points in the United States, all in the AWS-3 band. The literature shows as of 2017, and there are an estimated 215,000 eNB cell tower sites across the continental United States. Although the AWS-3 eNB provider data set is limited in quantity, the data set spans a large number of land cover types (morphologies) and gives data across significant regions in the United States. The two eNB location datasets are categorized into three morphologies (rural, suburban, urban) using the National Land Cover Database (NLCD).

4.1.2. **Grouping eNB Locations into Morphologies**

eNBs deployment locations and densities are based on numbers of users that could be served. For example, in low population densities of people, eNBs are spaced farther apart because they service fewer users than a more densely populated region. These regions in geography are hereafter referred to as morphologies. A morphology here is a

classification of terrain, residential, or building density, which is used as a sorting technique. The motivations for sorting eNBs into morphologies allow for the application of different propagation models. For example, the extended Hata (eHata) PL models use rural, suburban, and urban morphologies.

The eNBs in the datasets used are grouped into three clutter categories (hereafter referred to as morphologies), a sorting needed for applying clutter loss to the propagation distributions. The propagation channel between eNB and UE is ground-to-ground which is highly dependent upon the clutter, such as ground cover, buildings, foliage. The set of clutter categories, or morphologies, are urban, suburban, and rural. These morphologies were determined by the NLCD methodology described in [46]. The NLCD land use categories are determined by using 30 m by 30 m squares across the entire United States land area. An eNB location and generalized coverage area which is defined here as the circle made by the cell radius. Once eNBs are sorted into their respective morphologies, a distance to cell edge distribution can be calculated using a nearest neighbor algorithm.

4.1.3. **Calculating Cell Radii**

Once eNBs locations are sorted into their respective morphologies, cell radii distributions are then calculated using half the distances between the nearest neighboring eNB. Cell radius is used to describe the radius of an assumed circular signal coverage area of a cell tower, as a representation of its coverage area. This circular coverage region does not account for antenna patterns or variations due to terrain. The calculations assumed coverage from the same provider did not overlap (on average, there is an equal likelihood a user would attach to either eNB in an overlapping coverage scenario). The cell radius of an eNB is assumed to only reach as far as the nearest neighbor's cell radius without overlap.

For example, if two towers are one kilometer apart, the cell radius of each tower is 500 m (no overlapping was considered in this paper). The distance calculation method used is known as the *nearest neighbor* calculation. Specific implementation details of this calculation are provided in [46].

The ball tree algorithm [47] computes the nearest neighbor for each cell tower. A ball tree is a binary tree in which each level of the tree contains a ball that contains a subset of five eNBs. On the first level of the tree, every point is contained in a single ball. The second level of the tree splits the ball into two and the algorithm then is used to determine which coordinates are closest to the centroid of each ball. An eNB's coordinates are assigned to a single ball. As the height of the tree increases, the number of balls increases, and the number of coordinates contained within each ball decreases. After the algorithm terminates, the Haversine distance between a subset of the coordinates contained within each ball is calculated.

Latitude and longitude in decimal degrees and absolute distance between each eNB is found using the Haversine formula, shown in Equation (4).

$$d = 2r\ arcsine\left(\sqrt{sin^2\left(\frac{\varphi_2 - \varphi_1}{2}\right) + cos(\varphi_1)cos(\varphi_2)sin^2\left(\frac{\lambda_2 - \lambda_1}{2}\right)}\right) \quad (4)$$

Where:

φ_1, φ_2 = latitude of points 1 and 2

λ_1, λ_2= longitude of points 1 and 2

d = distance (km)

r = Earth's radius (km), here 6371 km is used

4.1.4. **Applying Path Loss Models to Calculated Cell Radii (Translating RF Powers into Distances)**

Once cell radii distributions are understood, the distances to the edge of a cell, one can then produce distributions of downlink predictions per each morphology using a pathloss model. The simplest pathloss model is FSPL, which will be used in the results as a comparison. The FSPL model is a direct line-of-sight model and only factors in the radius of each cell. FSPL serves as an upper boundary condition. This model works well in areas dominated by direct line-of-sight propagation with no obstructions, weather, or terrain effects. When FSPL is used to calculate the PL of other environments, such as suburban and urban, the free space model consistently underestimates the eNB emissions, since the cell radii are small and thus closer together. As a result, the free-space model does not reflect real-world conditions. The FSPL equation is shown in Equation (5) from [48]. The FSPL model serves as a reasonable starting point and is often used to establish best-case propagation limits, considering it does not factor in propagation through terrain or obstacles.

$$L = 20 \cdot log_{10}\left(\frac{4\pi R}{\lambda}\right) \quad (5)$$

The eHata model is appropriate since it has clutter coefficients for loss that apply to three different morphologies (rural, suburban, and urban). Equations (6) through (12) show the eHata model across three morphologies [49]. The eHata model is appropriate for frequencies between 1500 MHz to 2000 MHz and can be used for smaller cell radii as are found in LTE network deployments [49].

Arguments for the Extended Hata-Okumura equations are as follows:

L =Median path loss (dB)

f = Frequency of transmission (MHz)

H_B = Base station antenna effective height (m)

d = Link distance (cell tower radii for the purposes of this research) (km)

H_M = Mobile station antenna effective height (m)

$a(H_m)$ = Mobile station antenna height correction factor for urban areas (dB)

$$a(H_m) = (1.1 \cdot log_{10}(f) + 0.7) \cdot min(10, H_M) - \left[(1.56 \cdot log_{10}(f) - 0.8) + max(0, 20 \cdot log_{10}\left(\frac{H_M}{10}\right)\right] \quad (6)$$

$$b(H_b) = \min\left(0, 20 \cdot log_{10}\left(\frac{H_B}{30}\right)\right) \quad (7)$$

- Case 1: $d \leq 0.04\ km$

$$L = 32.4 + 20 \cdot log_{10}(f) + 10 \cdot log_{10}\left(d^2 + \frac{(H_B + H_M)^2}{10^6}\right) \quad (8)$$

Case 2: $d \geq 0.1\ km$

- Sub-Case 1: Urban

$$L_{Urban} = 46.3 + 33.9 \cdot log_{10}(f) - 13.82 \cdot log_{10}\big(max(30, H_B)\big) + 44.9 - 6.55 \cdot log_{10}\big(max(30, H_B)\big) \cdot log_{10}(d) - a(H_M) - b(H_B) \quad (9)$$

- Sub-Case 2: Suburban

$$L_{Suburban} = L_{Urban} - 2 \cdot log_{10}\left(\frac{f}{28}\right)^2 - 5.4 \quad (10)$$

- Sub-Case 3: Rural

$$L_{Rural} = L_{Urban} - 4.78 \cdot \left(log_{10}(f)\right)^2 + 18.33 \cdot log_{10}(f) - 49.94 \quad (11)$$

- Case 3: $0.04\ km\ < d < 0.1\ km$

$$L = L(0.04) + \frac{log_{10}(d) - log_{10}(0.04)}{log_{10}(0.1) - log_{10}(0.04)} \cdot \left(L(0.1) - L(0.04)\right) \quad (12)$$

With PL distributions to the cell edge one can then find the UE uplink power distributions required to close an uplink connection to the eNB. These uplink power distributions would inform spectrum coexistence modelers with informed uplink UE_EIRP (hereafter referred to as P_{UE}) distributions that could be effective in calculating LTE network effects on an incumbent spectrum users' mission.

4.1.5. **Methods of Calculating P_{UE} Distributions**

This dissertation utilizes distributions of PL and the LTE OLPC equation (Equations (13) through (15)) to produce P_{UE} distributions. The PUE curves will be shown in cumulative distribution functions (CDF) to mimic the technique used in the CSMAC AWS-3 feasibility reports.

4.2. Methods to Translate Field Measurements of eNB Downlink Powers

For the IAF portion labelled “Variabilities”, field collected RF received power collections will demonstrate that PL models (especially FSPL) do not quantify the clutter losses. Four examples of data collected in the field will be analyzed to demonstrate the OTA variabilities associated with RF propagation.

4.2.1. **Field Test Measurement Examples**

Many PL models are predominantly a function of distance, but data collected in the field will demonstrate that terrain and clutter losses in ground to ground RF paths dominate the loss values. The four collected data sets are:

4.2.1.1 *Stationary measurement example*

This example is performed with test equipment parked along a road with line of sight view of a macrocell LTE eNB. Seventeen minutes of RSRP values will be collected to investigate the stationary variability of the eNB emissions. This data collection would reveal eNB variabilities over a long-term collection (10,200 data points). The LTE downlink power is measured using a Sanjole Wavejudge powered by a vehicle’s electrical power with a received antenna with 0 dBi of gain. The receiver antenna will collect 17 mins of downlink RF power to measure the variabilities of power detected from 1.6 km distance to the line-of-site eNB.

Figure 9, The data collection setup for a stationary data collection of an eNB output power.

4.2.1.2 *A walking test using a smartphone example*

This example is designed to collect RSRP versus Latitude and Longitude beginning at the base of an eNB and moving to a distance of 1.2 km in three different directions with a smartphone collecting serving cell RSRP values (these three different directions are to account for the eNB's antenna gain normalizing its effects). Capturing one RSRP point per second with a walking pace of 3 mph across the three walking paths (out and back) results in 5370 data points. The results section will plot the RSRP versus distance. Subtracting the suspected eNB EIRP will yield the PL versus distance for this rural environment. The path from eNB to receiving smartphone is line of sight with no obstructions. Figure 10 shows the aerial map of the smartphone's walking paths.

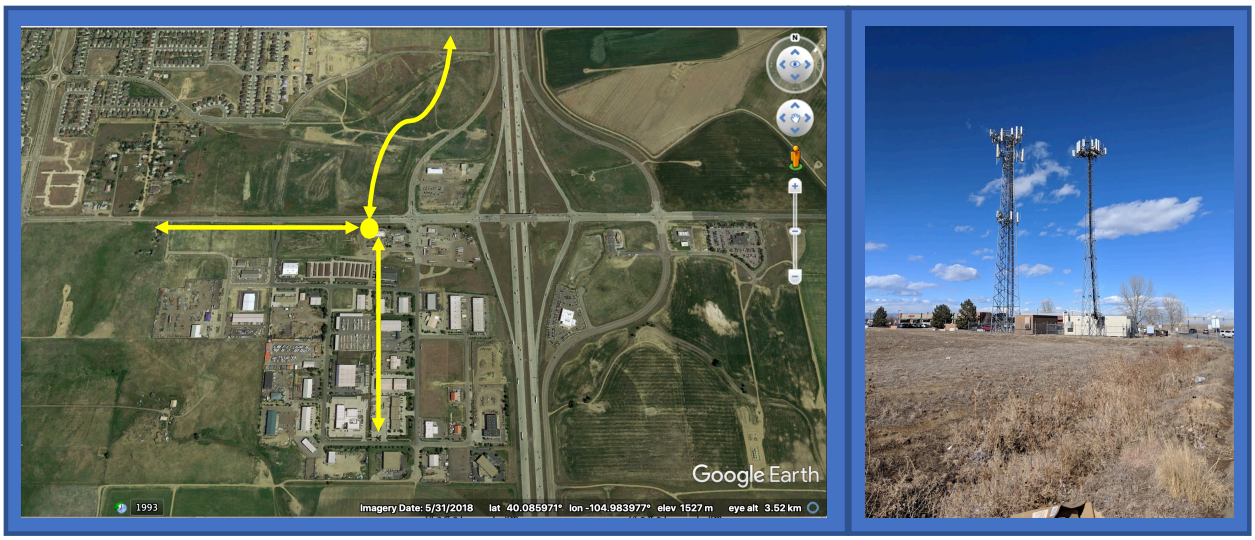

Figure 10, An aerial view of the walking paths in close proximity to an eNB using a smartphone to collect RSRP versus location data to measure path loss over distance and quantify the variabilities. Map provided by Google Earth.

4.2.1.3 *An urban walking test example*

This example uses a smartphone to collect RSRP versus Latitude and Longitude through an urban environment (Arlington, VA) with a smartphone collecting serving cell RSRP values while handing off to a few AWS-1 band eNBs. The goal of this walking test is to plot the RSRP values across the majority of the city, choosing routes with the most building clutter. Figure 11 shows the urban region where a walking data collection of RSRP will be collected. When walking through this area, the expectation is the smartphone will hand-over to more than one eNB. According to LTE protocols, the smartphone is continuously comparing signal strengths across eNBs that are within range. When a better link can be established to another eNB, the smartphone will transfer its RF link to that eNB.

Figure 11, An aerial view of the walking paths around an urban setting using a smartphone to collect RSRP versus location data to measure RSRP from the various AWS-1 eNBs in the area to quantify the variabilities. Map provided by Google Earth.

4.2.1.4 *Drive testing measurement campaigns performed by the NTIA ITS*

This example describes a measurement campaign performed by the NTIA ITS that demonstrates the widely varying PL values that occur when RF signals propagate through a variety of terrains, clutter categories, and atmospheric conditions. The rural drive test performed by NTIA ITS was to record PL measurements at Point Mugu in California. The propagation measurements were made with an attempt to control for many factors by using a constant output power, omnidirectional antennas, and a single frequency. A fixed[16] transmitter and a mobile receiver navigating a variety of roads were used. When driving

[16] A stationary transmitter location emitting one frequency (1780 MHz), emitting one power level (40 dBm), and using an omni-directional antenna. The receiving mobile antenna is omni-directional as well.

on the roads, the receiver's radial distance had overlaps; that is, multiple PL answers exist for the same distances. Received power from the fixed transmitter was collected at 1 second increments. The mobile receiver collected 8,678 points of received power and latitude/longitude position data (in dBm, in decimal degrees respectively). Absolute distance from the transmitting antenna was extracted from the latitude and longitude data.

This technique of grouping distances into 100 meter buckets is a method of treating PL as a distribution. PL distributions are more descriptive of how a wireless system behaves in an operational environment. Spectrum coexistence testing is concerned with power received from an unintentional source, finding that received power requires an understanding of the degradation of signals as they propagate through a channel (or path). Collecting field PL measurements reveals these PL distributions. Collecting measurements in this manner and treating the values as distributions gives the spectrum stakeholders and regulators valuable insight on how these systems will perform in their field deployments.

4.3. Methods to update the CSMAC UE EIRP Curves

As mentioned in the Literature Review, the methods for producing P_{UE} CDFs by the CSMAC were not revealed. With the LTE network assumptions, the CSMAC used in this dissertation will demonstrate a technique to reproduce those CDF curves. Then using eHata model predictions derived from actual eNB placements a recommendation is given of a method to calculate CSMAC UE EIRP CDFs. These UE CDF curves will then be further improved using field captures of eNB downlink powers (measured as RSRP) as seen by a UE. RSRP values are measured using a cell phone application called Network Cell Info available on the Android Platform (using a Samsung Galaxy Note 9), the application is pictured in Figure 12.

Figure 12, Screen capture of Network Cell Info application running on a Samsung Galaxy Note 9. The application is logging position (latitude and longitude) with RSRP.

The -61 dBm and -84 dBm values on the dials of Figure 12 are the RSRP values of the attached eNB and the neighboring eNB respectively. In the background, the smartphone's position (latitude versus longitude) and RSRP values are being logged into a comma separated value file (which also include eNB identifiers, time of day). The logged RSRP values will be converted into UE output power predictors (P_{UE}) and then used to reproduce or update the CSMAC P_{UE} CDFs using the LTE open loop power control (OLPC) equation, shown in Equations (13) through (15). Figure 13 describes the methods

for two sets of P_{UE} CDFs curve generating techniques with (a) using a fixed RSRP value to reproduce the CSMAC CDFs and (b) using field collected RSRP values to produce more real-world P_{UE} CDFs based on.

$$P_{UE} = P_0 + \alpha \cdot PL \tag{13}$$

$$P_{UE} = min(P_0 + \alpha \cdot PL, 23)\ dBm \tag{14}$$

$$P_{UE} = min\left(P_0 + \alpha \cdot \left(P_{eNB} - \left(RSRP - 10 \cdot log_{10}(600)\right)\right), 23\right)\ dBm \tag{15}$$

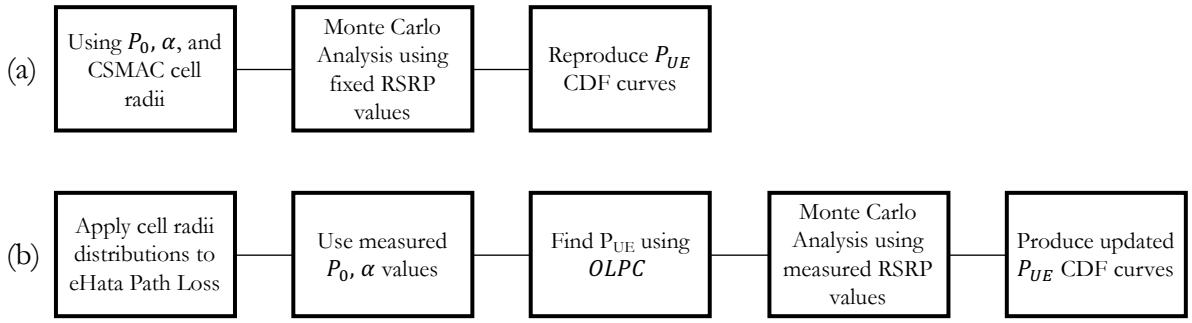

Figure 13, Methods for producing P_{UE} CDF curve (a) Reproducing CSMAC P_{UE} CDFs using CSMAC assumptions for cell radii, P0, α, using a fixed RSRP value which is used to represent average RSRP measured by a UE in a coverage area (b) an expansion of this technique using eHata path loss models, measured P_0 and α values, the OLPC equations, and measured RSRP values.

4.4. Calculating MU in Spectrum Coexistence Testing

The ANSI C63.27 describes methods for calculating MU in spectrum coexistence testing. MU is a well-defined science used by metrologists in their standards-based measurements [38]. To establish confidence in measurements, the IAF item 5 requires that all reported measurands include MU.

Finding sources of measurement uncertainty (in a test bed, field testing, and field deployments) is required for identifying, quantifying, and reporting confidence in measurement values in spectrum coexistence testing. On the subject of measurement science, in 1969 the National Bureau of Standards stated that "*a reported value whose accuracy is entirely unknown is worthless*" [44].

For completeness, quantifying and reporting MU is an important step for all measurement activities, including spectrum coexistence testing. Whether a test is over cables or in the field, as outlined in the C63.27, MU applies to all test methods listed in Table 6. Spectrum coexistence test reports should include:

- A list of the individual components used in testing and their associated individual uncertainty
- Values for the combined standard uncertainty of the measurement (which requires a measurement formula)
- A final expanded uncertainty value

A measurement formula for a series of RF components cascaded together is simply the sum of the parts used (when in logarithmic space); when a formula includes propagation, mixing components, and so forth, the calculations become more complex.

4.4.1. **Background Treatment for Measurement Uncertainty and Variability**

Measurements of spectrum phenomena, such as causal interference levels require an understanding of measurement science, or metrology. The process of measuring quantities is accompanied by measurement errors (capturing fixed point along a continuum of values in a random process) or nuisances (such as temperature drift or factors unaccounted for). Measurement process errors are the basic elements of uncertainty analysis. Once these fundamental error sources have been identified, we can begin to

develop uncertainty estimates. These estimates are important when making claims of precision or confidence in measurands (which, in the case of spectrum coexistence, are translated into spectrum service rule changes).

4.4.1.1 *Methods for Calculating Measurement Uncertainty*

Accuracy of spectrum coexistence test results depends on the ability to accurately measure (in the RF space) amplitude (or power), frequency, and time of the intended and *unintended*[17] signals. Standards-based testing methods will help achieve this end. Other measurements include the ability to accurately measure wireless performance[18] of the devices under test. Wireless performance metrics are described as key performance indicators in the parlance of this dissertation. The uncertainty of each of these metrics contributes to the final expanded uncertainty of a measurement. Data used to estimate performance metrics is represented as distributions that are based on either statistical or some type of non-statistical[19] information. To estimate the total uncertainty budget in a measurement result, each input is modeled and inserted into the measurement equation (denoted as Y) individually.

4.4.1.2 *Type-A Uncertainties*

Statistical models or summary statistics are used to describe each RF component and its range of values. Taking a series of measurements on an RF test component over many days in different environments will yield slightly different values. Describing the

[17] For simplicity, the general case of an incumbent wireless system operating in the presence of a new or proposed entrant to the spectrum is considered.

[18] The wireless performance is referred to as the functional wireless performance in the ANSI C63.27 standard.

[19] Such as engineering intuition.

range of those values in terms of mean (μ) and standard deviation (σ) will inform a MU budget. σ gives the typical absolute deviation between a random observation from the distribution and μ. Because taking measurements comes at a cost of time and other resources, a limited amount of data is used as a representative sample. From that limited sample, estimates of mean and standard deviation of the unknown parameters will be used. When MU data is collected from a test bed, sample mean ($\bar{X}$) and sample standard deviation (S) are used in MU budgets (where n is the sample number):

$$\bar{X} = \frac{1}{n}\sum_{i=1}^{n} X_i, \text{ and } S = \sqrt{\frac{\sum_{i=1}^{n}(X_i - \bar{X})^2}{n-1}} \quad (16)$$

When sample size is limited, $\bar{X}$ is an approximation for μ and each $(X_i - \bar{X})^2$ should be near $(X_i - \mu)^2$, the theoretical values based on σ. Averaging these values tends to even out any errors and makes S a good estimator for σ. The number of independent values of $(X_i - \bar{X})$ used to compute S is referred to as its *degrees of freedom*. *Standard uncertainty* (u_i) of $\bar{X}$ is a function of the number of sample measurements taken:

$$u_i = \frac{S}{\sqrt{n}} \quad (17)$$

which is frequently represented by $u(\bar{X})$, [50]. When cascading RF components together in a measurement test bed, the components' gain values sum together thusly:

$$Y = c_0 + c_1\bar{X}_1 + c_2\bar{X}_2 + \cdots \quad (18)$$

where Y is the test bed's measurement equation and coefficients c_i are linear constants. *Combined standard uncertainty* for Y is the square root of the sum of the squares:

$u_c = \sqrt{c_1^2 u_1^2 + c_2^2 u_2^2 \ldots}$, where u_i is the standard uncertainty of $\bar{X}_i$ *(19)*

Combining uncertainties for factors with nonlinear measurement equations (or factors that are not independent) is quantified by combining the squares of partial derivatives of measurement equation factors, as shown in Equation (20). The case where the measurement equation is a sum is a special case where partial derivatives are all equal to 1. The expanded formula is

$$Y = \bar{X}_1 + \bar{X}_2 - \bar{X}_3 \rightarrow \frac{\partial Y}{\partial \bar{X}_1} = 1, \frac{\partial Y}{\partial \bar{X}_2} = 1, \frac{\partial Y}{\partial \bar{X}_3} = -1 \quad (20)$$

$$u_Y = \sqrt{\left(1^2 u_{\bar{X}_1}^2 + 1^2 u_{\bar{X}_2}^2 + (-1)^2 u_{\bar{X}_3}^2\right)} = \sqrt{\left(u_{\bar{X}_1}^2 + u_{\bar{X}_2}^2 + u_{\bar{X}_3}^2\right)} \quad (21)$$

Nonlinear cases are out of scope of this thesis, and details for these treatments can be found in [44].

4.4.1.3 *Effective Degrees of Freedom*

Just as the degrees of freedom for each individual source of uncertainty indicate how much variability each uncertainty estimate has, the effective degrees of freedom of the combined standard uncertainty indicates its overall level of uncertainty. Low degrees of freedom (in the range $k = 0$ to $k = 4$) indicate that an uncertainty estimate is not very well known. The effective degrees of freedom, (ν_{eff}) for a combined uncertainty is calculated using the Welch-Satterthwaite formula [44]:

$$\nu_{eff} = \frac{u_Y^4}{\frac{c_{\bar{X}_1}^4 u_{\bar{X}_1}^4}{\nu_{\bar{X}_1}} + \frac{c_{\bar{X}_2}^4 u_{\bar{X}_2}^4}{\nu_{\bar{X}_2}} + \cdots} \quad (22)$$

The Welch-Satterthwaite formula is essentially a weighted average of the degrees of freedom of the individual standard uncertainties. The formula in Equations (20) through (22) works only when the values in the measurement equation Y are independent of one another.

4.4.1.4 *Expanded uncertainty*

A combined standard uncertainty quantifies how much a measurement result will typically deviate from the measurand. An expanded uncertainty quantifies how much a measurement result will deviate from the measurand with a high probability (for example, 95% or 99% are commonly used). The expanded uncertainty is the expected range around a value given a certain confidence level. The expanded uncertainty (U) is the product of the coverage factor (k) multiplied by the standard uncertainty. k is found using Student's t-distribution. Equation (23) shows the final result of the expanded uncertainty, Y.

$$Y = y \pm U \quad (23)$$

This final value, Y includes the measurand and $\pm$ the expanded uncertainty to a 95% confidence interval. The size of the expanded uncertainty relative to the measurand value indicates how reasonable the value is. For example, an IPC of INR = (-6 ± 10) dB means with a 95 % confidence, the INR is between -16 dB and 4 dB. This interval is a wide margin of uncertainty and the test results should be called into question. Final values with expanded uncertainties should be graphed with the measurand as a solid line and the MU

values in dashed lines. Another alternative is to plot the measurand with a line whose thickness spans the MU.

4.4.1.5 *Sample Calculation*

To demonstrate the application of the MU calculations and propose alternative methods, the test block diagram shown in Figure 14 will be analyzed in the results section of this paper.

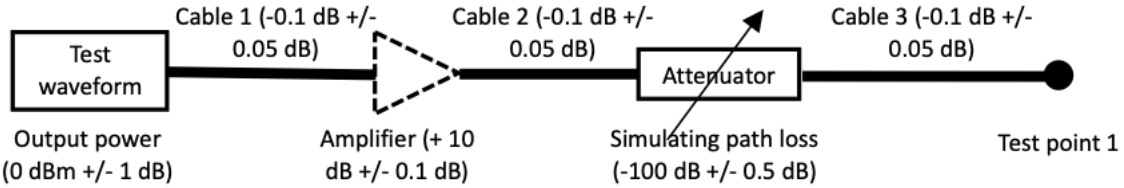

Figure 14. Example of an RF test path with an output stage (such as a signal generator) connected to an amplifier (gain stage), a variable attenuator (set to 100 dB). All losses, including cable losses, are assigned a measurement uncertainty value. The output is at test port 1.

$$P_{tp\_1} = 0\ \text{dBm} - 0.1\ \text{dB} + 10\ \text{dB} - 0.1\ \text{dB} - 100\ \text{dB} - 0.1\ \text{dB} = -90.3\ \text{dBm} \quad (24)$$

The simple cascaded gain formula is shown in Equation (24), and when in log-space (measured in dB) is the sum of the parts.

4.4.2. **Alternative Method Using Monte Carlo Simulations**

In this dissertation, the JCGM method of calculating MU will be compared to an alternative method. This alternative method will engage computational power to exercise the continuum of possible values across the measurement components' possible values using a Monte Carlo ("brute force") computational technique. Each component will be

treated as a distribution of values around its nominal value and the convolution of those distributions is the final value and its uncertainty.

If uncertainties and variabilities of the individual components are well defined, computational *for loops* can be applied to achieve an alternative method to the MU technique described above. A repeated for loop is referred to as a Monte Carlo method [51]. When repeating the possible output power of the RF test path in Figure 14 using the Monte Carlo method, the uncertainties therein are expressed in the following for loop (using MATLAB):

```
nsamp=1000;
for i=1:nsamp
  Pt= 0+(randn(-1 1))*0.5; %source power 0 dBm +/- 1
  G1= -0.1+(randn(-1 1))*0.05; %cable 1
  G2= 10+(randn(-1 1))*0.1; %gain stage
  G3= -0.1+(randn(-1 1))*0.05;%cable 2
  G4= -100+r(randn(-1 1))*0.1; %attenuator loss
  G5= -0.1+(randn(-1 1))*0.05;% cable 3
  Pr(i)=Pt+G1+G2+G3+G4+G5;%output power at test_point_1
end
```

Where P_t is the output of the 0 dBm source, G_n are the gains of the individual components (negative values when they represent losses), and P_r is the power at test point 1. The command “rand(1)” is a MATLAB function used to generate a uniformly distributed random number between 0 and 1. If the distributions were normal (Gaussian), then the command “randn(1)” would be used in its place.

The Monte Carlo method has an advantage of leveraging the relative low cost of computational energy afforded by low-cost computing. This method also allows the user to insert any type of distribution of for each component in the RF chain of components.

4.4.3. Treating Field Measurement Variability as an MU

This dissertation applies the MU techniques to the variabilities in propagation PL values. In a measurement that includes received power over a known distance is a case where antenna gains, transmit powers, and distances need to be well understood. When possible, a spectrum coexistence testbed should include RF propagation effects (also known as the *air interface*) as part of the wireless communications link, and link variations and uncertainties must be considered when using these data for spectrum coexistence determinations. To properly translate testbed measurements to field operations, variability in an RF link must be considered when evaluating spectrum coexistence testing.

4.4.4. Integrating Uncertainties into an RF Test Bed

An example of inserting field measurements, such as those collected in this paper, into an RF block diagram is shown in Figure 15. The cascaded RF gain through the circuit is the sum of the gains of the individual part, shown in Equation (25). In Chapter 5, the cascaded power through this circuit is plotted with PL represented as a distribution.

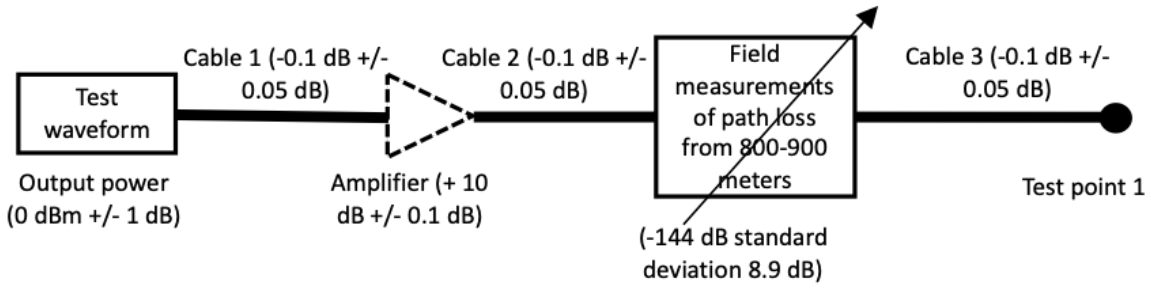

Figure 15. Example RF test path revisited with block of measured data

$$P_{tp\_1} = 0\ dBm - 0.1\ dB + 10\ dB - 0.1\ dB - 144\ dB - 0.1\ dB = -134\ dBm \quad (25)$$

Chapter 5 also contains the resulting plots of cell radii and PL distributions as applied to both (i) the carrier provided and (2) randomized real eNB location data sets. The regeneration of the CSMAC curves using RSRP CDF distributions is plotted with a sample of eNB variations. Then the RSRP distributions are used for predicting P_{UE} distributions. The RSRP arrays contain variabilities of the RF channel, therefore predicting UE output powers using field collected RSRP distributions also contains the variabilities of the RF channel because P_{UE} is monotonical derivation from RSRP.

In the results Chapter the Monte Carlo analysis technique (generated using MATLAB), produce MU and PL variabilities examples. The Monte Carlo results is applied to MU calculations form the GUM formulas. The results are provided in the form of PDFs, CDFs, and box plots.

4.5. Converting RF Powers to Stand-Off Distances

Item 6 in the IAF is labelled "propagation variabilities", this section proposes methods of quantifying variabilities using MU techniques to find stand-off distances with confidence regions. A method for comparing PL models to measured PL data is applied to a sample case using Figure 7, Impact of a 29 dBW Cellular Base Station Transmitting at 1530 MHz on a High Precision GPS/GNSS Receiver [76]. The FSPL model will be tested against other PL models and measured data to determine if the 14 km figure is supportable. Four models were taken from Philips et al. in "A Survey of Wireless Path Loss Prediction

and Coverage Mapping Methods" and plotted over the measured data described in subsection 4.2.1 [52]. Measured LTE power data captures are region-specific, capturing anomalies and variabilities over areas of clutter, terrain, and other RF signal impediments. In the use case for the IAF in Chapter 6, the stand-off distances recommended by GPS testing efforts will be revisited using the LTE downlink power measurements described in subsection 4.2.1.

4.6. Summary

This Chapter has provided methods for improving spectrum coexistence testing by using eNB datasets to predict LTE uplink and downlink powers, standards-based techniques for calculating MU and path loss variabilities. These methods are representative of what the IAF requires to provide science-based spectrum coexistence analyses suitable for regulators' decision-making processes. The following Chapter presents the results and analyses of the methods from Sections 4.1 to 4.5.

5. RESULTS AND ANALYSIS

In the IAF the *technical details* portion could include many types of spectrum-dependent systems. These systems can have standards that define their operating characteristics; for example, 4G LTE systems are described by the 3rd Generation Partnership Project (3GPP).[20] However, the 3GPP LTE system descriptions alone are not sufficient; many details are open ended and allow the carrier implementations dictate network details.

Deployment details from a carrier may also be required to assess interference effects. Carrier specific details are needed to describe cell tower lay-down densification – which will affect the uplink behavior. The LTE network technical details require thorough detail, well enough to craft a spectrum coexistence test method. CSMAC attempted to describe LTE laydown details in years 2012-2013, but these details change as new versions of LTE are released, or as users and features change. For example, since 2013 voice over LTE, VoLTE is a ubiquitous service. VoLTE uses a fewer number of LTE physical resource blocks than typical data transmissions and may have different interfering effects to incumbent spectrum users.

Section 5.1 will describe LTE deployment results and will provide plots of predictive LTE cell sizes (using cell radii) that better inform LTE network details for groups like CSMAC. These cell radii are then used to show PL model predictions using

[20] http://www.3gpp.org/

eHata model which groups PL clutter predictions into 3 morphologies which is more detailed than FSPL. Section 5.2 provides results of four OTA LTE downlink power captures. These downlink results are provided as distributions and grouped into likelihood plots. Section 5.3 provides results of reproducing and modifying the CSMAC LTE uplink (also referred to as UE EIRP curves) predictions. The methods allow for reproducing these curves to include updates to the deployment assumptions and network densities. Section 5.4 provides results of the LTE uplink predictions using the downlink measurements and LTE network assumptions. Both the uplink and downlink measurements and predictions are useful distributions for predicting interference effects from LTE deployments. Section 5.5 provides results of the MU formulas and a comparison between the GUM method to a Monte Carlo method.

5.1. Results and Analyses of LTE Network Cell Tower Deployments

5.1.1. Distributions from the eNB Location Datasets

Cell radii distributions results across randomized real (RR) and carrier provided (ProvData) datasets after sorting into rural, suburban, and urban morphologies.

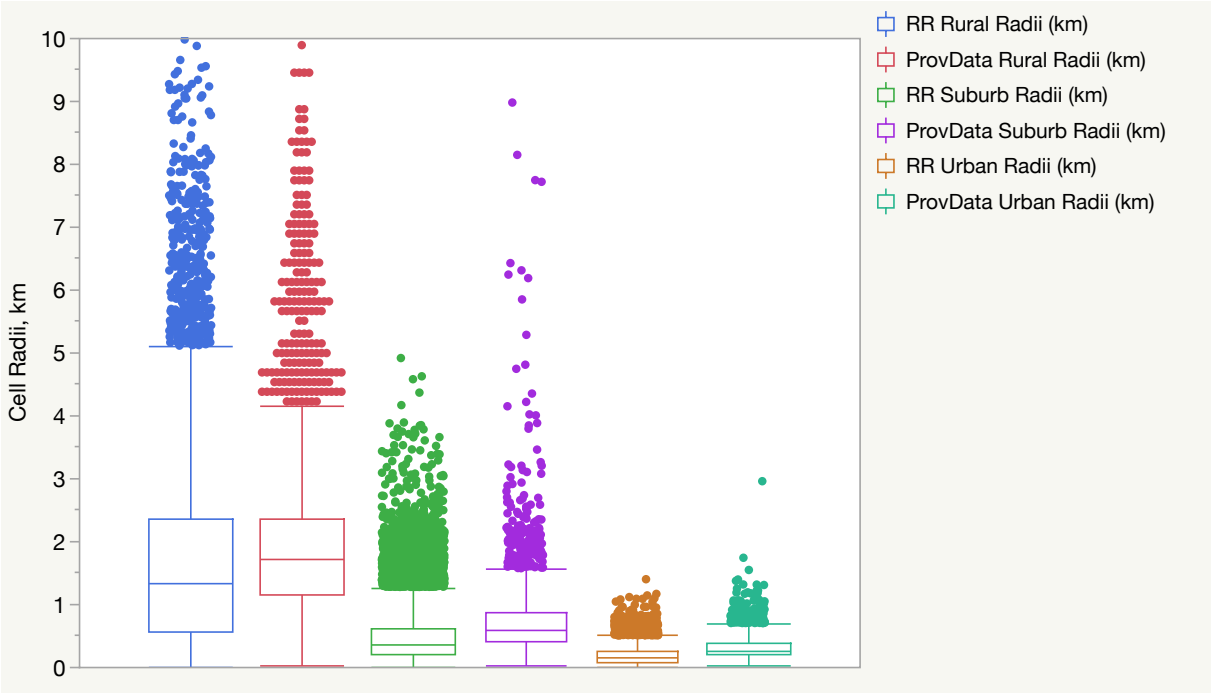

Figure 16, Box plots showing two datasets (Randomized Real (RR) and ProvData (data provided by a national carrier)) cell radii distributions across three morphologies (rural, suburban, and urban), in km.

The resulting boxplots in Figure 16 demonstrate the differences between the RR and ProvData datasets. The RR datasets was provided to CSMAC for LTE network analysis and the actual locations were obfuscated to protect their proprietary interests. Their obfuscation process is not in the literature and could have pushed many eNBs into different morphologies skewing the results of the sorting algorithm in an unknown direction. The ProvData is a list of absolute eNB locations and therefore the sites are in the actual morphologies and the sorting algorithm is more accurate. These cell radii distributions are similar between RR and ProvData and the trend that eNBs are closest together in an Urban setting and farthest away in rural meets the intuitive sense. CSMAC grouped urban and suburban results together for their analyses and the results from Figure 16 (summarized in

Table 7 with median values, $\tilde{x}$ and standard deviation, σ) show they are similar (all under 1 km radius).

Table 7, Summary statistics (median and standard deviation) from the bow plots in Figure 16.

Summary Statistics			
	Rural	Suburban	Urban
Median ($\tilde{x}$) and Standard Deviation (σ) of Cell Radii	Provider dataset: $\tilde{x}$ = 1.7 km, σ = 1.3 km Rand. Real dataset $\tilde{x}$ = 1.3 km, σ = 1.6 km	Provider dataset: $\tilde{x}$ = 0.84 km, σ = 0.53 km Rand. Real dataset $\tilde{x}$ = 0.36 km, σ = 0.41km	Provider dataset: $\tilde{x}$ = 0.38 km, σ = 0.18 km Rand. Real dataset $\tilde{x}$ = 0.15 km, σ = 0.13 km

With the cell radii distributions sorted into the three morphologies, applying the eHata PL equations to each distribution will produce distributions of PL to the cell edge of each point in the distributions.

5.1.1.1 *Applying Path Loss Models to Calculated Cell Radii (Translation of km to dB)*

Applying the cell radii distributions and the eHata equations, the following plots show the PL distributions to the cell edges across the three morphologies. Figure 17 shows the RR and ProvData eHata PL distributions and the median and standard deviations are summarized in Table 8.

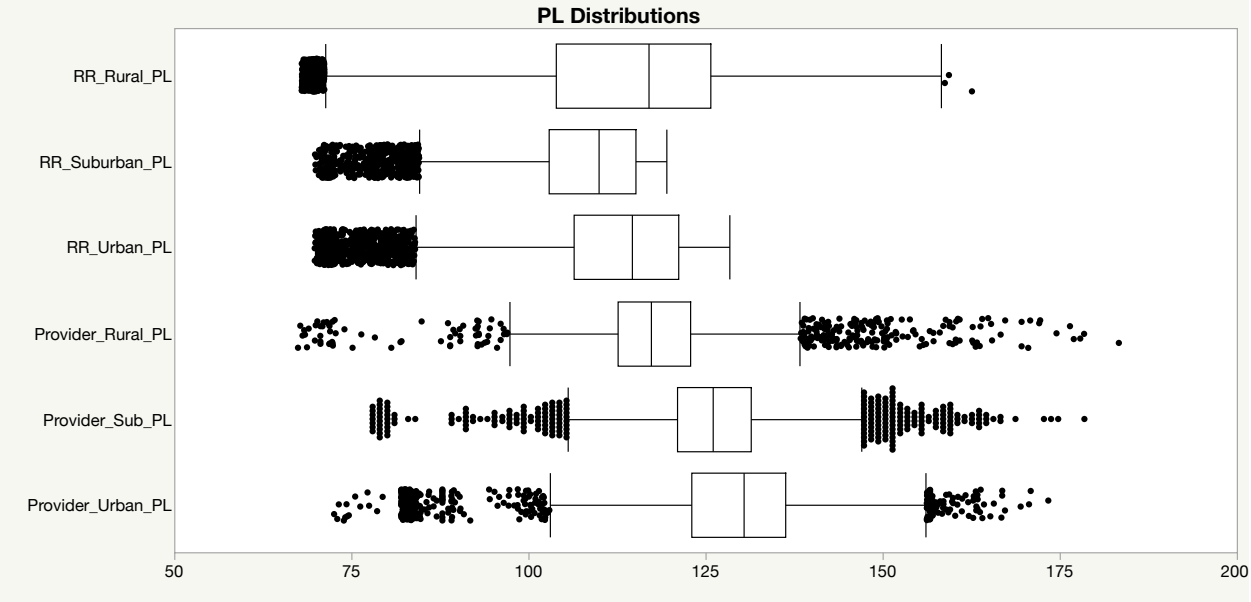

Figure 17, Box plots showing two datasets (Randomized Real (RR) and Provider (data provided by a national carrier)) path loss distributions across three morphologies (rural, suburban, and urban), in dB.

Table 8, Summary statistics (median and standard deviation) from the path loss distributions box plots in Figure 17.

Summary Statistics			
	Rural	Suburban	Urban
Median ($\tilde{x}$) and Standard Deviation (σ) of Path Loss	Provider dataset: $\tilde{x}$ = 117 dB, σ = 11 dB Rand. Real dataset $\tilde{x}$ = 117 dB, σ = 17 dB	Provider dataset: $\tilde{x}$ = 126 dB, σ = 10 dB Rand. Real dataset $\tilde{x}$ = 112 dB, σ = 10 dB	Provider dataset: $\tilde{x}$ = 130 dB, σ = 15 dB Rand. Real dataset $\tilde{x}$ = 117 dB, σ = 14 dB

5.1.1.2 *Applying the OLPC equation to the path loss distributions to predict P_{UE}*

One interesting observation is the compression in the differences across the datasets and morphologies. The median cell radii deviate by more than ten-fold (from 0.13 km to 1.6 km), however, the median PL deviation is approximately 15 dB (from 115 dB to 130 dB). The log of the ratio of the distances of 0.13 km and 1.6 km is ~11 dB the difference between the 15 dB and the 11 dB figures can be explained by the loss terms the eHata model differning from real-world clutter. Since LTE network planning is designed to provide similar SNRs to it users regardless of morphology, it makes intuitive sense that the median PLs are similar.

5.1.2. **LTE Received Power Measurements**

The calculations in section 5.1 are all predictions using an eHata PL which accounts for clutter categories, were taken from mobile testing (in Japan, [53]). Although these measurements include urban building or residential housing clutter, they are not necessarily applicable to an area of sharing interest by spectrum stakeholders. The observation is: if spectrum sharing is a multibillion-dollar decision, performing drive testing and mobile measurements are worth the time and effort.

5.2. Results in Translating Field Measurements of Downlink Powers

This section provides the results of the field measurement collection efforts performed for this dissertation. The following four examples of spectrum received powers demonstrate how variability of RF paths. The first example is a stationary LTE eNB measurement of downlink power using a Sanjole Wavejudge LTE protocol analyzer.

5.2.1. **Field measurements examples**

5.2.1.1 *Stationary Measurement*

The first measurement was performed using a Sanjole Wavejudge connected to a stationary vehicle's power supply with a short 0 dBi gain monopole antenna in view of an eNB. The measurement system was parked 1.6 km away from the eNB under test and 17 minutes of data was recorded. There was no building clutter between the eNB and the Sanjole's receiving antenna. However, there are dips in the eNB power from 10 dB to 18 dB that are from vehicle traffic driving between the eNB and the receiving antenna. Figure 18 shows the RSRP versus time plot of the data collection.

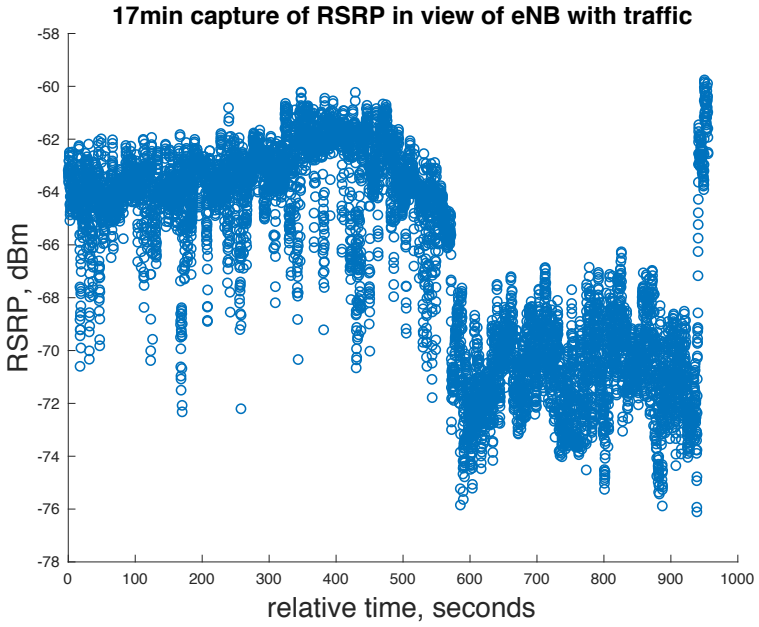

Figure 18, 17 minutes collection of RSRP values from a stationary position demonstrating the variability from a non-mobile ground to ground RF propagation channel.

There are short time dips in eNB power from 500 seconds to 950 seconds. These power fades correspond to vehicular traffic on the road between the eNB and the Sanjole Wavejudge receiving antenna. A 60 foot truck takes approximately 1.2 seconds to pass by the receiving antenna and the observed dips in power are approximately that duration.

5.2.1.2 *Walking test under an LTE macrocell*

The second measurement is a walking test using a smartphone to collect RSRP, beginning at the base of the eNB in a rural environment. The eNB is approximately 60 feet tall and the walking paths were intended to be in the main lobes of the eNB's sector antenna elements (while remaining safely on the roads). The walking path had no building or vehicle clutter between the receiving smartphone and eNB. The data was collected using the Network Cell Info app and points were collected at a rate of one per second. Figure 19, (a) is a plot of the raw data from the walking data collection from 0 km to 1 km from an eNB, overlaid on this plot is the predictions from FSPL and eHata model for a rural morphology. (b) is the same data converted to path loss and bucketized into 100 meter distributions.

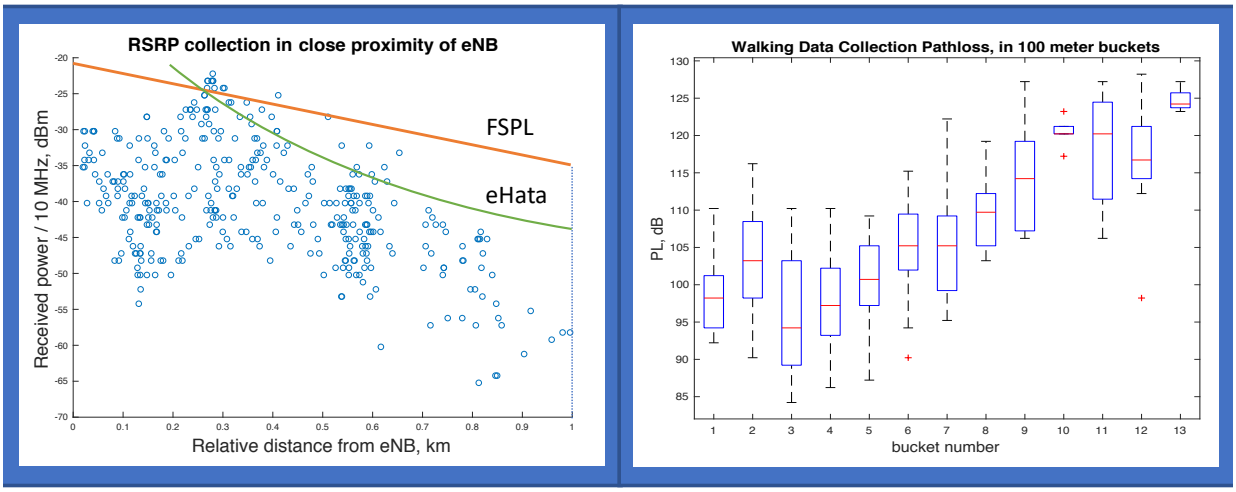

Figure 19, (a) is a plot of the raw data from the walking data collection from 0 km to 1 km from an eNB, overlaid on this plot is the predictions from FSPL and eHata model for a rural morphology. (b) is the same data converted to path loss and bucketized into 100 meter distributions.

From Figure 19, the FSPL and eHata overpredict the received power by the smartphone. Tracing up any one distance value has many answers (dots in the raw data) for received power. For example, at 500 meters, the RSRP has results from approximately -55 dBm to -30 dBm, a difference of 25 dB.

Another observation when inspecting the raw data is the RSRP values rise between 200 meters and 300 meters. Intuitively, received power should decrease when distance increases. The likely explanation for this rise in power as distances increases is because of the shape of the eNB antenna lobes. Directly under the eNB is not in the main lobe of the eNB sector antenna. This is a reasonable observation (not confirmed with antenna pattern details as this is an observational study, not an antenna characterization study) because this eNB was placed here to offer wireless services to people using the surrounding roadways.

Offering wireless service to the roads behooves the carriers and directing the antennas' main lobes to those roadways would serve that purpose.

The second plot in Figure 19 is a plot of the raw RSRP converting to PL data using 62dBm (the assumed EIRP of the eNB) minus the PL values. The data is grouped into 100-meter buckets and displayed as box and whisker plots. The box plots extend out to 1.3 km. The medians are shown as a red stripe and the boxes contain the inner two quartiles and the whiskers extend to 95% of the data. Red plus signs show outliers beyond the 95%. The box plots give a visual representation of the PL distributions a UE or spectrum stakeholder may utilize to predict interference effects.

Through the box plots, Figure 19 (b) demonstrates that knowing the likelihood of received power is more useful than using PL models. This technique is repeated in the next subsection in an urban morphology.

5.2.1.3 *Walking through an urban area attaching to many eNBs*

The third measurement is a walking test around Arlington, VA in an urban environment. The Network Cell Info application was used on a smartphone to collect RSRP and latitude and longitude data at intervals of one second per data point. A total of 11387 points were collected. Throughout the walking path, the smartphone used to collect RSRP data attached to fourteen eNBs. All of these eNBs were installed by Verizon Wireless and the phone was locked to Verizon Wireless service and the AWS-1 band. Figure 20 is a plot showing RSRP distributions using box and whisker plots versus eNB. The eNBs are shown as physical cell identifiers. Across the fourteen eNBs, the median RSRP values vary from approximately -105 dBm to -75 dBm. The precise locations of the eNBs in this walking path was not known, so a plot of the PL versus distance is not calculable.

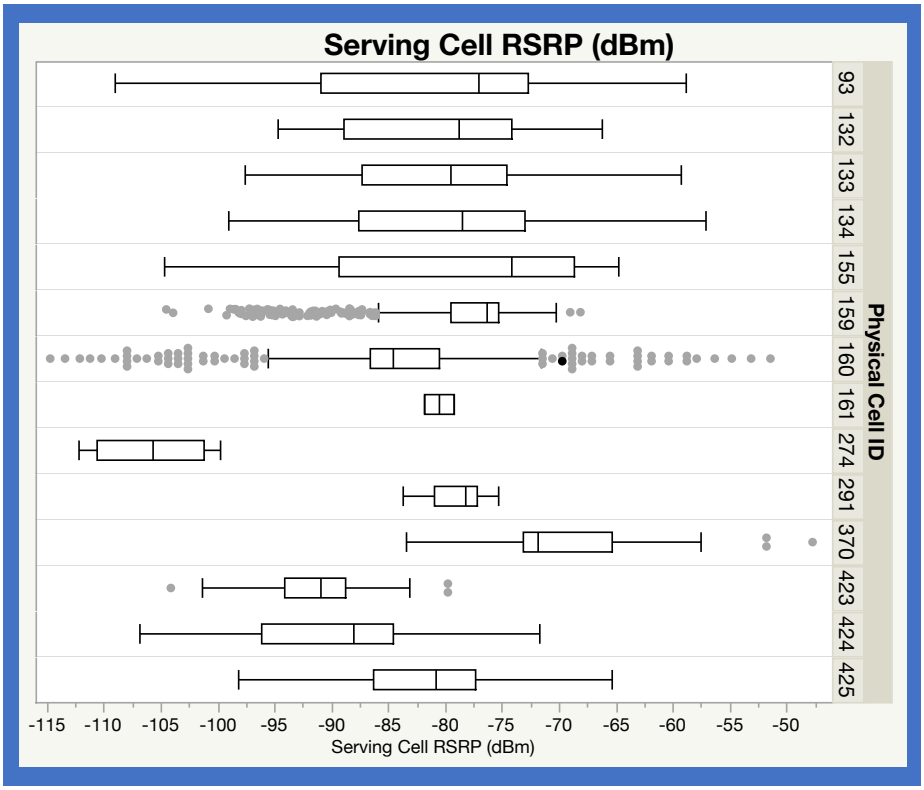

Figure 20, RSRP distributions versus serving cell.

This urban walking path had building and vehicle clutter between the receiving smartphone and each attached eNB. The decision for the smartphone to hand-over to a different eNB is made at the eNB and RSRP levels drives that decision. The map of the RSRP levels versus geolocation is shown in Figure 21, Histogram and map of Urban walking RSRP collection. The histogram is a representation of the entire raw data set across the fourteen eNBs, the map shows the NLCD clutter category and the colors of the walking path is color coded to show RSRP values. The majority of the NLCD color codes shows urban high intensity, with regions of low intensity as well. The low intensity corresponds to lower RSRP values.

This urban data collection was in a region approximately 6 square kilometers. Using the Ball tree nearest neighbor algorithm, the fourteen eNBs have a median cell radius of 0.3 km, which is indicative of the values described in subsection 5.1 of this paper. The NLCD color codes verify the morphology for these RSRP data is in an urban environment.

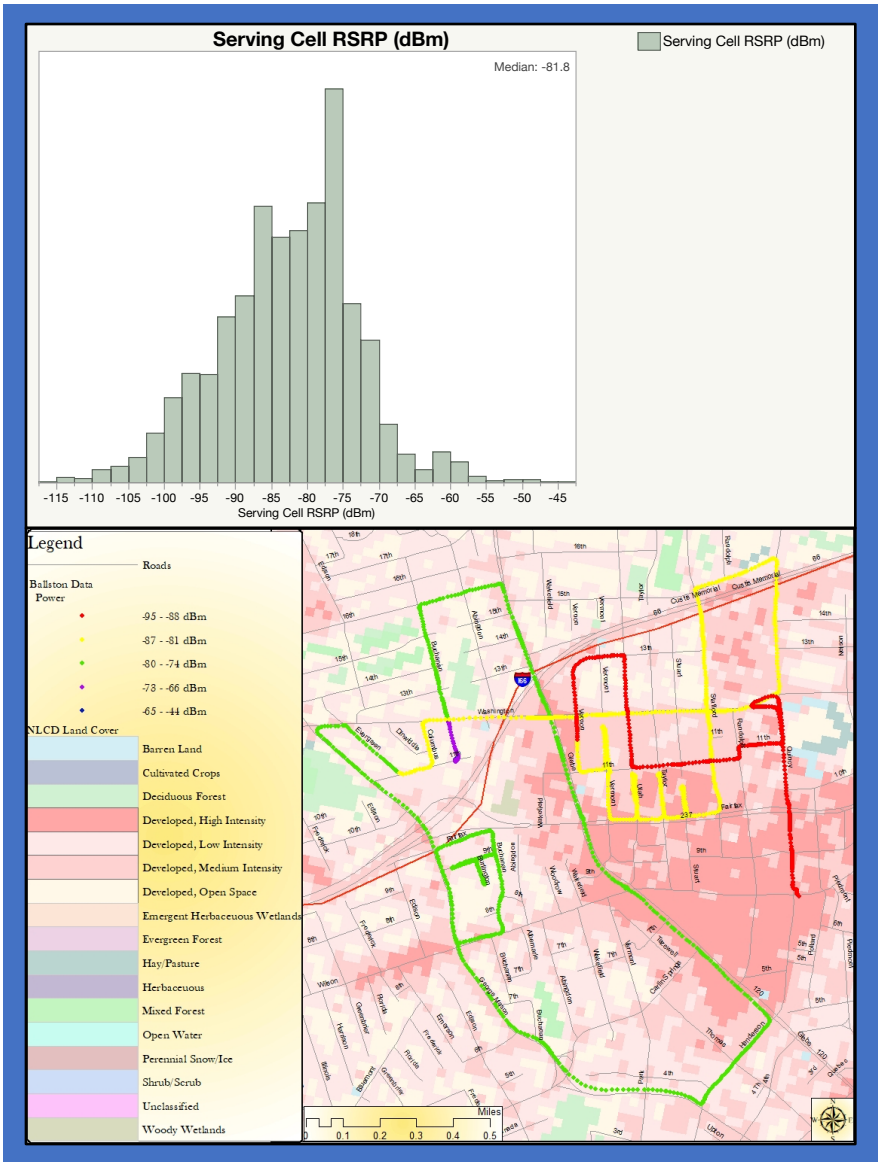

Figure 21, Histogram and map of Urban walking RSRP collection. The histogram is a representation of the entire raw data set across the fourteen eNBs, the map shows the NLCD clutter category and the colors of the walking path is color coded to show RSRP values.

5.2.1.4 *Drive test using NTIA ITS data*

The fourth PL measurement is a driving test around Point Mugu, CA, in a rural environment. This drive test attempted to control for RF emissions, antenna effects, and frequency. Even when holding those factors constant, the signals (and therefore resulting PL predictions) have a wide variability.

The propagation measurements were made with an attempt to control for many factors by using a constant output power, omnidirectional antennas, and a single frequency. A fixed[21] transmitter and a mobile receiver navigating a variety of roads were used. When driving on the roads, the receiver's radial distance had overlaps; that is, multiple PL values exist for the same distances. Received power from the fixed transmitter was collected at 1-second increments. At the mobile receiver, 8,678 points of received power with position data were collected in the form of dBm, latitude, and longitude values (in decimal degrees). The latitude and longitude measurements were converted to absolute distance from the fixed 10-watt transmitter.

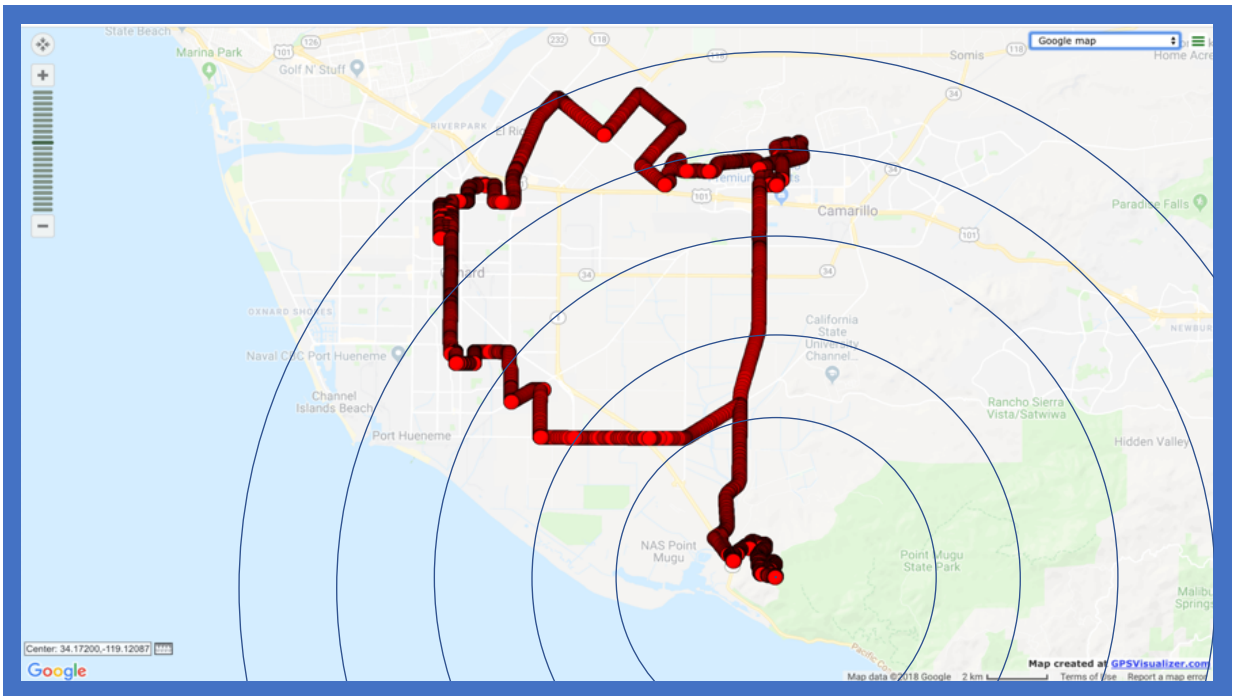

Figure 22, NTIA ITS drive test in a rural environment. The concentric rings show that there are frequently more than one location that has the same radius from the transmitter. These data are unpublished collections from ITS and were provided for this paper by ITS staff.

Figure 22, NTIA ITS drive test in a rural environment. The concentric rings show that there are frequently more than one location that has the same radius from the transmitter. These data are unpublished collections from ITS and were provided for this paper by ITS staff. shows a map of the rural data collection drive path contains rings at 3 km, 5 km, 7 km, 9 km, and 11 km distances from the transmitter for illustration of how radial distances can have many points of PL measured at different locations. For example, the 5 km arc intersects the driving path at points northwest and north of the transmitter. The drive path navigated through neighborhoods of flat terrain that is considered rural (i.e., no structures above one story tall).

To visualize the collected data, Figure 23 Path loss measurements from NTIA ITS in rural environment (a) raw data from 0 km to 18 km and (b) bucketized into 100 meter buckets from 1 km to 4.2 km. shows both a scatterplot of the raw (a) and box plots of bucketized (b) PL data. In Figure 23b, the data were segmented (bucketized) into 100-meter buckets and a box plot for each bucket is displayed. Bucket 1 is from 100 meters to 200 meters, bucket 2 is 200 meters to 300 meters, and so on. The rectangles of the box plot hold the middle two quartiles of the 100-meter bucket and the red line is the median value. The whiskers in the box plots display the outer two quartiles to 95%. Outliers beyond that are shown as red plus signs (+). The bucketized representation is truncated to 42 buckets and not shown out to the entire 18 km of data collection.

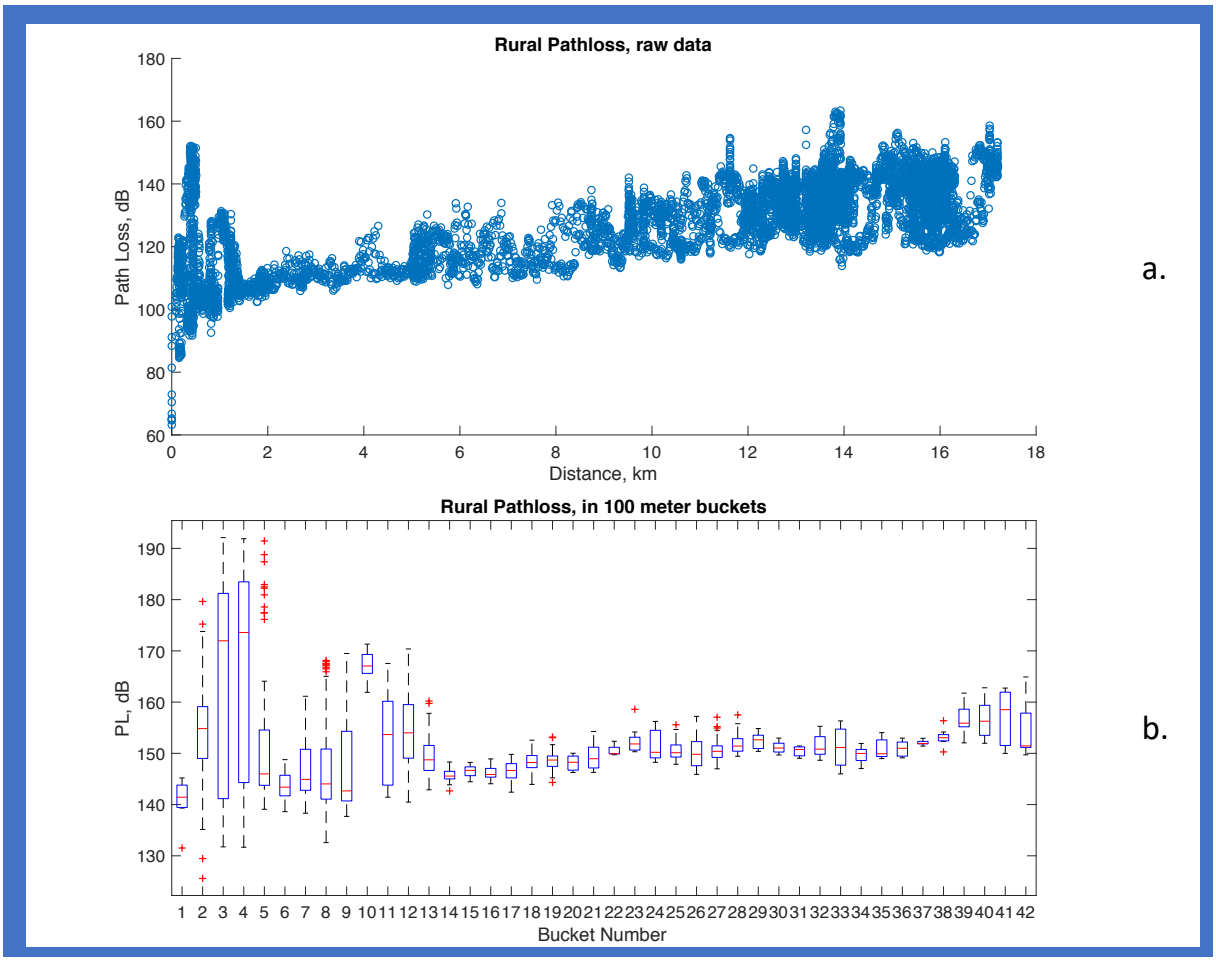

Figure 23 Path loss measurements from NTIA ITS in rural environment (a) raw data from 0 km to 18 km and (b) bucketized into 100 meter buckets from 1 km to 4.2 km.

The technique of grouping distances into 100-meter buckets is a method of treating PL as a distribution. These distributions are more descriptive of how a wireless system behaves in an operational environment. Spectrum coexistence testing is concerned with power received from an unintentional source, finding that received power requires an understanding of the degradation of signals as they propagate through a channel (or path). Collecting field measurements reveals these PL distributions. Treating the field

measurement values as distributions gives the spectrum stakeholders and regulators valuable insight on how these systems will perform in their field deployments.

These four spectrum data collection efforts and their analyses demonstrate the risk of translating results from a well-controlled spectrum coexistence test (that accounts for MU and variability) to an actual RF environment. The RF environment has more variability than what is represented when using a PL prediction model. In spectrum coexistence determinations, operational considerations also need to be accounted for.

5.3. Updates to the CSMAC UE EIRP Curves

In the previous section of this Chapter, LTE downlink powers were collected using RSRP measurements from smartphones. These methods are appropriate in the case of interference predictions involving eNB emissions. When predicting UE emissions, such as how CSMAC did use UE EIRP CDF curves, the recommend approach is to use the OLPC and cell radii distributions.

The CSMAC WG1 report (during the AWS-3 auction planning stage) presented UE EIRP curves shown in Figure 24, from [16] to predict interference to incumbent spectrum stakeholders from LTE uplink emissions. These analyses by the CSMAC predicted interference effects to these incumbent users if the AWS-3 Auction 97 were to move forward. The output power distributions for the LTE UEs (P_{UE} predictions) were displayed in a CDF and the methods for their generation were not explained. In this section, a Monte Carlo method using the median P_{UE} values and the same LTE network assumptions were used to reproduce and update using RSRP data collections.

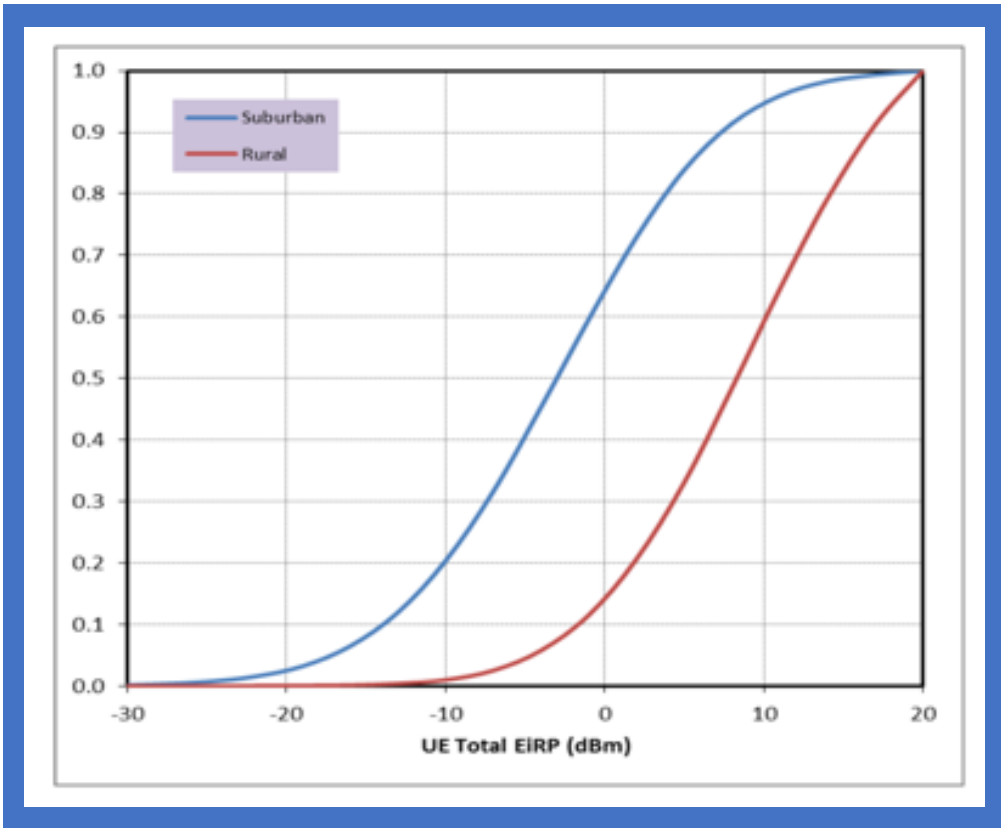

Figure 24, CSMAC UE EIRP CDF curves used to predict UE output powers that incumbent spectrum users may encounter, from [16].

5.3.1. **Reproducing the CSMAC curves for LTE UE EIRP**

By using the 0.5 (mean) points in the CDF of Figure 24 for the rural red curve (7 dBm) and for the urban/suburban blue curve (-4 dBm). Using equation (3) the downlink RSRP is calculated in Equation (26), where RSRP = -87 dBm.

By inspection, the median P_{UE} for rural (with a P_0 = - 90 dBm, 10 MHz = 600 resource elements (9 MHz / 15 kHz), and α = 0.9), the corresponding RSRP value

measured to produce such a PUE is calculated with the LTE OLPC equation, shown in Equation (26).

$$P_{UE} = P_0 + \alpha * (PL) \rightarrow 7dBm \quad (26)$$
$$= -90 + 0.9 * (62\ dBm - 10$$
$$* log(600\ resource\ elements) - RSRP)$$

$$\boldsymbol{RSRP = -87\ dBm}$$

By inspection, the median P_{UE} for suburban and urban (also with LTE network assumptions of: P_0 = - 90 dBm, 10 MHz = 600 resource elements (9 MHz / 15 kHz), and α = 0.9), the corresponding RSRP value measured to produce such a P_{UE} is calculated in Equation (27), where RSRP = -73 dBm.

$$P_{UE} = P_0 + \alpha * (PL) \rightarrow -4\ dBm \quad (27)$$
$$= -90 + 0.9 * (62\ dBm - 10$$
$$* log(600\ resource\ elements) - RSRP)$$

$$\boldsymbol{RSRP = -73\ dBm}$$

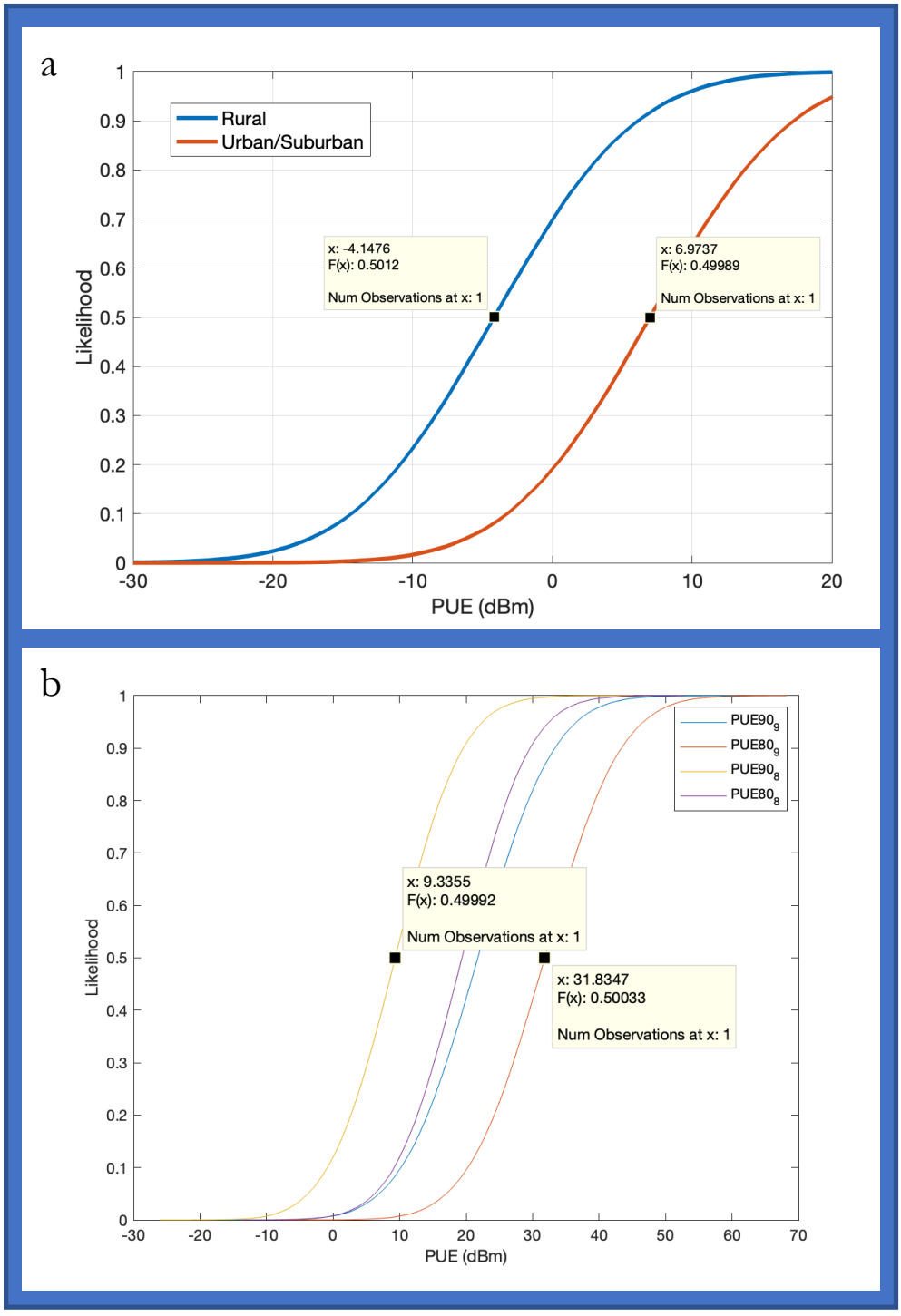

Figure 25, (a) Output of Monte Carlo simulation of RSRP values set to median for two morphologies, iterated +/- 10 dB over 10 000 trails. (b) Output of Monte Carlo simulations of RSRP values set to median for two morphologies, iterated +/- 10 dB over 10 000 trails, the P0 and alpha are set to (-90, 0.9), (-80, 0.9), (-90, 0.9), (-80, 0.8).

The results from Equations (26) and (27) are the median RSRP a UE will measure in rural and urban/suburban settings (-87 dBm and – 73 dBm respectively). Using these calculated median P_{UE} values, the Monte Carlo method to reproduce the "CSMAC UE EIRP CDFs" results are shown in Figure 24 by using the median RSRP values iterated +/- 10 dB using a Monte Carlo loop with 10,000 trials. Figure 25 (a) shows the reproduction on the CSMAC curves using Gaussian distributions of RSRP predictions.

To demonstrate the effects of the P_0 and α assumptions, Figure 25(b) shows the P_{UE} distribution sensitivity using the same Monte Carlo method across for LTE network values. The movement of the P_{UE} curves are a function of the open loop power formula terms, their effects are visible in this plot. For better insight of the EIRP output powers needed to close the UE—to—eNB link, the CDFs are allowed to drift past the 23 dBm maximum output power of the UE. In practice, however a UE's output power is capped at 23 dBm.

Table 9, Summary of the median values from Figure 25(b) across four combinations of P_0 and α.

P0	α	Median UE EIRP
-90 dBm	0.9	9.3 dBm
-80 dBm	0.9	12 dBm
-90 dBm	0.8	19 dBm
-80 dBm	0.8	> 23 dBm

Table 9 shows that a 10 dB difference in P_0 corresponds to a 3 dB difference in median P_{UE}, and a 0.1 difference in α corresponds to an approximately 10 dB difference in median P_{UE}. Therefore, P_{UE} prediction are most sensitive to the assumption of α and less

sensitive to the P_0 assumptions. α is a scaling factor of the PL which varies from 0.8 to 0.9 (or 10% to 20%) and P_0 varying from -80 dBm to -90 dBm is a factor of 10. Hence the PUE predictions are more sensitive to the changes in P_0.

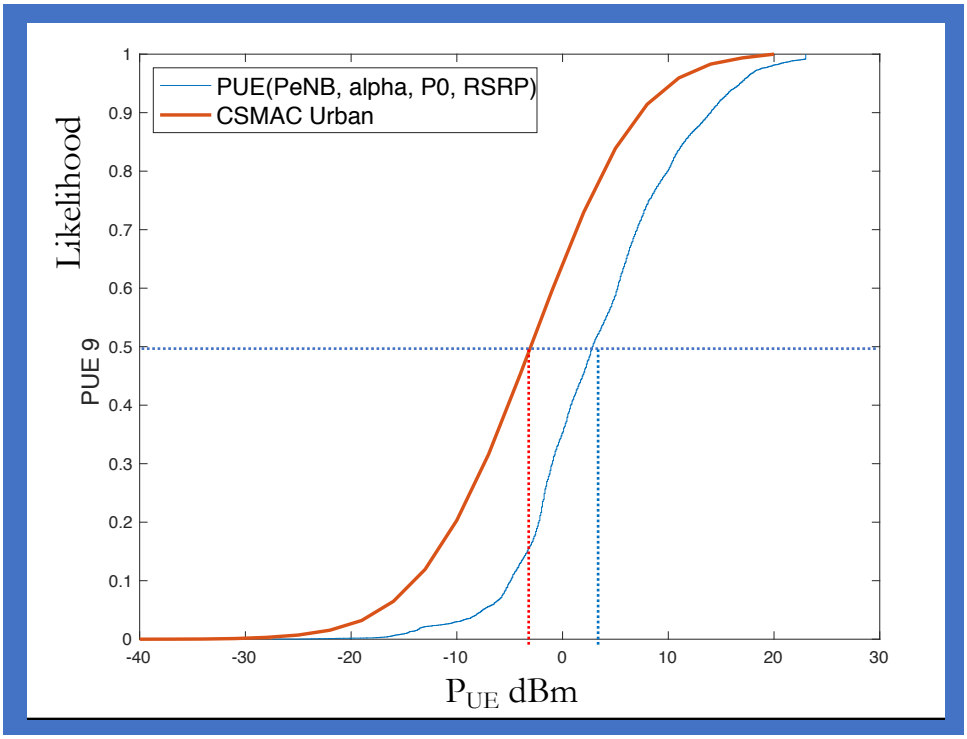

Figure 26, The CDFs of CSMAC Urban versus the calculated CDF of RSRP values using the Arlington, VA RSRP data collections inserted into the open loop power control equation.

5.4. Using Measured RSRP Data to Produce UE EIRP (or P_{UE}) Distributions

The CSMAC curves were reproduced in Figure 25(a) using the Mote Carlo method and the median P_{UE} values from the CSMAC literature. An alternative method is to use field collected RSRP arrays to create P_{UE} CDFs. In this section an urban example is used to test the method. Using the RSRP data collection while walking through the urban area

of Arlington, Virginia results are shown in Figure 21. This data collection is across many eNBs and yields a better understanding of the spectrum users' emissive behavior when in this urban region.

Using the combined RSRP for the entire Arlington, VA walking route, the RSRP distribution has a median value of -81 dBm with peak values in the mid -40 dBm range (this will become important when considering likelihoods of interference). The array of collected RSRP (considered urban/suburban morphology) distribution was inserted in to the LTE OLPC equation (as described in Figure 13) to produce the P_{UE} distribution in Figure 26 which is displayed in CDF form and plotted (in blue) with the CSMAC CDF curve (in red) from Figure 24. The CDF curve was produced using the MATLAB® ECDF function. The CDF has the same general shape as the CSMAC Urban CDF curve, but is offset by approximately 6 dB. For example, a P_0 = -90 dBm was used to produce this curve, but the actual value may have been -80 dBm. This offset is likely explained by the eNB LTE network settings. This P_{UE} distribution is measured and then calculated off a real deployed LTE network. Acquiring the LTE network's settings from the commercial carrier could help with producing uplink power predictions. If the P_{UE} curves are expressed in terms of path loss predictions and the UE is equally likely to be in a cell from 100 meters to cell radius (the cell radius is a distribution). Then the PUE predictions are expressed as a CDF whose thickness expresses a uniform distribution of possibilities, shown in

Figure 27.

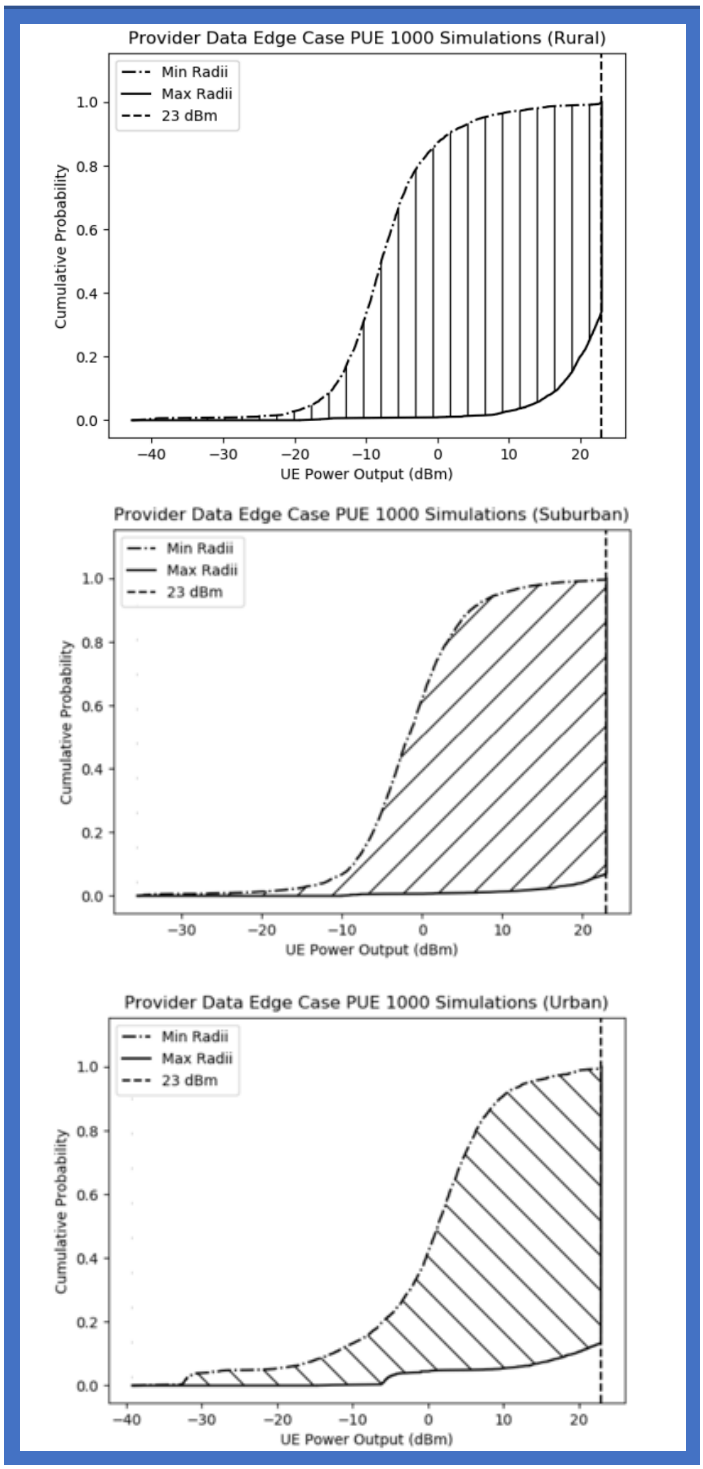

Figure 27, The continuum of P_{UE} values across all locations with an LTE cell.

5.4.1. **Summary**

If an incumbent spectrum user or spectrum regulator wishes to understand better the impacts of a spectrum service rule change or a new spectrum user accessing the spectrum, techniques such as these can yield insight to the behaviors of those new entrants. Collecting field measurement observational data can be used to answer the questions of spectrum users' emissive behavior. Data collections such as these may have an associated cost and resource consumptions, but the insight to spectrum behavior is more complete and answers regarding spectrum policy decisions can be improved.

The extrapolation of these results may be inappropriate as differences in clutter conditions, or terrain may affect results or contribute any more uncertainty to the results. Regardless, the insight given here is a better representation of what PL variabilities one can expect in field deployments, better than models with no conditions of likelihood of occurrences. The continuum of CDFs shown in

The plots in

Figure 27 show that a UE could be emitting any number of output powers and a and of CDFs is more descriptive of UE behavior than a thin line with no variabilities. The wide plots of P_{UE} show that uplink emissions are probabilistic in emissions intensity versus position in a cell. If a regulator wishes to make rules based on 95% confidence, the CDFs in Figure 27 show a range of approximately 10 dB (from 13 dBm to 23 dBm) exists across the three morphologies. Also the trend is revealed that the more clutter, the higher P_{UE} power distrbutions (as with the urban morphology in Figure 27c).

5.5. Calculating MU in a Spectrum Coexistence Testbed

As was described in ANSI C63.27 and applied in test reports such as the NIST Technical Note 1954 [43], the considerations of MU when quantifying spectrum coexistence measurements is crucial to understanding a test bed's results. For example, if a MU of +/- 2 dB exists in a spectrum coexistence test bed, then one cannot confidently describe effects less than that uncertainty.

5.5.1. Sample Calculation

Figure 14 shows a series of RF parts connected in a way that could be used for an RF spectrum coexistence test. A test waveform is sent to an RF gain stage (or amplifier). This amplified signal is connected to a variable attenuator that could be used to simulate PL where an increase in attenuation is proportional to increased distance in a field deployment. In this example, the PL attenuator is set to 100 dB. The six parts shown have gain (or loss) figures with their associated uncertainties. Given the example RF test block diagram in Figure 14, the expected output power at test point 1 is the test waveform output summed with the gain/losses of the individual parts:

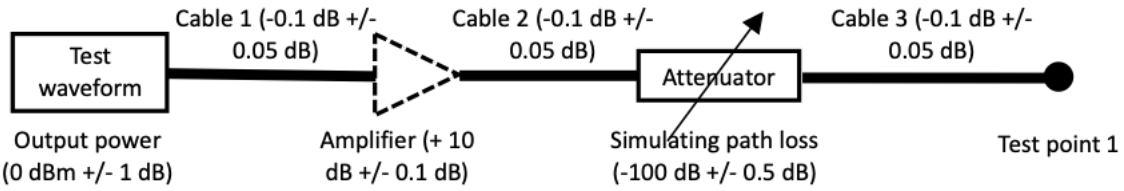

Figure 28. Example of an RF test path with an output stage (such as a signal generator) connected to an amplifier (gain stage), a variable attenuator (set to 100 dB). All losses, including cable losses, are assigned a measurement uncertainty value. The output is at test port 1.

$$P_{tp\_1} = 0\ \text{dBm} - 0.1\ \text{dB} + 10\ \text{dB} - 0.1\ \text{dB} - 100\ \text{dB} - 0.1\ \text{dB} = -90.3\ \text{dBm} \quad (28)$$

Without accounting for the associated uncertainties, the summed gain of the path is -90.3 dBm. When applying this appendix's MU with uniform distributions, assuming the cable uncertainties are type-B and $n = 10$ (samples of uncertainty measures). The standard uncertainty is $u_c(y) = 1.12$ dB, at 95% confidence, the Student's t-test coverage factor, $k = 2.13$ resulting in an expanded uncertainty, $U(y) = \mathbf{2.4\ dB}$. The output power of this RF circuit is therefore expressed as -90.3 dBm $\pm$ 2.4 dB with a 95% confidence interval.

Table 10. n sample measurements versus expanded uncertainty

Measurement sample (*n*)	Output value (dBm)	Combined standard uncertainty	Effective degrees of freedom	Expanded uncertainty (dB)
10	–90.3	1.13	15.1	2.4
9	–90.3	1.13	13.7	2.4
7	–90.3	1.13	10.7	2.5
5	–90.3	1.13	7.8	2.6
3	–90.3	1.13	4.7	2.9
2	–90.3	1.13	3.2	3.5

One assumption made in this example is that the measurement of source output power was made with sample $n = 10$ for the type-A uncertainties. When fewer measurement samples are made on an RF component used in testing, the expanded uncertainty increases. Table 10 shows the comparison of expanded uncertainty increasing versus number of measurement samples made on an individual part (in this case it is test waveform output power).

When compared to field testing, a laboratory environment is less costly for taking many sample measurements. In a non-laboratory setting, increased *n* sample measurements can be costly to obtain when components are difficult to access, or operational conditions are difficult to reproduce. For example, field test measurements are costly to obtain, if the *n* sample measurements is low, the uncertainty will be high. Since field test PL measurements have a large variability, the MU is less critical (for example, a PL variability of ± 2.4 dB is less critical when PL variability is ± 25 dB). In summary, MU is critical to

quantify in a bench test bed and increasing sample size of measurement collections will increase confidence of the MU applied to collected measurands.

5.5.2. **Alternative Method Using Monte Carlo Simulations**

If uncertainties and variabilities are well defined, computational *for loops* can be applied to achieve an alternative method to the MU technique described above. A repeated for loop is referred to as a Monte Carlo method. When repeating the possible output power of the RF test path in Figure 14 using the Monte Carlo method, the uncertainties therein are expressed in the following for loop (using MATLAB, randn is a Gaussian distribution)):

```
nsamp=1000;
for i=1:nsamp
  Pt= 0+(randn(-1 1))*0.5; %source power 0 dBm +/- 1
  G1= -0.1+(randn(-1 1))*0.05; %cable 1
  G2= 10+(randn(-1 1))*0.1; %gain stage
  G3= -0.1+(randn(-1 1))*0.05;%cable 2
  G4= -100+r(randn(-1 1))*0.1; %attenuator loss
  G5= -0.1+(randn(-1 1))*0.05;% cable 3
  Pr(i)=Pt+G1+G2+G3+G4+G5;%output power at test_point_1
end
```

Where P_t is the output of the 0 dBm source, G_n are the gains of the individual components (negative values when they represent losses), and P_r is the power at test point 1. The command "rand(1)" is a MATLAB function used to generate a uniformly distributed random number between 0 and 1. If the distributions were normal (Gaussian), then the command "randn(1)" would be used in its place. Figure 29 shows three plots—the

histogram, cumulative distribution function (CDF), and box plot—of the 1,000 samples in the for loop.

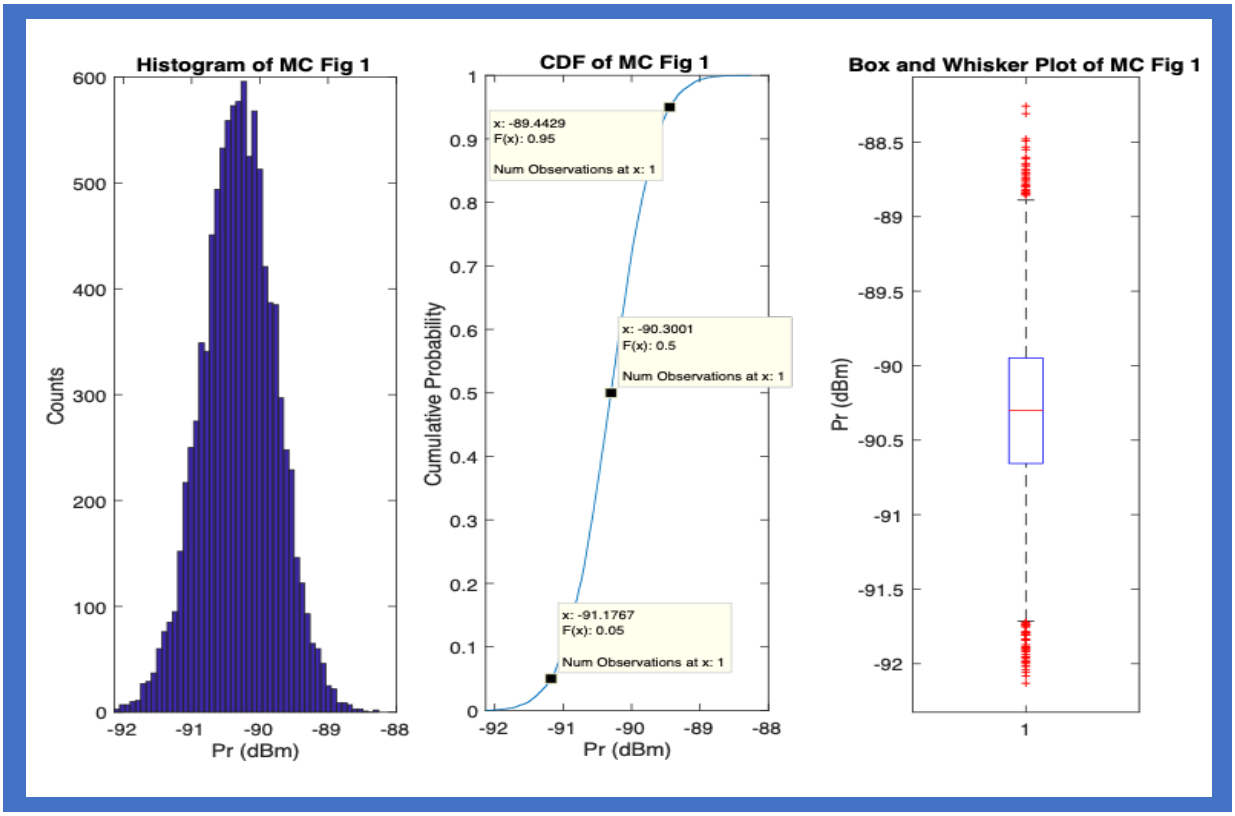

Figure 29. Monte Carlo output RF components Results of Monte Carlo method as applied to the RF block diagram from the data from Figure 14. The data are displayed here as a histogram, CDF, and Box Whisker plot.

The CDF has labels for the 5%, 50%, and 95% points. The median = –90.3 dBm, and the delta between 95% and 5% is **2.2 dB**. This value is close to the expanded uncertainty ($U(y)$) of **2.4 dB** MU calculated above. The advantage of the Monte Carlo method is that it can use inputs of PL distributions, making the conversions from RF power to distances. This Monte Carlo MU method can also apply actual distributions of received

RF powers taken from the field. This uncertainty determination using Monte Carlo is a useful alternative to using the MU techniques.

The Monte Carlo method has an advantage of leveraging the relative low cost of computational energy afforded by low-cost computing. This method also allows the user to insert any type of distribution of for each component in the RF chain of components.

5.5.3. **Treating Field Measurement Variability as an Uncertainty**

In a measurement that includes an air interface, RF propagation effects are part of the wireless communications link, and the link's variations and uncertainties must be considered. Variability in an RF link must be considered when evaluating spectrum coexistence testing.

5.5.3.1 *Drive Test Measurement Example*

Applying the NTIA ITS drive test measurements to the same test bed described in Figure 28, substituting the PL attenuator with the distributions of the data collected near Point Mugu, CA.

Inserting the field measurements, as shown in Figure 23 into an RF block diagram is shown in Figure 30. Substituting the variable attenuator with measured PL data propagates the variations in the measured data by treating them as MUs. In this example, the inserted PL data is from the rural measurements, from 800 to 900 meters distance (bucket 8 in Figure 30). This bucket contains 110 measurement points with median PL of 144 dB, standard deviation of 8.9 dB, a minimum of 133 dB, and a maximum of 168 dB.

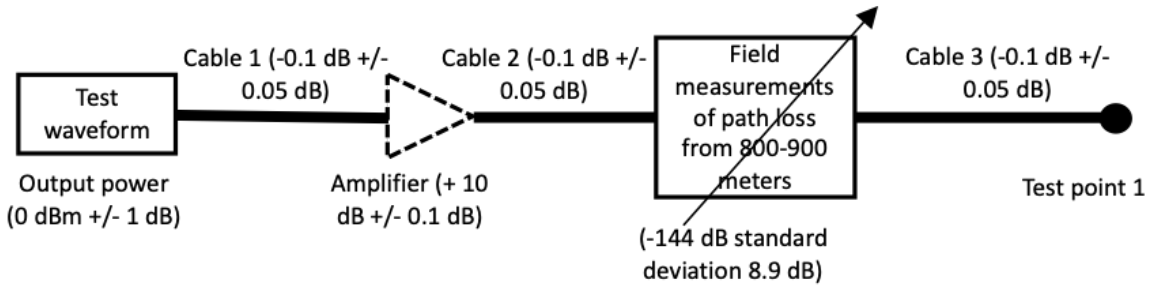

Figure 30. Example RF test path revisited with block of measured data.

$$P_{tp\_1} = 0\ dBm - 0.1\ dB + 10\ dB - 0.1\ dB - 144\ dB - 0.1\ dB = -134\ dBm \quad (29)$$

Without accounting for the associated uncertainties, the summed gain at test point 1 of the path in Figure 30 is -134 dBm. When applying MU with the same uniform distributions and assuming the cable uncertainties are type B and n = 10 (samples of uncertainty measures) in the same manner as example in section 4.4.1.5, the standard uncertainty, $u_c(y) = 8.96\ dB$, at 95% confidence, the Student's *t*-test coverage factor, $k = 2.23$ resulting in an expanded uncertainty, $U(y) = 20$ dB. The output power of this RF circuit is therefore expressed as $\mathbf{-134\ dBm\ \pm 20\ dB}$ with a 95% confidence interval.

Applying the Monte Carlo method to the RF test path from Figure 30 shows the MU of the circuit, describing the minimum measurable quantities. The measured rural data is not uniform and resembles a normal distribution for the middle 75% of the data, shown in Figure 31, which displays the histogram and quantile-quantile plots. The latter is a comparison with a gaussian (45-degree, red-dashed diagonal line).

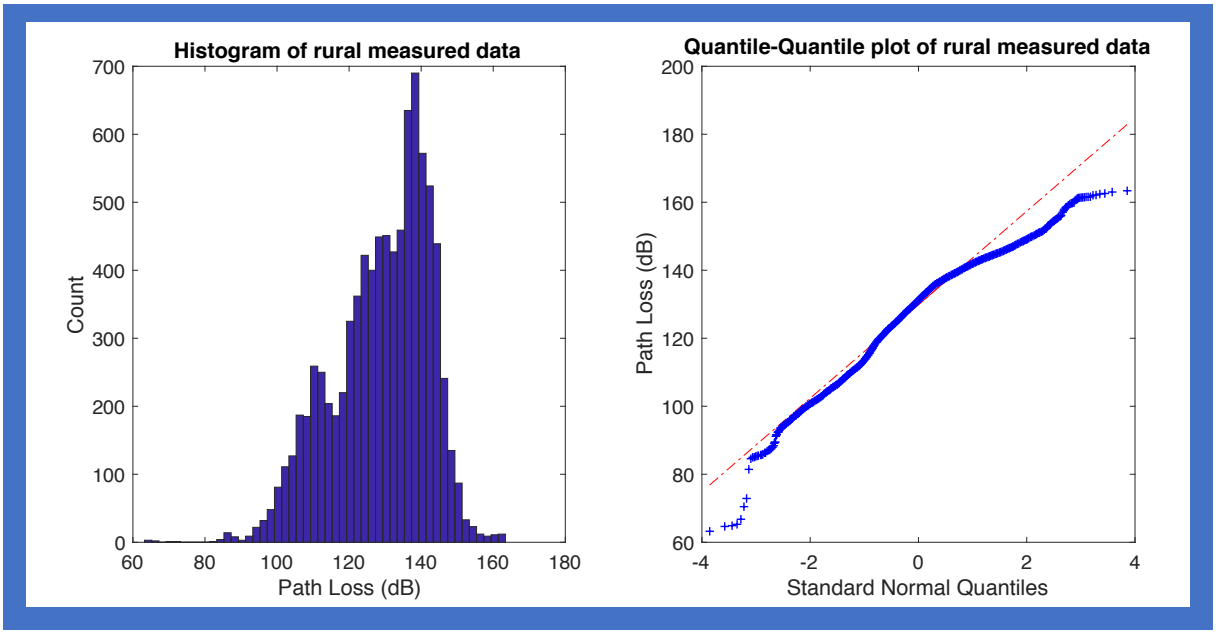

Figure 31. Histogram and quantile-quantile plot of rural measured data

Treating the PL data as normally distrusted and the remaining $G_n s$ as uniformly distributed, the Monte Carlo MATLAB code is copied here:

```
nsamp=1000;
for i=1:nsamp
  Pt= 0+(randn(-1 1))*0.5; %source power 0 dBm +/- 1
  G1= -0.1+(randn(-1 1))*0.05; %cable 1
  G2= 10+(randn(-1 1))*0.1; %gain stage
  G3= -0.1+(randn(-1 1))*0.05;%cable 2
  G4= -134+(randn(-1 1))*8.9*2; %measured path loss
  G5= -0.1+(randn(-1 1))*0.05;% cable 3
  Pr(i)=Pt+G1+G2+G3+G4+G5;%output power at test_point_1
end
```

Figure 32 shows three plots of the output of the Monte Carlo method across the example RF test path with measured data inserted from Figure 23 Path loss measurements

from NTIA ITS in rural environment (a) raw data from 0 km to 18 km and (b) bucketized into 100 meter buckets from 1 km to 4.2 km. Figure 32 contains a histogram, cumulative distribution function, and box whisker plot. The cumulative density function (CDF) has labels for median (at 0.5) $= -134$ dB, 2.5 % and 97.5% points are -151 dB and -116 dB respectively. The 95% confidence interval of the results is the difference of $(-116\text{ dB}) - (-151\text{ dB}) = 35\text{ dB}$. Therefore, the output power at test point 1 is $\mathbf{-134\ dBm \pm 17.5\ dB}$ with a 95% confidence. This is comparable to the -134 dBm $\pm$ 20 dB with a 95% confidence that resulted from the MU technique in section 4.4.4.

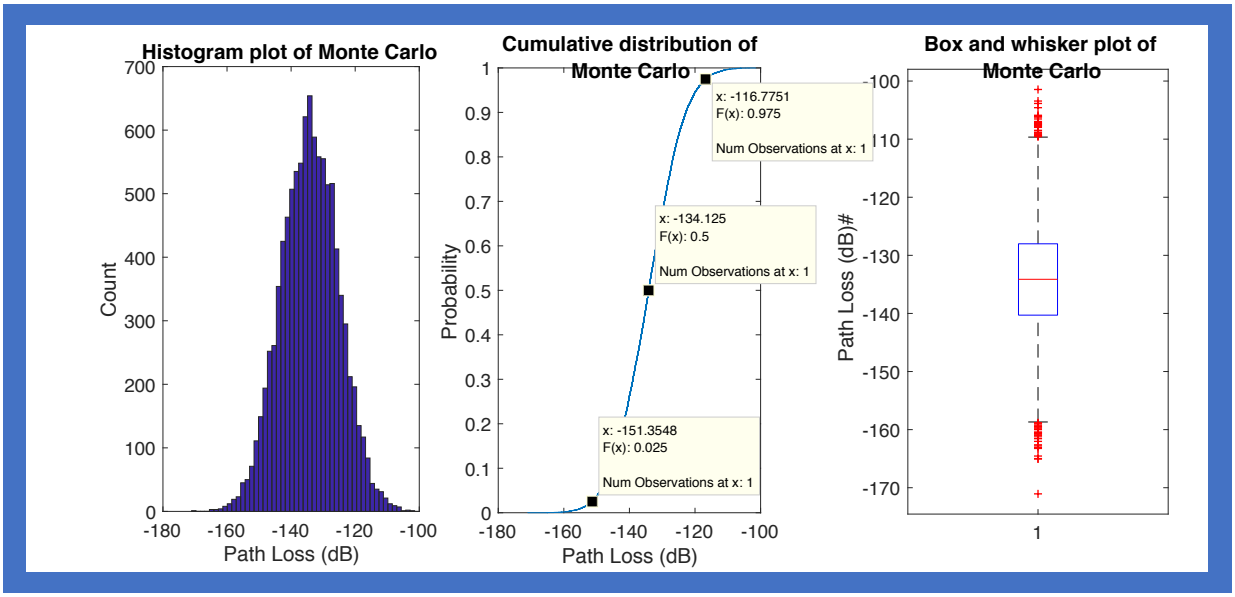

Figure 32. Results of Monte Carlo method as applied to the RF block diagram from Figure 30. The data are displayed here as a histogram, CDF, and Box Whisker plot.

5.5.4. **Conclusion**

The impacts of uncertainties and variabilities in a spectrum coexistence test need to be reported as part of the results. Wide variations of values that come from MU and variabilities demonstrate that the answers in spectrum coexistence tests are more accurately represented as a range or distribution of values (rather than single-point solutions). More complex measurement equations, such as signal to noise plus interference ratios (SINRs) must include all associated uncertainties and variabilities to provide valuable insight to spectrum coexistence repercussions. Section 5.1 through 5.3 contain examples of item 2 of the IAF, a detailed reporting of the "affected system platforms". That item is satisfied with the LTE uplink and downlink system performance and operational descriptions. Sections 5.4 and 5.5 demonstrate techniques and results for items 5 and 6 of the IAF are "MU" and "variabilities".

6. USE CASE: LTE OPERATIONS ADJACENT TO GPS BAND

This Chapter provides a use case for exercising the IAF. The 2 systems used for analysis are LTE downlink adjacent band to GPS receivers. The testing was not performed for this dissertation, this example uses results from the NASCTN test (which used actual KPIs to measure interference effects). In sections 6.9 and 6.10, 2 different risk analyses were used (an area impact, and CCDF of likelihood).

6.1. Introduction

This use case serves to exercise the proposed IAF for spectrum coexistence determination. The systems analyzed in this section are (a) a proposed entrant commercial mobile radio service (CMRS) operating adjacent to (b) level one (L1) GPS and co-channel to Mobile Satellite Services (MSS). The IAF will provide regulators with a comprehensive suite of information as considerable leverage for making better-informed spectrum management regulatory decisions.

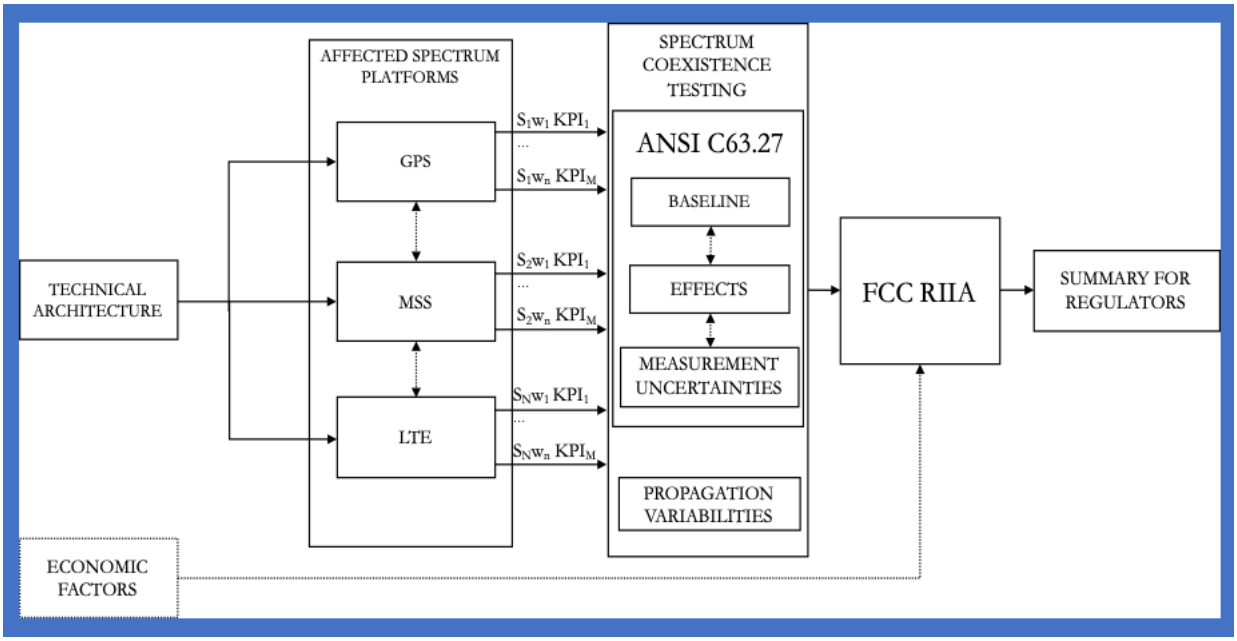

Figure 33, A modified copy of Figure 8 from this document. This IAF will be illustrated in this chapter by examining an actual FCC use case. Each of the corresponding blocks are described in the subsections of this chapter.

6.2. IAF Application

The IAF in Figure 8 (and Figure 33) consists of system descriptions, deployment specifics, KPI determination, weighting KPIs, coexistence testing, incorporation into a risk interference assessment, and a summary for regulators.

6.3. Technical Architecture

At this stage of the framework, technical and operational descriptions are provided by the users of the spectrum. For example, the proposed band plan, service rules, and new entrant operational details.

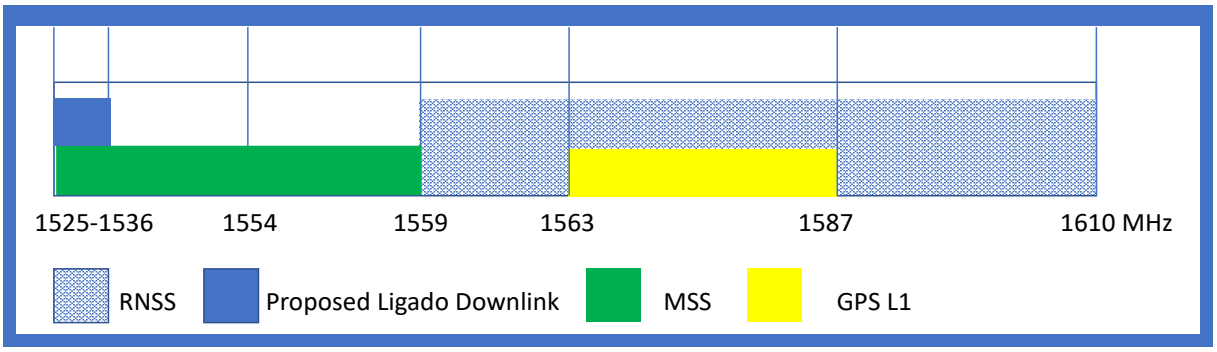

Figure 34. L-Band spectrum allocations, including the 10-MHz downlink proposed by Ligado Networks

6.3.1. **The Proposed New Entrant to the Band**

In 2012, Ligado Networks[22] proposed a deployment of LTE CMRS in the bands adjacent to GPS under the ancillary terrestrial network rules where MSS operate. The proposed bands are shown in Figure 34. Ligado's network proposals included paired (uplink and downlink) in the L-Band. By 2012, Ligado pooled together MSS spectrums to build out an LTE network when the FCC, under pressure from the GPS community and early test results, withdrew the spectrum-use licenses [54]. For the purposes of the IAF, System 1 is the incumbent GPS, System 2 is the incumbent MSS, and System 3 is the proposed LTE mobile broadband network.

6.4. Affected System Platforms

The proposed CMRS network is in the L-Band surrounding the global navigation satellite service band, of which GPS operates in the 1500 MHz L1 band. This sample test

[22] At the time, Ligado Networks was called LightSquared.

case concerns many technologies and stakeholders; for example, the United States Air Force owns and operates the GPS satellite cluster; commercial, industrial, and safety-of-life receiving systems are dependent on this Federal service [32]. Commercial GPS device sellers build on the broadcast information in the Federal GPS cluster to offer timing and positioning services to their customers. Current service rules allow MSS (with an ancillary terrestrial component) in the band adjacent to GPS L1.[23]

6.4.1. **System 1: GPS**

GPS is a subset of the services offered in the Radio Navigation-Satellite Service (RNSS) group of frequency bands. GPS, L1 specifically, is a civilian service broadcast in the L-Band from a cluster of satellites in the 1559 MHz to 1610 MHz range.

Space-based GPS was initially designed and operated as a satellite navigation system for the Department of Defense (DoD) in the 1970s. Although GPS was intended to function as a positioning system for the DoD, other applications for the system emerged in the commercial sector [32]. For example, civilians found uses for the positioning and timing features provided by the satellite cluster to help with mapping and directions. Because GPS is a broadcast system,[24] there is no limit to the number of users able to access the signals.

The original GPS design used two frequencies: one centered at 1575.42 MHz, called L1, and a second centered at 1227.60 MHz, called L2. Other bands were added later, such as L5, used for instrumentation aviation and safety of life [27]. This paper focuses on

[23] L1 GPS is subset of the spectrum allocated for the Radio-Navigation Satellite Service band.
[24] To use GPS, only a receiver is required.

the L1 legacy civilian band of GPS because it is widely used in consumer and industrial products and is most at risk of harmful interference effects by the proposed commercial LTE networks seeking to enter the adjacent lower band.[25]

At its inception, GPS had no strong emitting spectrum neighbors, and this has allowed for cheap design of GPS equipment without regard to adding strong front-end filers to block nearby band energy. Terrestrial GPS receiver signal levels are quite low: In the frequency allocation filing, the L1 satellite power is listed as 25.6 W [32]. The antenna gain is listed at 13 dBi. Thus, based on the frequency allocation filing, the power would be approximately:

$$P_{dBm} = 10 \cdot log_{10}\left(\frac{1000 \cdot P_{\text{Watts}}}{1\ \text{Watt}}\right) \rightarrow EIRP_{dBm} \tag{30}$$

$$= 10 \cdot log_{10}\left(\frac{1000 \cdot 25.6}{1\ \text{Watt}}\right) + 13\ \text{dBi} = +57\ \text{dBm}$$

The PL from a satellite 21,000 km away is about 182 dB [32]; $57\ \text{dBm} - 182\ \text{dB} = -125\ \text{dBm}$. This signal level is low compared with a terrestrial-based networks, and is degraded further by the following conditions:

- Being indoors
- GPS transmitting satellites near the horizon
- Urban clutter, also known as "urban canyon"
- Forests, high trees, and foliage
- Weather effects, such as rain and fog
- Other overhead structures, such as tunnels and bridges

[25] L1 is closest to the CMRS band identified in the Introduction of this paper.

By contrast, terrestrial-based LTE eNBs transmitting at 52 dBm to 62 dBm EIRP, and LTE handsets—including, but not limited to smartphones—operate well when receiving downlink signals from -110 dBm to -40 dBm. These downlink signals are much stronger than the GPS signals from space [45]. If LTE and GPS must operate at the same time and place, frequency must separate them to minimize harmful interference effects. Currently, the lower adjacent service is the MSS.

6.4.2. **System 2: MSS**

Since 2003, GPS has had an adjacent band neighbor. The band lower adjacent to GPS became home to MSS, which due to its compromised coverage areas could expand service to include terrestrial base stations.[26] Historically, the 1525 MHz to 1559 MHz band is an MSS allocation [55] and the GPS community agreed to the terrestrial use of base stations called an ancillary terrestrial components (ATC) which could be used for service augmentation. When deployed correctly, ATC would allow indoor service for MSS users. A more exhaustive description of the response to the proposals for MSS ATC components appears in Appendix A section A.5 . Since 2003, many consider the satellite phone spectrum underutilized, while 3G (third-generation) and now 4G (fourth-generation) markets dominate [54]. Most MSS users operate in areas without typical cell phone coverage—such as low population areas or over large bodies of water. Given the low

[26] The MSS band is called the Auxiliary Terrestrial Component (ATC) and has been authorized in the 1525–1559 MHz band since 2003. These satellite phones were allowed to augment their downlink signals with terrestrially based base stations.

density of use for this band, the spectrum could be shared on a co-primary basis using large separation distances. Figure 35[27] shows an example MSS portable transceiver, or phone.

Figure 35, MSS phone by Motorola

MSS in the L-band has not seen the type of growth as was originally anticipated. Platforms including 4G LTE have become a ubiquitous technology occupying a majority of the CMRS market share. MSS systems are widely used where LTE systems are not available, making spatial reuse optimal for sharing. For example, if every satellite phone contained an LTE radio as well, the satellite phone could hand off to the LTE network when in range, thus ensuring persistent coverage [54].

MSS is a disadvantaged communication system requiring *view* of the sky (i.e., outdoor use only). In a 2002 proposal to augment the operations of MSS, companies like Mobile Satellite Ventures L.P. (MSV) proposed the use of an ATC to the FCC. In this proposal to protect GPS, the stakeholders agreed upon the out of band (OoB) emissions in

[27] Image labeled for non-commercial reuse, https://commons.wikimedia.org/wiki/File:Iridium_phone2.jpg

the 1559 MHz to 1605 MHz GPS band level of –100 dBW/MHz [56]. The FCC accepted and adopted this IPC in the Flexibility for Delivery of Communications by MSS Providers [57]. By contrast, Canada Industry created MSS ATC base station maximum interference power in the GPS band at –70 dBW/MHz, a 30 dB difference (or 1,000 times greater in absolute power) compared with the limits imposed by the U.S. [58]. The current literature presents no description or explanation for why power limits differ substantially between the U.S. and Canada for the GPS band. Either –100 dBW/MHz is overly conservative, or –70 dBW/MHz harms GPS. The literature gives no evidence as a basis for either figure of merit, and is an area for future study.

In 2017 a Satellite Industry Association report [59], stated from 2012 to 2016 the U.S. market size of the MSS sector of satellite communications has been $400 million to $500 million. This service remains a relevant assured communications system for regions of the globe where cellular technologies do not currently provide coverage.

6.4.3. **System 3: Ligado LTE**

LTE has become the dominant standard for 4G mobile broadband services. Widespread LTE deployments will support innovative, new use cases—autonomous cars, Internet of Things, remote surgery, telehealth, etc. Any growth seen in the 4G technologies has paved the way for 5G services currently deploying. The popularity of 4G services is forcing companies to look at how they are using the spectrum and consider a transfer to LTE mobile broadband services.

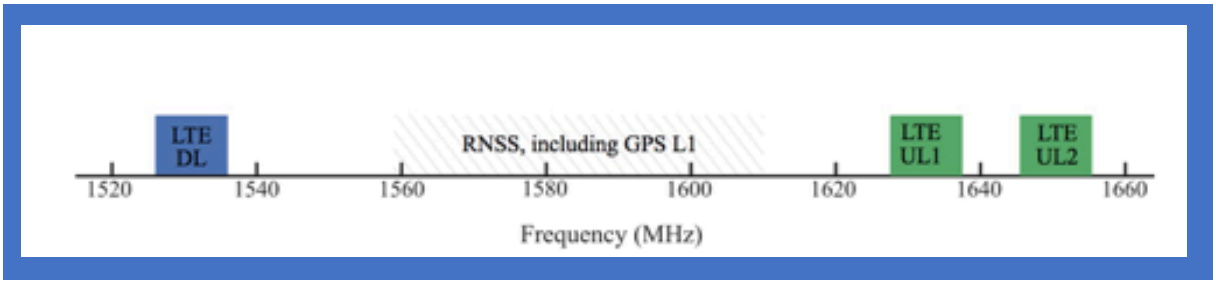

Figure 36. LTE bands proposed by Ligado Networks

In 2012, Ligado Networks proposed a deployment of LTE services in the bands adjacent to GPS under a modification in the ATC rules where MSS operates. Its network proposals included paired (uplink and downlink) in the L-Band. Ligado spent resources to build out an LTE network in the band shown in Figure 36 when the FCC, under pressure from the GPS community and test results,[28] withdrew the licenses [54].

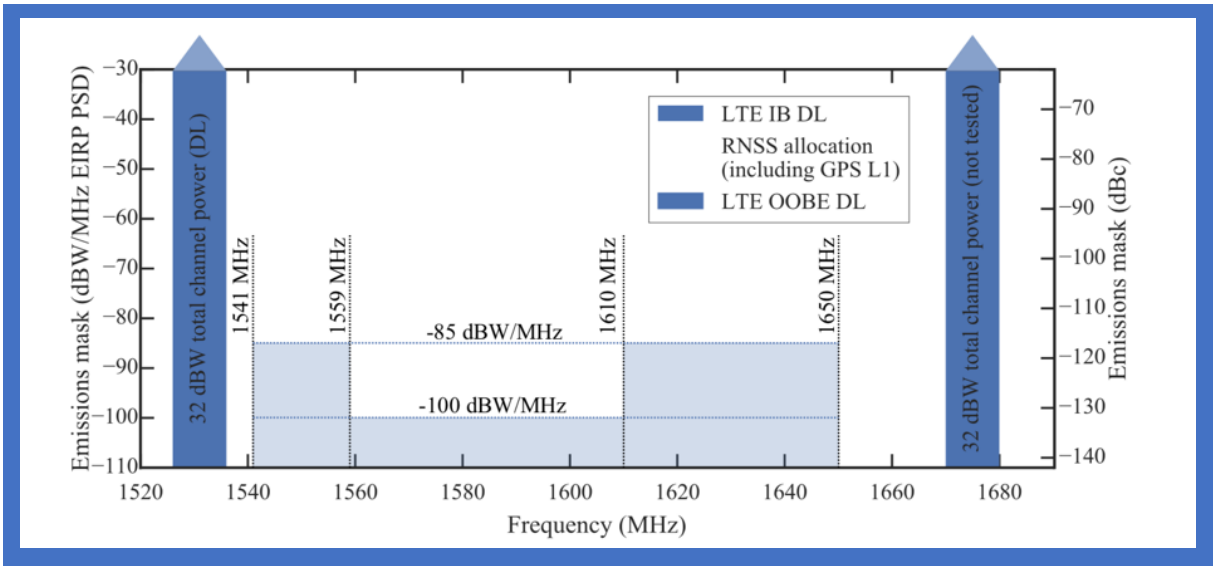

Figure 37. Ligado's proposed network emissions masks. The light shaded blue shows the multi-level protection mask created to protect GPS receivers. Copied from [63, Figure 2.4.a.]

[28] Results of testing are summarized in appendix section Appendix A.

The region of the spectrum where interference is most likely to occur is the spectrum adjacent to the high-powered LTE downlink from its proposed eNB emissions at 1526 MHz to 1536 MHz. In an effort to mitigate interference, the FCC reduced the allowable eNodeB emissions to 32 dBW and added a notch to the OoB emissions mask. The in-band and OoB masks are shown in Figure 37. Ligado had originally proposed downlink operations in the 1545 MHz to 1555 MHz band, but later withdrew its authority to operate out of concerns of interfering with L1 GPS. Ligado's hopes were that the 23 MHz between 1536 MHz (edge of their proposed downlink) and 1559 MHz (the lower edge of the RNSS band) was a sufficient guard band. Ligado had precedents for protecting GPS using an IPC of –100 dBW/MHz [56], using the band for LTE instead of MSS ATC signals.

6.5. KPIs

Interference protection from adjacent band emitters requires measuring system performance with and without the presence of other signals. Performance criteria are the KPIs of that system. More specifically, they are a system's response variables that are deemed descriptive of system performance. Some response variables are more valuable to end users and adding weights to those criteria aids in describing impacts during a spectrum coexistence test. Weighting KPIs is outside of the scope of this dissertation, but it may be an effective way to differentiate service priorities across a variety of stakeholders.

6.5.1. **Harmful Interference to the Incumbent System**

To demonstrate harmful interference, a measurable impact to performance needs to be shown. Typical performance measures for communication systems include an increase in BER or information latency. Other spectrum-dependent systems such as radionavigation or radiolocation are concerned with performance measures such as position uncertainty, timing accuracy, detection range, or track accuracies. Performance measures should be descriptive of why the spectrum-dependent system was designed, agreed on, and explicitly defined by the stakeholders.

6.5.2. **Control Factors and Response Variables**

As per the ANSI C63.27 spectrum coexistence testing standard states, KPIs are defined as a subset of relevant response variables, as shown in Figure 38. Response variables are variables or factors of a spectrum-dependent system that change in response to a change in conditions (such as SNR or BER) or in response to an increase in adjacent channel power. Response variables show an effect, and KPIs show an effect determined as critical to system performance. Critical can be described as causing reduced performance, service degradation, or service outages.

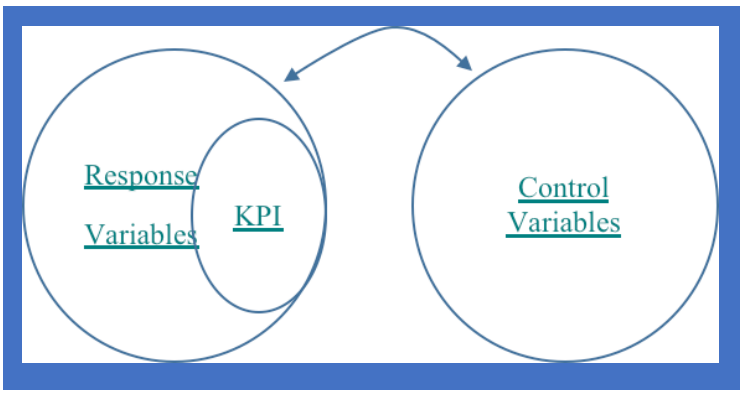

Figure 38. KPIs are a subset of response variables

The KPIs of interest when considering an LTE network deployed near (in frequency) to GPS are response variables that affect GPS performance. The presence of interference to a GPS system as defined by the ITU is an INR of –6 dB, meaning interference power can be at a level of ¼ power of the noise. Another way to represent INR is in terms of the coarse acquisition carrier power divided by the noise power density, expressed as a carrier power to noise ratio, $\frac{C}{N_0}$.

$$\text{Noise power density in dB/Hz } N_0 = 10 \cdot log_{10}(k \cdot T) \tag{31}$$

Where,

- k is the Boltzmann's constant $1.38 \cdot 10^{-23} \frac{\text{Joules}}{\text{Kelvin}}$
- T is the noise temperature in degrees on the Kelvin scale

When T = 290K,[29] N_0 = –204 dBW/Hz, (or –174 dBm/Hz).[30]

[29] 290 K is approximately 62 degrees Fahrenheit.
[30] As temperature ranges from –10 to +140 degrees Fahrenheit, N_0 ranges from –205 to –203 dBW/Hz, respectively.

Received carrier power to GPS receiver is expressed as $P_R = P_T - PL + G_R$, where

- P_R is the received carrier power
- P_T is the transmitted carrier power
- PL is the loss of carrier power from PL effects
- G_R is the gain of the receiver's antenna in the direction of the received satellite signal

The carrier power received by the receiver is nominally –158.5 dBW (Petovello, 2010, p. 22). For a GPS L1 coarse/acquisition (C/A) signal the nominal $\frac{C}{N_0} = -158.5\ \text{dBW} - \left(-204\frac{\text{dBW}}{\text{Hz}}\right) = 45.5\ \text{dBHz}$.

6.5.3. **C/N_0 variability in 30 seconds**

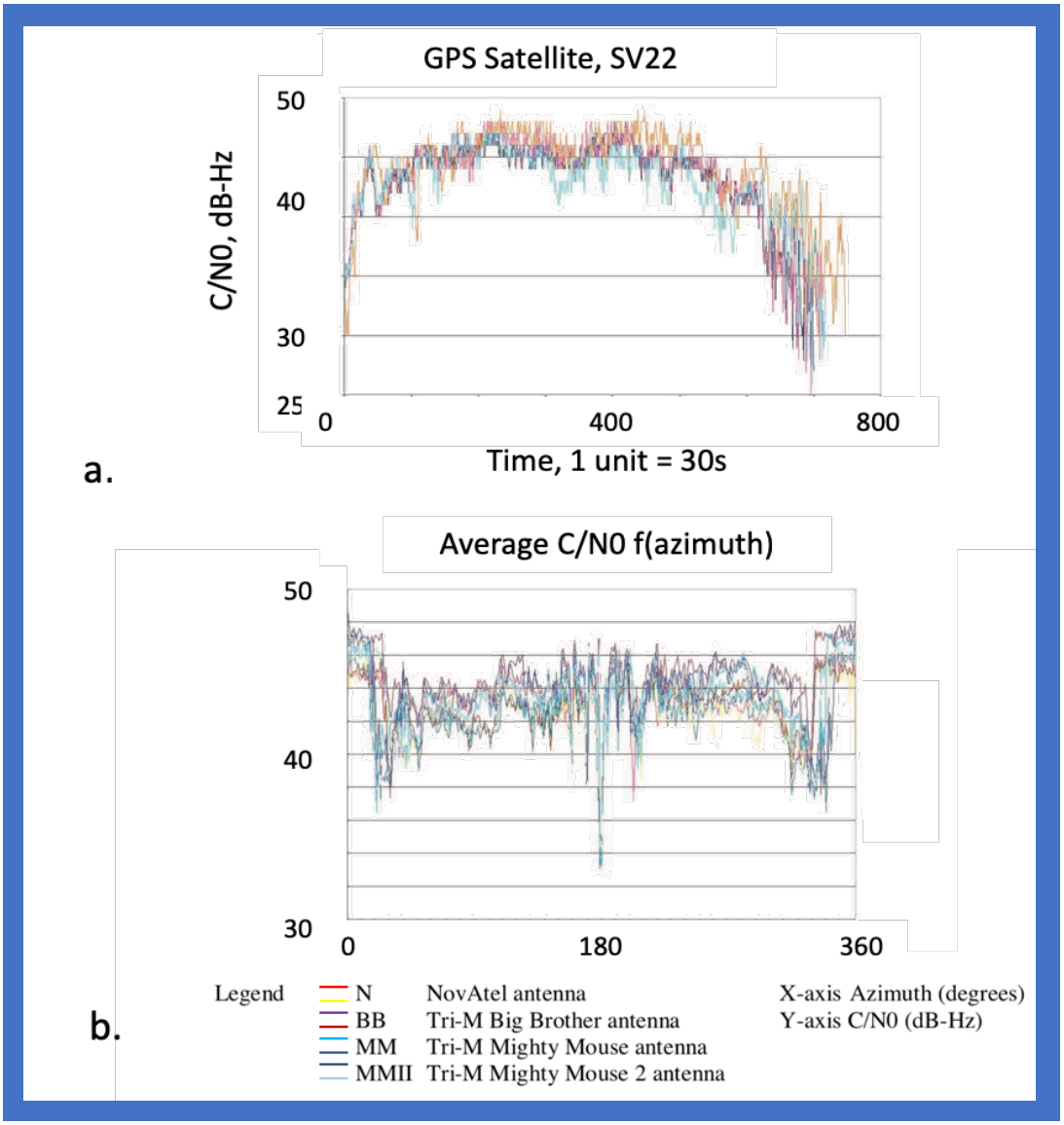

Figure 39. Baseline variations in (a) C/N_0 versus time for the SV22 GPS satellite; (b) C/N_0 azimuth angle (degrees) showing the normal operations for GPS receivers is a varying C/N_0 condition, (reprinted from (Hetet, 2000))

As an operational baseline (*normal* GPS behavior), $\frac{C}{N_0}$ varies as a GPS satellite passes across the sky. Figure 39 demonstrates observational measurements of $\frac{C}{N_0}$ variations

over time[31] for the SV22 GPS satellite [8]. Across the measurement period, $\frac{C}{N_0}$ varies from $25 < \frac{C}{N_0} < 48$ dBHz. Each tick mark is a 30-second measurement period. The plots in Figure 39 demonstrate the potential variations in $\frac{C}{N_0}$ in *baseline conditions* (i.e., absence of adjacent band signal conditions). Figure 39b shows average $\frac{C}{N_0}$ over azimuth angles of satellite travel. Each line shows a different GPS device overlaid on the same plot. From 0–20 and 340–360 degrees the satellites are directly overhead and the average $\frac{C}{N_0}$ ranges from -45 dBHz to -48 dBHz.

6.5.4. **CINR**

Interference from other spectrum users can degrade the C/N_0, therefore the interference enters the ratio in the denominator. CINR, measured in dB, is expressed as the carrier power divided by the noise plus interference, $\frac{C}{I+N_0}$.

One method of quantifying the maximum tolerable (not based on a performance measure) interference is an interferer equal to 25% of the noise power. This interference is quantified as a degradation of the C/N_0 by 1 dB using the following relationship:

$$CINR_{abs} = \frac{C}{N_0 + I} = \frac{C}{N_0 + \frac{N_0}{4}} = \frac{C}{N_0 \cdot (1.25)} \rightarrow CINR_{dB} = 10 \cdot log_{10}\left(\frac{1}{1.25}\right) \quad (32)$$

$$= -0.96 \text{ dB, or approx.} -1 \text{ dB}$$

[31] Time is along the x-axis equates to movement of the satellite across the sky, while the reporting receiver is stationary and ground based.

A quarter power of the noise that equates to an INR of –6 dB (and the equivalent 1 dB CINR degradation) is used as a measure of harmful interference [60]. This 1-dB degradation of CINR applies to aeronautical devices, as stated by the ITU in note 2 of M.1903:

> *NOTE 2 – The 6 dB aeronautical radionavigation safety margin, as discussed in § 3 of Appendix 1, was developed for a specific aeronautical radionavigation application of the RNSS and ARNS in the band 1,559-1,610 MHz and was not intended to be applied to non-aeronautical applications. The level of the safety margin, if any, to be applied to non-aeronautical safety applications of RNSS is to be established on the basis of further study [61].*

Yet this conservative 1 dB CINR degradation is interpreted as the harmful interference threshold for non-aeronautical RNSS systems [62]. The ITU 1903 Note 2 indicates the use of INR = -6 dB, (which is equivalent to CINR = -1 dB) is not an appropriate harmful interference KPI for non-aeronautical IPC. However, monitoring CINR can serve as a leading indicator of harmful interference.

6.5.5. **Additional GPS KPIs**

C/N_0 is not a directly measurable, by a piece of test equipment that is traceable to a standard criterion instead it is “measured” by the GPS system under test. The general approach to how the C/N_0 is calculated (see the previously cited reference) by the GPS device is understood; however, if this criterion is to be used as the sole Spectrum Management criterion a more thorough understanding of the absolute value is required. Further, the specific method for calculating and reporting the C/N_0 value is dependent on the specific hardware and algorithms used by the manufacturer of the Global Positioning System chip.

Table 11. KPIs for various GPS device classes

KPI / Device Class	time	position	C/N0	# of satellites in view	fix type	pseudo range	Carrier phase	1 pulse per second
GLN	√	√	√	√				
HPP	√	√	√	√	√	√	√	
RTK	√	√	√	√				√
GPSDO	√	√	√	√	√			√

Instead of merely classifying harmful interference to a power level that may interfere, describing interference as a degradation of a KPI relevant to the intended service is more useful. In spectrum coexistence testing, tracking KPIs that measure the services' performance can be used to better define harmful interference in terms of usability. For example, KPIs used in the NASCTN test hosted at the NIST facility are listed in NIST Technical Note 1952 [63]. CINR was one of many KPIs tracked in the presence of interference and all KPIs were used to describe system performance effects. Tracking all relevant KPIs allows for a reporting of actual effects to the GPS link from the injection of LTE adjacent band interference.

GPS KPIs are specific to the type of GPS receiver class type being evaluated. The four device classes of GPS receivers are general location and navigation (GLN), high precision positioning, real-time kinematics, and GPS disciplined oscillator devices. Device classes versus KPIs used in the NASCTN test are shown in Table 11. GLN devices are analyzed in this use case, therefore the KPI of position uncertainty is of most interest to the

GPS user. When position accuracy is uncertain, the GPS user is unsure of their precision location which makes location services less reliable.

6.6. Spectrum Coexistence Testing

As described by the IAF, the standards-based spectrum coexistence testing with appropriate treatment of test MUs and deployment variabilities adds information valuable to spectrum regulators. Spectrum coexistence testing is performed in hopes that the results can be extrapolated to performances seen in actual deployments. This dissertation identifies two standards that could be used to fulfil this framework component.

6.6.1. Example of a Standards-Based Spectrum Coexistence Test

The NASCTN test of impacts of LTE on GPS [63] serves as an example of a hybrid test following the C63.27 spectrum coexistence standard. The test was executed in a large, RF-shielded anechoic chamber. The LTE interferer (plus adjacent band energy) was summed together with GPS downlink energy over coaxial cables. The summed energy was transmitted through an antenna and received by the GPS receivers under test.

For GPS downlink energy, the NASCTN test used a Spirent GSS8000 GPS emulator emulating realistic movements of 35 minutes of GPS satellites. This emulator includes RF channel effects in its emissions. The emulations were designed to resemble satellites arcing across the sky at Yuma, Arizona, from 01:35:18 UTC until 02:10:18 UTC [63]. The GPS emulation was replayed for each test case. The emulated GPS downlink transmitted 15 minutes of pure GPS followed by 20 minutes of GPS plus LTE. The automated test bed collected GPS receiver KPIs for the entire 35 minutes. These 35-minute sweeps were repeated for different power levels of LTE. The emulated satellite movement

contained actual RF propagation channel details including variations in C/N_0 (and subsequently CINR). The advantage of using actual GPS receiver hardware was that the testers could observe effects such as warm-up time, shown in Figure 40. Device warm-up time is a factor that can add a large uncertainty to the measurement of C/N_0. As demonstrated by Figure 40 the device under test took more than 2 minutes for position uncertainty and approximately 10 minutes for C/N_0 to settle to steady-state value in the presence of the baseline satellite emissions [63, p. 106].

The hybrid method used in the NASCTN test allowed for antenna effects but provided a level of control[32] of other factors.

[32] Other factors included a repeatable 35 minutes of GPS satellite movement and calibrated measures of LTE power through splitters inserted into the test set's cabling.

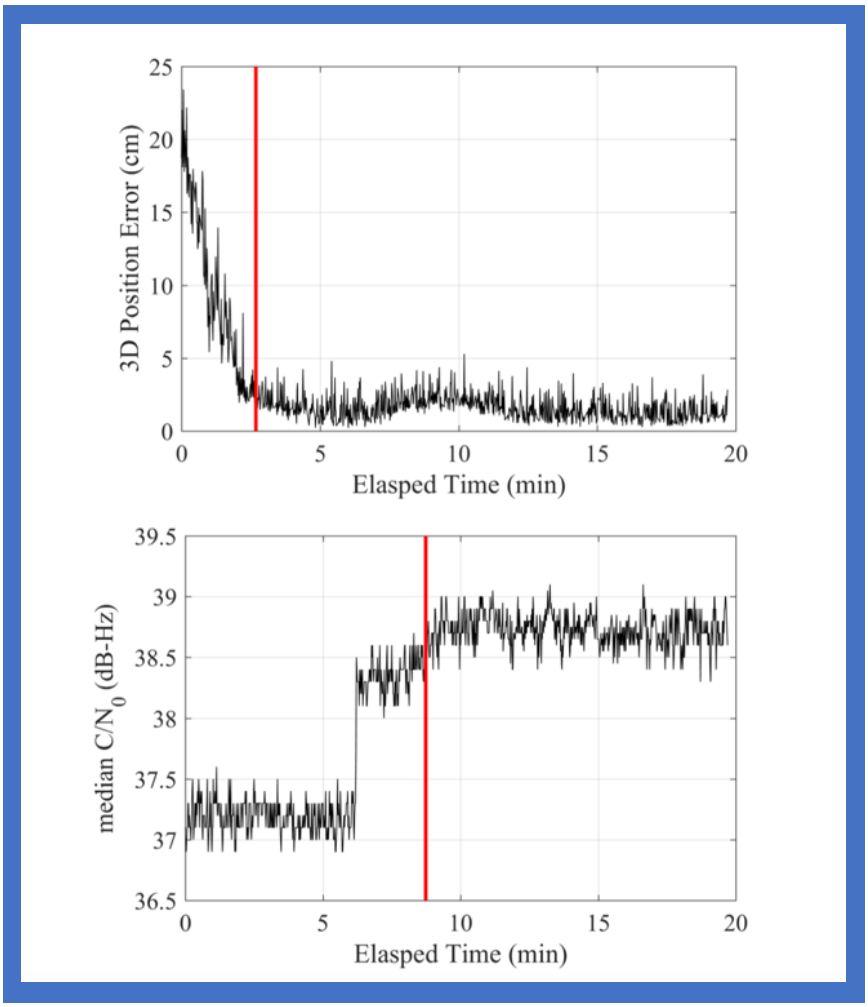

Figure 40. Estimations of warm-up time for (a) 3D position error, and (b) median C/N_0 data (reprinted from [63, pp. 106, Figure 5.3])

6.7. In-Field Spectrum Coexistence Testing

This section describes some of the complexities of field testing and how some benefits of field testing can be introduced to cabled or hybrid testing setups.

6.7.1. Over the Air Testing

A fully outdoor OTA test would include realistic propagation and channel effects, but repeatability would be difficult. For example, GPS satellite clusters change throughout

the day and other factors would reduce repeatable test conditions. Externalities like weather, mobility, and terrain[33] will vary the baseline and test conditions, and increased test time is needed to conduct a well-controlled test. A comprehensive understanding of these externalities is required for determining spectrum coexistence.

6.7.2. **Injecting Operational Realism to Laboratory Testing**

Field testing and measurements in realistic operational scenarios have the advantage of including all variations and uncertainties that can occur in deployment of spectrum-dependent systems and include propagation effects. For example, in the scenario in Figure 41, the intended path from P_T to P_R through RF channel PL_1 has a potential source of interference from P_{T2} through RF channel PL_2. If this scenario was tested in a laboratory environment and RF channels were emitted through RF coaxial cables then the realism of RF channels would be removed from the testing scenario. If the channel effects are measurably significant, the conclusions made from the test could change.

[33] This is not an exhaustive list of externalities that can contribute to the variability of spectrum coexistence measurements.

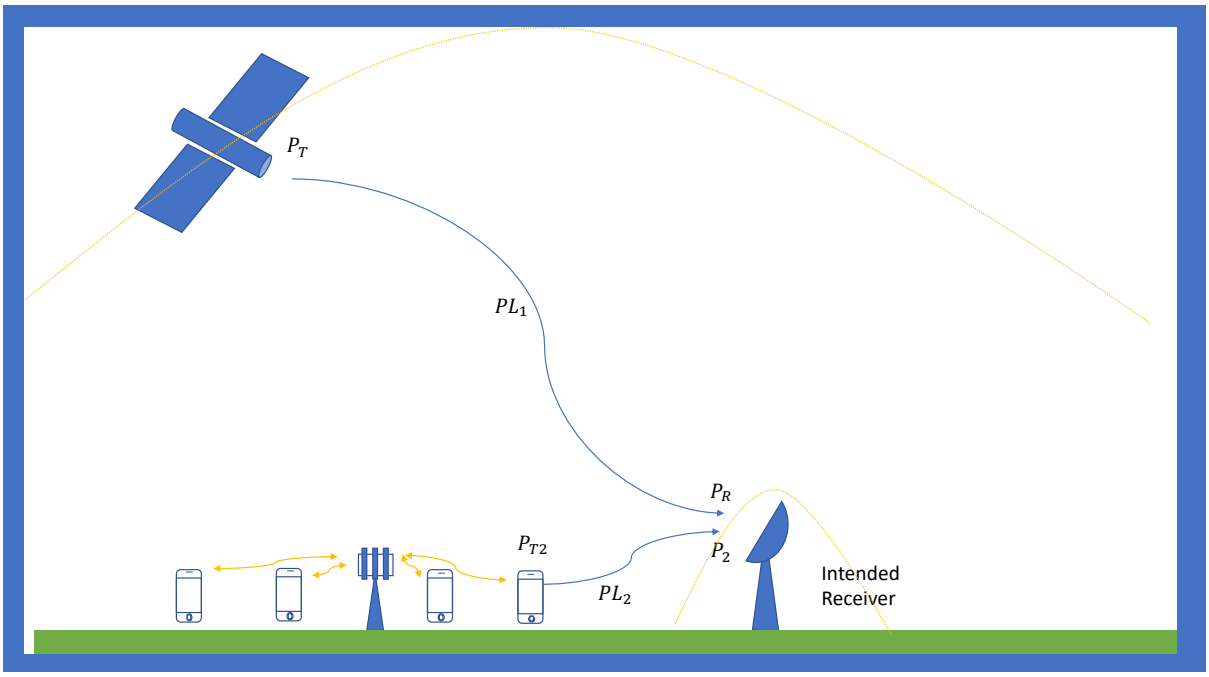

Figure 41. Test scenario graphic, showing an orbiting GPS satellite, a ground-based receiver, and incoming LTE cell network energy.

A technique suggested in this paper for adding a more realistic P_{T2} propagating through PL_2 is done by collecting P_{T2} emissions from actual deployments of LTE UEs in situ. Collecting RF recordings from UEs operating in their intended environments includes realistic variations of signal power, channel effects (including time varying channel effects, multipath, clutter, etc.), and duty cycle.[34] RF recordings can be made using test equipment such as a vector signal transceiver. Injecting such RF recordings into a test bed will contribute to the realism of laboratory spectrum coexistence test.

[34] The term duty cycle refers to the "on" time of a UE's transmitter. A UE that is sending a large amount of data will request many resource blocks and, once granted, will transmit large amounts of energy compared with a UE attached to an eNB sending only control signals. Specific details regarding LTE network behavior are beyond the scope of this paper.

6.7.3. **Measurement of LTE Power to Position Error**

Using measurements of position error from NIST Technical Note 1952, the LTE downlink power's effect on position error for three different consumer-off-the-shelf GLN devices is shown in Figure 42. According to Figure 42, a downlink power greater than –20 dBm for the devices under Tests 1 and 3 shows a degradation in position error. This error could lead to poor navigation or a negative impact for emergency services trying to locate someone who called 911 (and is using the emergency 911 location feature on a smartphone). The width of boxes surrounding the points of measure in Figure 42 are a 95% MU. The width corresponds to the ~ $\pm$ 2.7 dB MU calculated in NIST Technical Note 1952. When including MU, it is not possible to make assertions that a degradation of 1 dB was experienced with any confidence. For device under test (DUT) 1, there are repeatable perturbations to position error when LTE power reaches -20 dBm $\pm$ 2.7 dB. DUT 3, however, saw no measurable position error with LTE signals at their maximum tested values. For this use case, the expected value of -20 dBm LTE downlink power will be carried forward into the risk assessment.

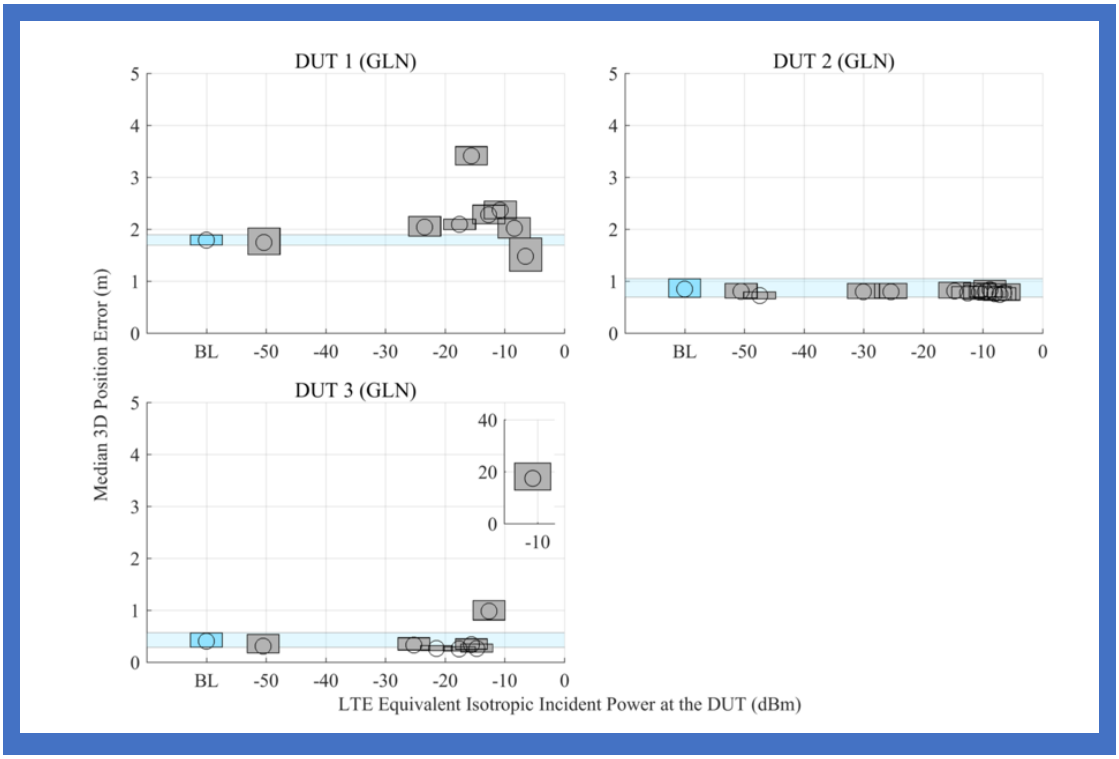

Figure 42. Position error versus LTE downlink power. These three plots are copied from NIST Technical Note 1952 as a representation of measurements displayed with bands of uncertainty surrounding the measurand [63].

6.8. Risk Assessment

The assessment of risk is now armed with results from a standards-based spectrum coexistence test. Analysis of LTE impacts to GPS, as described in section 6.6, the NASCTN testing of LTE effects on GPS (a) followed a standards-based approach (C63.27), (b) collected KPIs that describe GPS receiver performance, and (c) measurements included an uncertainty analysis. These three items satisfy the spectrum coexistence testing items of the IAF.

The variability of RF path loss as experienced in the field makes translating -20 dBm LTE power into a stand-off distance a matter of likelihood-of-interference and can benefit from field measurements. The following subsections will apply eNB locations and determine harmful interference likelihood using path loss models and then through the application of field measurements.

6.8.1. **Measuring Impacts Using Path Loss Models**

An existing LTE network is used in this section as an analog to the proposed Ligado Network. In an early analysis of the data from cellmapper.net (eNodeB locations) some inferences can be made by the distribution of eNodeB locations such as how eNBs cluster near heavily commuted roads. When in close proximity to an eNB in the lower Ligado downlink band, the signal may reach powers that can adversely affect GPS receivers. The RIIA cumulative distribution functions that chart likelihood versus consequence can be applied at this point. The likelihood measure is a random distribution of how likely one is to be in an area of interference on the map of Figure 43. This is called an *area of impact* determination—an analogous LTE deployment at a different frequency band is used—a T-Mobile eNB laydown in Band 4[35] is plotted over a 17 km by 10 km region.[36] Area of impact in this context would be the area free from harmful interference divided by the area where harmful interference would occur. The color coding in Figure 43 (red, yellow, green

[35] For comparison purposes, the eNB in LTE Band 4 is selected due to its wide adoption offering reasonable service coverage for users in the region selected.

[36] This technique can be easily performed on any region, including the entire United States. The small sample area is used for illustration purposes.

shading) represents a heatmap of powers emitted using free-space (and eHata for suburban) PL models for propagation characteristics. In this selected 170 km^2 area, businesses, residences, and heavy commuting areas are included and is served by 24 eNBs.

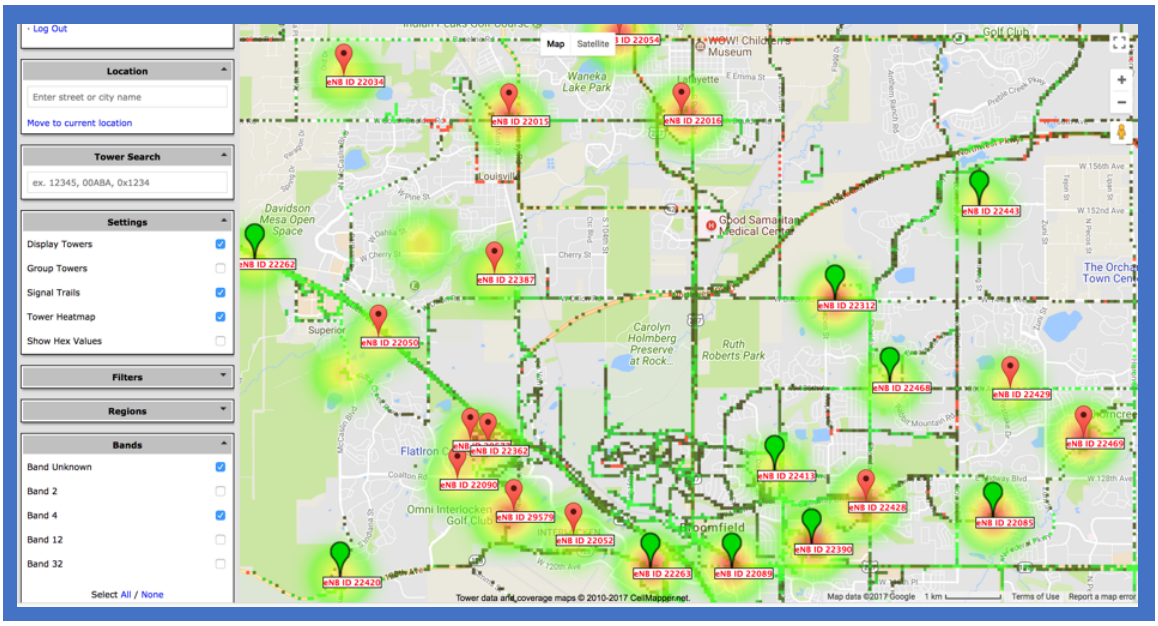

Figure 43. Screen capture from the mapping feature on www.cellmapper.net, using display features LTE, Band 4, show heatmap, T-Mobile Network.

To translate the -20 dBm LTE downlink interference level to an outdoor deployment of an LTE network requires calculating the power versus distance for various eNBs over the land area from Figure 43. The free-space propagation model[37] from NIST Technical Note 1952 [63] with inserted dashed lines to show distance where -20 dBm

[37] Free-space path loss is not appropriate to use for ground-to-ground communications because it does not account for the additional RF path losses from buildings, terrain, and vegetation. Free-space is sometimes considered a boundary condition—least path loss. A more detailed explanation of various path loss models is described in section 4.4.3.

occurs is shown in Figure 44. Using Figure 44 as a free-space propagation calculator, an eNB downlink power is −20 dBm at a distance of 160 meters.

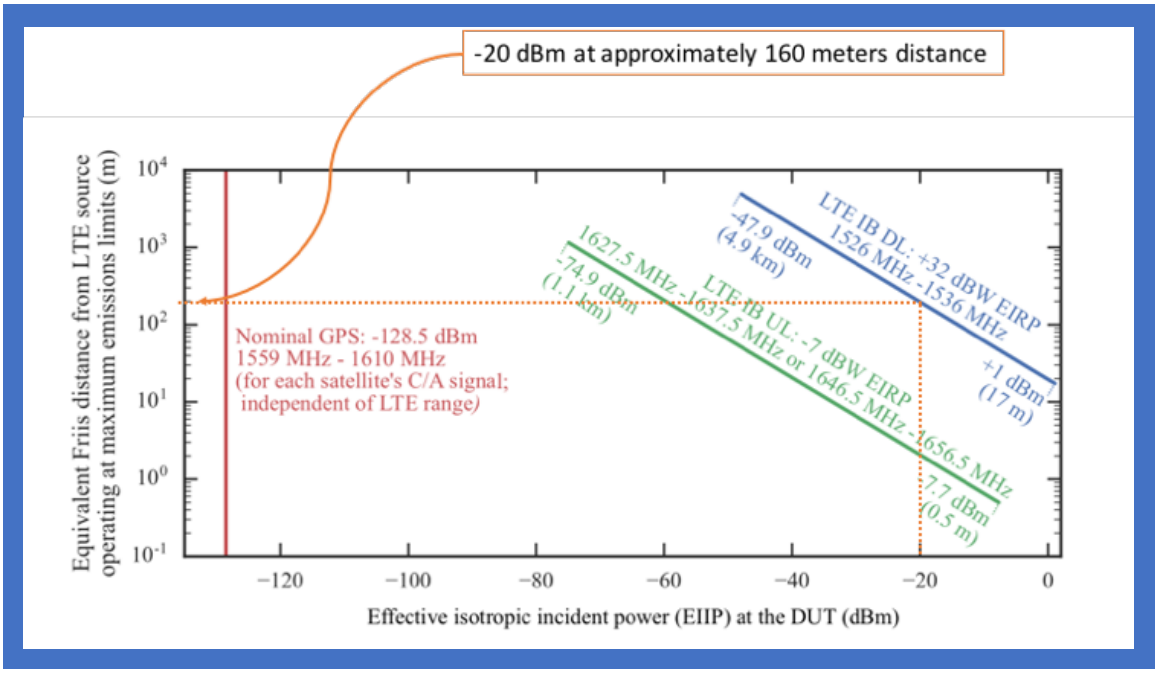

Figure 44. Propagation calculation from the NIST Technical Note 1952, the added dotted red lines show the distance (approximately 200 meters) where the power reaches -20 dBm. This figure is annotated to show the -20 dBm / 160 meter point.

The FSPL model does not account for any clutter, presenting a path loss model that includes cluter will reduce the 160 m stand-off distance. Because there is clutter loss in the suburban region shown in Figure 43, applying a path loss model that includes clutter loss is more appropriate. The eHata model applies additional loss factors that were derived from drive testing through cluttered environments [64]:

$$PL = A + B \cdot log(d) + C \qquad (33)$$

$$A = 69.55 + 26.16 \cdot \log(f_c) - 13.82 \cdot log(h_b) - a(h_m) \quad (34)$$

$$B = 44.9 - 6.55 \cdot \log(h_b) \quad (35)$$

$$C = -2 \cdot \left[\log\left(\frac{f_c}{28}\right)\right]^2 - 5.4 \quad (36)$$

$$a(h_m) = (1.1 \cdot \log(f_c) - 0.7) \cdot h_m - (1.56 \cdot (f_c) - 0.8) \quad (37)$$

Where d is distance between transmitter and a receiver; h_b and h_m are heights in meters of mobile UE and base station (eNB), respectively; and f_c is the center frequency of the emissions of concern.[38] Note, the calculation for C is for suburban areas; there are other C values for rural and urban applications [64, Appendix 7.A]. Equation (38) uses the Hata model to solve for distance given a known PL of 92 dB. Knowing PL and solving for distance, d = 150 meters; see Equations (39) and (40).

$$+62 \text{ dBm (eNB EIRP)} - \big(-30 \text{ dBm (power at GPS receiver)}\big) = 92 \text{ dB} \quad (38)$$

Solving for d:

$$92 = 69.55 + 26.16 \cdot \log(1531) - 13.82 \cdot log(30) - (1.1 \cdot \log(1531) - 0.7) \cdot 1.5 - (1.56 \cdot (1531) - 0.8) + [44.9 - 6.55 \cdot \log(30)] \cdot \log(\boldsymbol{d}) - 2 \cdot \left[\log\left(\frac{1531}{28}\right)\right]^2 - 5.4 \quad (39)$$

[38] In this case f_c = 1531 MHz, the center of the proposed Ligado Networks Downlink band.

$d \cong 150\ meter$ (assuming suburban clutter loss) *(40)*

Using the eHata model for a suburban morphology results in a stand-off distance of **150 meters**, (Equation (40)).

6.8.2. **Comparison of Path Loss Models to Measured Data**

Figure 45 is plot of 5 PL models overlaid on top of measured data from subsection 4.2.1.4 in Chapter 4. Past interference predictions have leveraged FSPL yet other ground to ground PL models differ by orders of magnitude. The COST 231 model tends to converge with this drive test data after approximately 1.2 km (the 12th bucket). This further proves that field collecting data is crucial to making informed spectrum coexistence determinations.

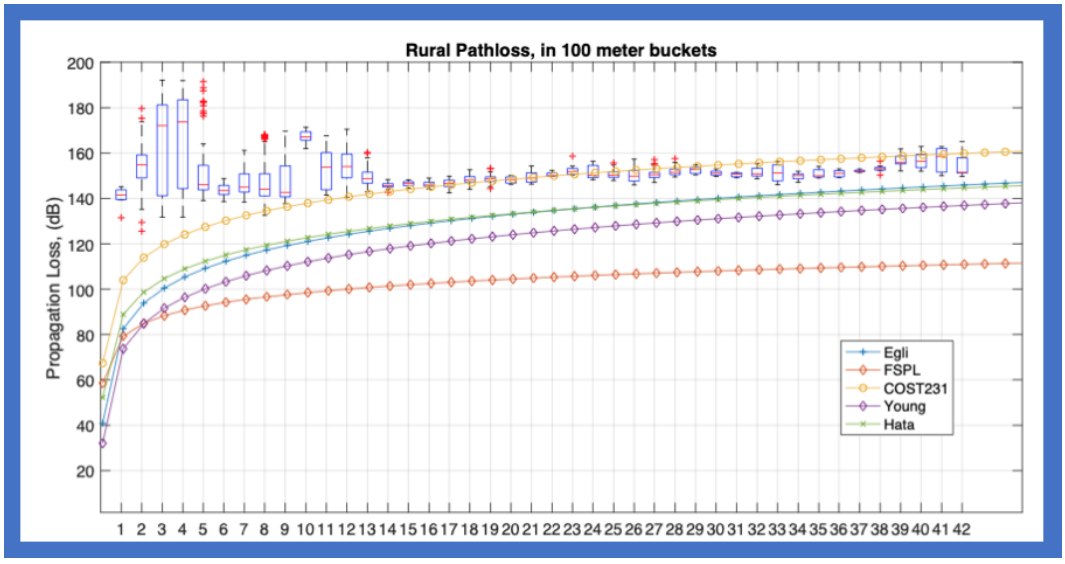

Figure 45, Path loss model comparison to measured data.

6.8.3. **Interpreting Test Data by Quantifying Interference Regions**

The following subsections describe the likelihood of interference using the test results and projecting those results to realistic operational deployments to better define operational impact.

6.8.3.1 *Using an area impact study*

Assuming each eNB in Figure 43 is operating at 32 dBW (62 dBm) EIRP at the proposed Ligado downlink frequencies, the weakest of the three GLN devices would see a degradation of position error within a radius of 150 meters from each eNB.

To calculate the expected value (in percent of the area affected), the following equation divides the area of the resulting 24 circular regions in Figure 43 having a radius of 0.15 km, affects an area of 1 % (expected value of the distribution is calculated in Equation (41)) of total area.

$$\%\ area\ affected = \frac{Area_{impacted}}{Area_{total}} = \frac{24 * \pi * 0.150^2\ \text{km}}{10\ \text{km} * 17\ \text{km}} = \mathbf{1}\% \qquad (41)$$

When considering use cases for consumer GPS, note that GPS only works outdoors and that mobile use on roads is a common application. LTE eNBs are typically located along roads, providing travelers location-based services. In the 17 km x 10 km region from Figure 43, there are approximately seven well-traveled east–west roads and 10 north–south, making the linear distance of well-traveled roads equal to $17\ \text{km}\ (7) + 10\ \text{km}\ (10) = 219\ \text{km}$.

$$\% \, roads \, affected = \frac{Length_{roads,impacted}}{Length_{roads,total}} = \frac{24 * 2 * 0.150 \text{ km}}{219 \text{ km}} = 3.2\% \quad (42)$$

Continuing the generalization, if these eNBs are transmitting in the Ligado band, then 1% of the land area and 3.2% of the linear road distance would show an increase in GPS position error.

6.8.3.2 *Quantifying interference effects using grid mapping*

This subsection is an example of how to account for the impacts of this footprint of GPS interference. The 17 km x 10 km ($n \times m$) region encompasses suburban and rural terrains with heavy commuting routes. The eNBs shown are Band 4 (2110 MHz to 2155 MHz LTE downlink) T-Mobile service. These eNBs were chosen to represent a "typical" deployment scheme. Colored circles show the heatmap of eNB power: red cells in Figure 46 indicate harmful interference region has a radius of 150 m, r_i.

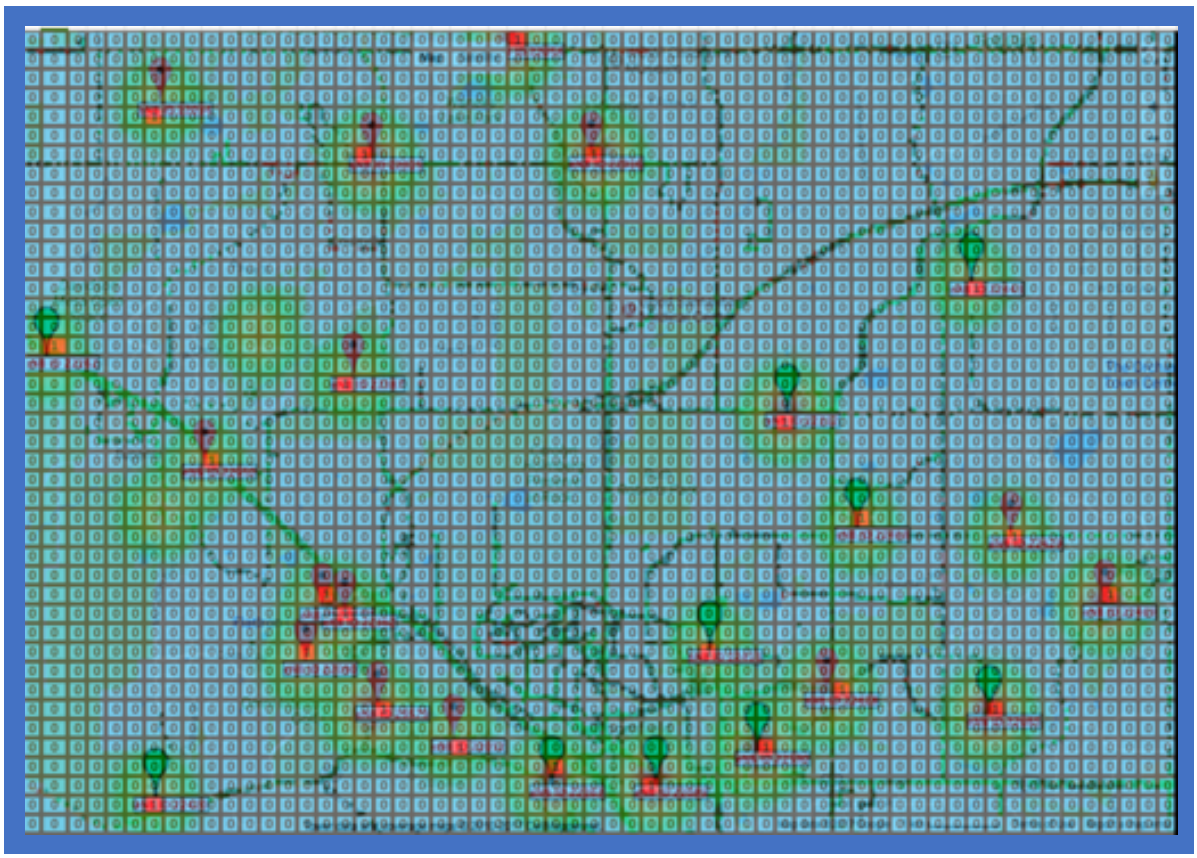

Figure 46. Grid overlaid on LTE downlink heatmap

Figure 46 shows a grid overlaid on the LTE downlink heatmap. Grid size is $j \times k$ where $j \approx 240\ m$, $k \approx 170\ m$. The cells of the grid are labeled with zeroes or ones based on a threshold value of –20 dBm, $p_{interference} \geq -20$ dBm; 24 out of 2,520 grid cells exceed the interference threshold. The area of interference likelihood is thus calculated as

$$\frac{24}{2520} = 0.95\% \qquad (43)$$

It takes approximately 20 seconds to drive past a 150 m radius (320 m diameter) circle surrounding an eNB, at 35 mph. There are five eNBs located along a heavily

commuted route (shown on the map as Route 36). According to labor statistics,[39] 58,000 people work in this town and approximately 33% commute into town. The average commuting time is 22 mins (1,320 seconds) so driving by five eNBs offering 320 m of interfering power would impact 7.5% of the commute.

Extrapolating these numbers to statewide figures, out of 2.5 million commuters statewide 74.7% drive alone ($2.5e6 \cdot 0{,}747 = 1.87e6$ commuters). If a commuter passes an eNB every 2 km ($35 \text{ mph} \cdot 22 \text{ minutes} = 21 \text{ km}$), $\rightarrow$ therefore commuters pass 10 eNBs during their commute to and 10 eNBs from work. At 20 seconds of service interruption with each eNB, a commuter will experience a total of 400 seconds of GPS service interruption per day: $400 \text{ seconds} \frac{400 \text{ seconds}}{2 \cdot 1320 \text{ seconds}} = 15\%$ of driving time through a degraded area due to eNBs.

6.8.3.3 *Changes to received power using field-measured data*

The 150 to 160 m interference distances were calculated using the FSPL model and eHata model. If this PL was based on data collected in the field and included variabilities, the "keep-out distance" is different than predicted.

PL model predictions can be replaced with actual field measurements of a particular environment. The advantages of inserting field-measured data are that the true contributions of clutter, ground bounce, atmospheric effects, boresight of antenna, etc. are present in the RSRP values. In an attempt to search for the actual power levels a UE would experience, the field measurement data collected by moving a UE physically next to a

[39] Data can be found at https://datausa.io/profile/geo/boulder-co.

macrocell eNB, then walking 1 km away in three different directions (south, north, and west) while recording latitude, longitude, and RSRP (as shown in Figure 19). The center frequency of the eNB was operating in the advanced wireless services 1 (AWS-1) band and the RSRP numbers are being treated as if they were in the 1531 MHz band.

RSRP points were collected at 1-second intervals using a slow walking rate of approximately 3 miles per hour along the yellow path shown in Figure 29. This moving speed translates to an RSRP data point collected every 1.3 meters. RSRP is measured across an LTE resource element, which is 15 kHz wide. In the 10 MHz wide eNB emissions there are 600 resource elements [29]; the translation of power in 15 kHz to the 10 MHz LTE band. The results of the data collection effort are shown in Figure 19(b). RSRP values, according to the scatter plot shown, have no values exceeding the laboratory tested -20 dBm harmful interference threshold. These results intuitively make sense; there is no reason in a CMRS network for a UE to receive a relatively high-power level; providing a level of power that serves the most consumers should be of primary concern for the eNB network deployments. The eNB is close to major roadways and covering these roadways can be best achieved by directing the energy to the roads, achieving power levels that are relatively consistent for all consumers of the service. Actual beam patterns, downtilt angles, and eNB operating details are outside the scope of this dissertation.

Figure 19, (a) is a plot of the raw data from the walking data collection from 0 km to 1 km from an eNB, overlaid on this plot is the predictions from FSPL and eHata model for a rural morphology. (b) is the same data converted to path loss and bucketized into 100 meter distributions. buckets (with the same technique as in section 4.2.1). This set of box plots demonstrates the uncertainty of measuring RF power over the air even when signaling

conditions are free of clutter. RSRP measurements were taken close to the LTE base station, in line of sight conditions, and fixed antenna heights (both base station and smartphone) the data collected is a distribution that does not follow a simple r^{-n} or eHata model.

6.8.4. **Quantifying Interference Effects Using Field RSRP Measurements**

Rather than using propagation models and areas of impact, field collected eNB downlink powers applied in Figure 47 that summarizes RSRP data collected from an Urban (Arlington, VA) and Rural (East of Boulder, CO) locations. Each data set was recorded using a Samsung Galaxy S9 and the NetworkCellInfo application which records latitude, longitude, and RSRP (downlink energy in a 15 kHz bandwidth). After converting to power in 1 MHz, the arrays of RSRP are plotted using the complimentary cumulative density function as recommended in the RIIA documentation. Figure 47 is plotted using only the values of eNB downlink power as a user moves through the regions of interest. Over the geographical areas the received LTE downlink power varies as a function of distance, terrain, antenna details (such as antenna gains, heights, 3 dimensional angles, lobe shape). Only a field test can apply all of these factors into a set of data and using the wireless hardware that the test is concerned ensures the data is relevant.

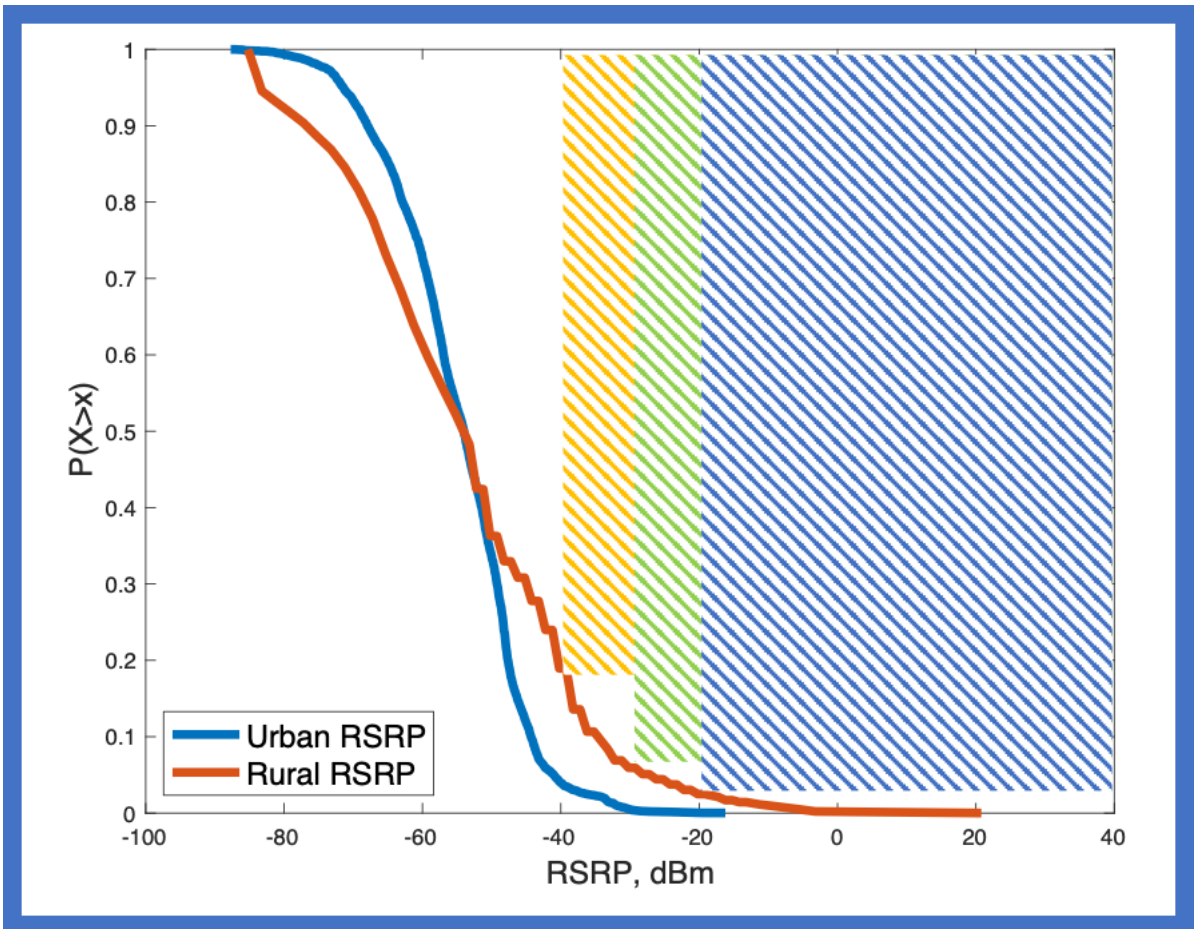

Figure 47, CCDF of RSRP values collected with three boxes demonstrating likelihood of power levels -20 dBm, -30 dBm, and -40 dBm.

Figure 47 contains the CCDF curves of RSRP arrays, two morphologies are plotted. The solid blue CCDF is Urban and in red CCDF is Rural. In predicting the likelihood an LTE downlink power level exceeds a value of concern, the CCDF is used by the FCC RIIA. On the roads where these RSRP values were recorded, there is an approximately **2.5%** chance of LTE power exceeding -20 dBm (illustrated by the lower left corner of the blue hatched rectangle), a 6 % chance of power exceeding -30 dBm (in green hatched), and approximately 19 % chance the power will exceed -40 dBm (in orange hatched).

The advantages of using RSRP field collections is the values are representative of a fully deployed LTE network. These arrays have values across many eNBs, their handovers, through representative RF channel conditions, and antenna effects. The field test application more closely resembles what a user will experience in the RF environment tested.

6.9. Summary

This chapter does not predict actual values for the decision of the proposed Ligado Networks LTE deployment (the -20 dBm value only applies to the GLN position erro acrss a few GPS receivers); instead, the use case serves as a demonstration of utilizing the IAF to inform the regulatory decision process. When employing appropriate scientific rigor, which includes actual KPIs (as required by the ANSI C63 and implemented in NIST Technical Note 1952), the coexistence test has meaning to the operational requirements of the systems involved. When applying MU to a spectrum testbed (as required by the C63), the reported measurands are transparent, and making measurements under that range lacks certainty. For example, as shown in Figure 42, the $\pm$ **2.7 dB** MU was calculated through repeated measures makes assertions that a **1 dB** degradation in CINR has occurred. These standards-based spectrum coexistence testing approaches with the inclusion of variabilities and uncertainties, realistic field measurements, and spatial areas of impact yield more descriptive interference risks. When translating spectrum coexistence measurements to operational conditions factors such as the propagation variabilities of channel models, position, equipment, antenna pointing vectors, MU yield very different results (and/or statistical distributions of results).

Field measurements capture propagation variabilities for a particular RF channel. In the LTE example, using field collected RSRP at the AWS-1 band lends insight to AWS-3 operations. These field-collected values make more informed interference prediction because all RF propagation channel effects are contained in the data. Distributions of likelihood must be provided to the FCC's RIIA and reported to spectrum regulatory bodies before decisions are made. The example of actual eNB downlink power measurements shows that propagation prediction formulas may not accurately predict a receiver's experience in the real world. This IAF use case demonstrates the types of information and testing methods that should be considered when making impactful spectrum regulatory considerations and provide quality inputs to RIIA. Furthermore, collected field measurements is crucial to informing spectrum coexistence decisions. Performing targeted field measurements to predict interference likelihoods comes at an expense of human capital and drive time. The expense should only be incurred if the economic consequences of interference between different systems outweighs the cost of data collection.

The framework proposed in the following chapter of this dissertation would add increased rigor leading to more defensible risk-based spectrum management assessments. Requiring a standards-based spectrum coexistence testing stage after the NOI and substituting results submissions in place of a comment period would increase the quality of information used by regulators to make decisions.

7. CONCLUSION – SUMMARY – AREA OF FUTURE RESEARCH

This chapter is divided into three main sections: a short summary of the chapters; recommendations for researchers, spectrum regulators and stakeholders; and identification of areas for future work.

7.1. Summary of Chapters

Chapters 1 and 2 are an introduction and literature review, focusing on improving the suite of information that spectrum regulators have afforded to them. These Chapters describe the value of spectrum growth and describe spectrum coexistence test methods and data collection techniques. Chapter 2 describes the current methods that spectrum regulators, such as the FCC, use to make spectrum policy changes. The FCC's adoption of risk-informed assessments is an improvement to their process; however, the quality of the information feeding those assessment is crucial. Requiring standards-based spectrum coexistence testing with best practices of measurement science is recommended. In Chapter 3, an extended framework (the interference analysis framework, IAF) is created to feed information into the RIIA. RIIA, as developed by the FCC TAC, includes the quantification of risk in spectrum policy change considerations. Both the IAF and the RIIA treat spectrum related measurements, deployment details, output powers, and deployment details as random processes. Chapter 4 describes methods for predicting LTE deployment and operating details, as well as techniques for quantifying measurement uncertainties and variabilities associated with spectrum related random processes. These deployment analyses techniques are an update to CSMAC's studies from 2013 and can be applied to future networks beyond 4G LTE. Chapter 5 provides plots, results, and analyses of these

methods' results to examples of LTE deployments and PL measurement campaigns. Results include eNB spacing, distributions of KPIs with considerations of MU ad path loss variabilities. Chapter 6 applies the IAF to a test case of LTE downlink operations adjacent to GPS. Using the IAF, impacts to GPS GLN receivers are described in terms of area impact and eNB downlink power distributions. These results are displayed in the methods described by the FCC's RIIA. Appendix A provides a history of GPS spectrum coexistence testing, both co-channel and adjacent band. This history reveals the use of the different IPC definitions used to claim harm to GPS receivers including the use of the 1 dB C/N_0 harmful interference metric when the ITU states it is not proper for non-aeronautical GPS receivers.

7.2. Recommendations

This dissertation has shown spectrum coexistence studies that were conducted using a variety of methods, such as through simulations and engineering intuition, measurements to a power level, and measurements to the performances of the spectrum-dependent systems themselves. As an example of a measurement to a power level, the FAA ABC study shows where $\geq$ 1 dB C/N_0 degradation occurs after converting relative powers to distances. The lighter blue region of Figure 48 shows that an approximately 14 km keep-out region is needed to prevent the harm threshold of $\geq$ 1 dB C/N_0 degradation to the GPS receiver. However, loss of lock from low-elevation satellites ends at an approximately 3 km stand-off distance. This dissertation has demonstrated that a measurable service performance degradation (in the form of a service-related KPI) is more representative of harmful interference, rather than a measurand that is not descriptive of system-level performance. Position uncertainty occurs when approximately 150 meters from an eNB, which is orders of magnitude closer than the 14 km distance predicted in Figure 48. MU of

spectrum coexistence test beds are shown (in a simple test bed) to exceed 2 dB, therefore making a 1-dB change in a measurand unquantifiable with any degree of confidence.

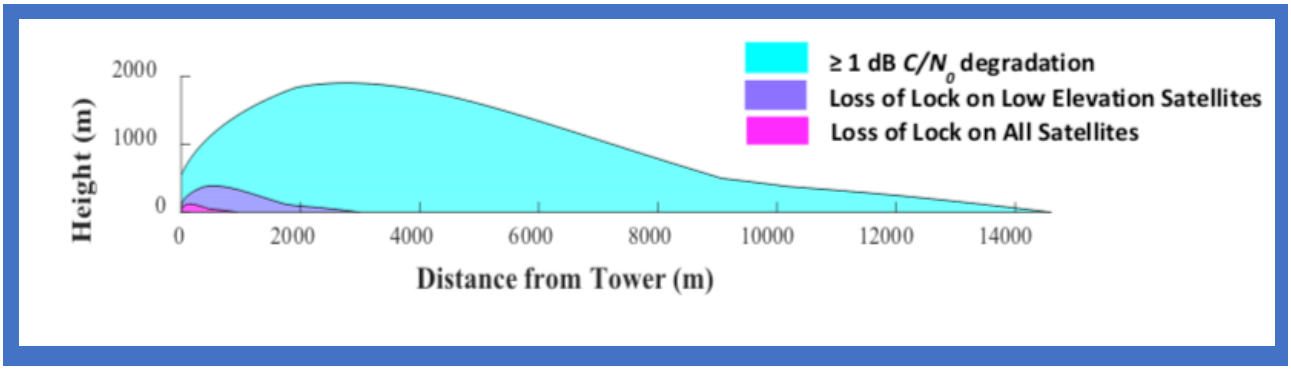

Figure 48. GPS keep-out regions in meters, eNB is located at 0 meters. Plot copied from [76].

By contrast, a testing effort that used the effects on mission performance versus values of co-channel *interference* (in this case, levels of LTE) is the NTIA ITS 14-507 report [65]. In this report, synthetic targets were injected into the radar's receiver at a power level that mimics a variety of realistic distances as a baseline condition. While the synthetic targets were present, varying levels of LTE energy was injected and the INR levels were recorded. Harmful interference was identified as when the targets were difficult[40] to visually resolve. The results summarized in Figure 49 demonstrate that the total number of observable targets is diminished when INR ≥ -6 dB. The number of "targets" are clear when INR $= -9$ dB and -6 dB. At higher values of INR, the target resolution degrades. Three different INRs are shown in Figure 49. This result is clear and useful for the 3.5 GHz band citizen broadband radio services (CBRS) LTE entry to the 3.5 GHz spectrum. This

[40] Difficult was defined as unclear in the opinion of a qualified radar operator who was recruited to assist with the test.

INR impact is visible to the operations of the radar and the KPI used is the ability to track multiple targets. There is a problem when these results such are extrapolated to other types of interferers or other types of incumbent systems.

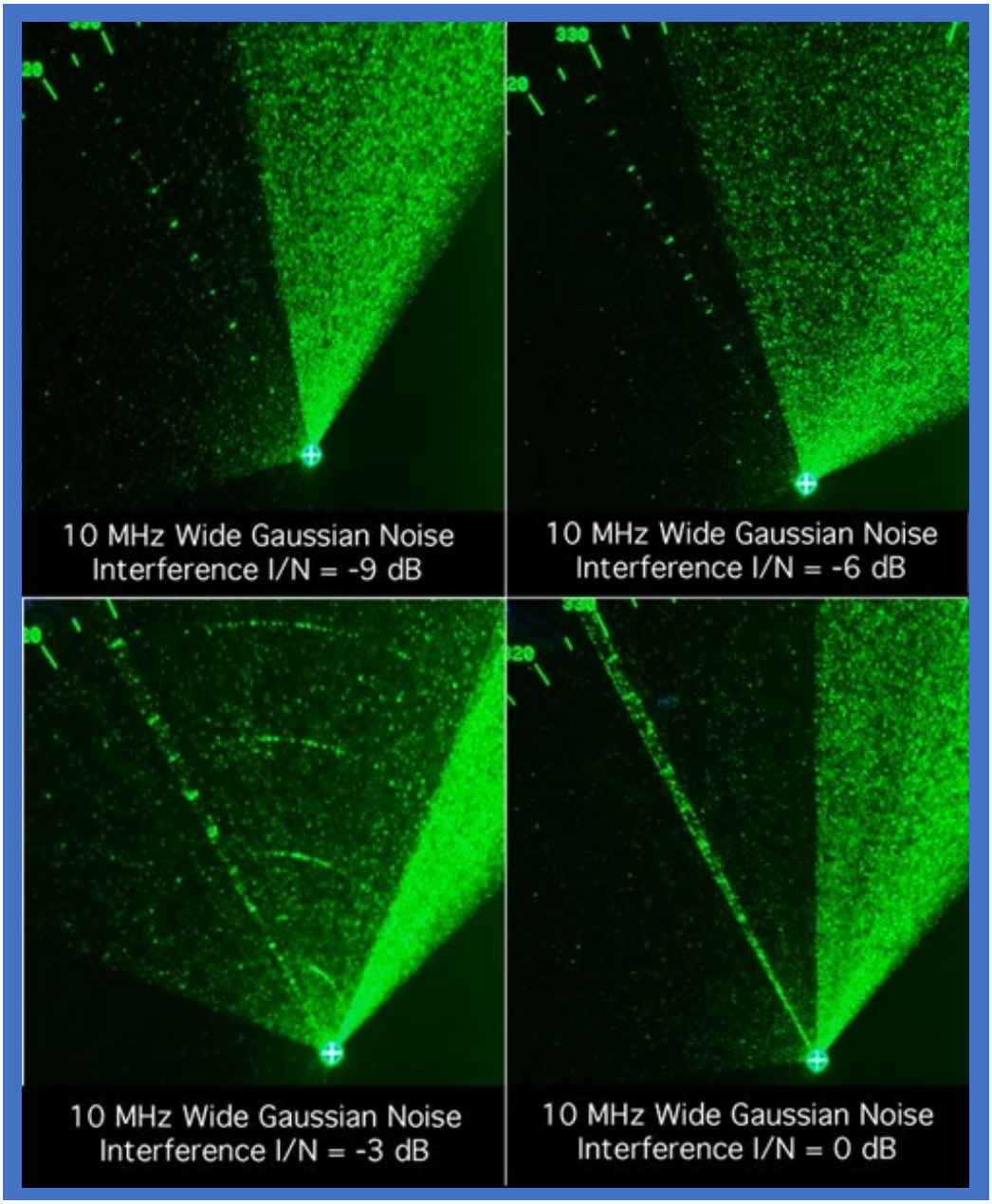

Figure 49. Navy RADAR SPN-43 performance versus INR (from TDD LTE), [68]

Translating the power levels that cause an INR of -6 dB to stand-off distances requires an application of PL models or when possible—field testing. Or both, to better understand PL specific to a region, this dissertation suggests taking measurements in the field of the locations of interest. Field measurements with uncertainties and variabilities will better predict power levels at the receivers of interest. These efforts will make results more defensible and lead to more informed decision making from spectrum regulators.

Since wireless systems have become ubiquitous and rights to spectrum use has become competitive, reduction of risk of interference has been the guiding principle. Now that maximizing spectrum use is becoming more important, those same regulators need a broad interdisciplinary suite of information (including metrology, statistics, and RF engineering) to make well-informed decisions.

7.3. Areas of Future Work

This dissertation describes a framework for assessing interference by defining the inputs to the FCC's RIIA. Included are proposed test methods to demonstrate a use case that gives regulators more information that can be used to make more informed spectrum regulatory decisions. There are many ways to continue this work through more extensive field collections of UE RSRP data collections and application to more use cases (such as the CBRS band or other bands currently being evaluated for service rule changes). Another logical extension of this work is to add economic effects to the IAF as shown with dashed lines in Figure 8. MU GUM techniques should apply to economic predictions (in the form of cost benefits analyses) in the same way it is applied to PL models and test beds in this dissertation. The spectrum stakeholder and regulatory community both desire ways to

improve the quality of information accuracy for making spectrum use and interference predictions. Techniques like the RIIA and now the IAF are helping make that happen. When translating interference power levels to distance, field measurements offer a distinct advantage over path loss models by inherently including RF channel factors in the measurements. However due to the expense and area-specificity of the results a method of automating such collections would benefit the data collecting efforts. For example, if a users' smartphone were able to record LTE downlink power and its own emissive behavior automatically, then mobile network uplink and downlink behavior would be better understood and interference predictions would be improved.

BIBLIOGRAPHY

[1] Ericsson, "Ericsson Mobility Report 2018," June 2018: https://www.ericsson.com/assets/local/mobility-report/documents/2018/ericsson-mobility-report-june-2018.pdf. [Accessed October 2018]

[2] B. Obama, "Presidential Memorandum for the Heads of Executive Departments and Agencies, Unleashing the Wireless Broadband Revolution," 1 July 2010. [Online]. Available: http://www.whitehouse.gov/the-press-office/presidential-memo. [Accessed 2 May 2018].

[3] United States Congress, House Resolution 1314 - Bipartisan Budget Act of 2015, Washington DC: United States Congress, 2015.

[4] United States Senate, S.19 MOBILE NOW Act, Washington DC: United States Senate, 2017.

[5] United States Congress, H.R.4953 - AIRWAVES Act, Washington DC: United States Congress, 2018.

[6] Federal Communications Commission, "FCC.gov," 4 June 2019. [Online]. Available: https://www.fcc.gov/document/comm-orielly-remarks-wi-fi-alliance-annual-member-meeting. [Accessed 15 August 2019] “Remarks of FCC Commissioner Michael O’Rielly Before the Wi-Fi Alliance Annual Member Meeting”.

[7] D. Coleman and B. Gunter, A DOE Handbook: A Simple Approach to Basic Statistical Design of Experiments, San Bernardino, CA: CreateSpace Independent Publishing Platform, 2014.

[8] S. Hetet, "Signal-to-noise ratio effects on the quality of GPS observations," 30 August 2000. [Online]. Available: http://gauss.gge.unb.ca/papers.pdf/hetet.report.pdf. [Accessed October 2018].

[9] Rondla Prasad, G.Shanmukh, Rajesh Karvande, “Analysis of Various RF-Interference Effects in GPS L1 C/A Code Receiver in Tracking Mode”, Published in: International Conference on Computing and Communication Technologies, 11-13 Dec. 2014

[10] International Telecommunications Union, "International Telecommunications Union, Radio Regulations Articles, Edition of 2016," 2016. [Online]. Available: http://search.itu.int/history/HistoryDigitalCollectionDocLibrary/1.43.48.en.101.pdf. [Accessed 4 April 2018].

[11] J. Kiddoo, “Engineering & Technology,” Federal Communications Commission, 30-Oct-2018. [Online]. Available: https://www.fcc.gov/engineering-technology. [Accessed: 15-Nov-2019].

[12] “OET - Technical Documents,” Federal Communications Commission, 06-Jun-2019. [Online]. Available: https://www.fcc.gov/general/oet-technical-documents. [Accessed: 10-Nov-2019].

[13] Federal Communications Commission, “Measurements of LTE into DTV Interference (Tests on four ATSC DTV Receivers of OFDM 64 QAM Co- and Adjacent-channel Interference)” 17 June 2014. [Online] https://docs.fcc.gov/public/attachments/DA-14-852A2.docx

[14] Department of Commerce, "NTIA Homepage," [Online]. Available: https://www.ntia.doc.gov.

[15] Department of Commerce, "CSMAC Search for 500 MHz Working Group," 10 November 2011. [Online]. Available: https://www.ntia.doc.gov/files/ntia/publications/csmac_search_1755-1850_recommendations_final.pdf. [Accessed 4 July 2019].

[16] Commerce Spectrum Management Advisory Committee, "Final report Working Group 1 – 1695-1710 MHz meteorological-satellite," Department of Commerce, Washington, DC, 2013.

[17] Commerce Spectrum Management Advisory Committee, "1755-1850 MHz Airborne Operations Aeronautical Mobile Telemetry Sub-Working Group Report," March 2014. [Online]. Available: https://www.ntia.doc.gov/files/ntia/publications/amt_swg_final_report_posted_03042014.pdf. [Accessed January 2019].

[18] H. Kumamoto and E. J. Henley, Probabilistic risk assessment and management for engineers and scientists, Piscataway, NJ: Wiley-IEEE Press, 2000.

[19] R. H. Coase, "The Federal Communications Commission," Journal of Law and Economics, vol. 2, pp. 1-40, 1959.

[20] C. Bazelon and G. McHenry, "Mobile Broadband Spectrum: A Vital Resource for the U.S. Economy," prepared for the CTIA by the Brattle Group, 2015.

[21] Federal Communications Commission, "FCC.gov," 9 May 2017. [Online]. Available: https://www.fcc.gov/about-fcc/fcc-initiatives/incentive-auctions#block-menu-block-4. [Accessed 4 April 2018].

[22] Ciganer and Hatch, R., "Working group 1: Assured availability - protect the clear and truthful reception of radionavigation signals. Technical report. National Space-Based Positioning, Navigation, and Timing Advisory Board," June 2014. [Online]. Available: http://www.gps.gov/governance/advisory/meetings/2014-06/wg1.1.pdf. [Accessed 4 April 2018]

[23] Federal Communications Commission Public Notice, "Office of Engineering and Technology Seeks Comment on Technological Advisory Council Spectrum Policy Recommendations," 1 December 2017. [Online]. Available: https://apps.fcc.gov/edocs_public/attachmatch/DA-17-1165A1.pdf. [Accessed 30 January 2018].

[24] National Institute of Standards and Technology, "Framework for Improving Critical Infrastructure Cybersecurity," NIST, Gaithersburg, 2014.

[25] The Spectrum and Receiver Performance Working Group of the Federal Communications Commission's Technological Advisory Council, "A quick introduction to risk-informed interference assessment," FCC, Washington, DC, 2015.

[26] The Spectrum and Receiver Performance Working Group FCC Technological Advisory Council, "A case study of risk-informed interference assessment: MetSat/LTE coexistence in 1695–1710 MHz," Federal Communications Commission, Washington DC, 2017.

[27] The Spectrum and Receiver Performance Satellite Communication Plan Working Group FCC Technological Advisory Council, "A risk assessment framework for NGSO-NGSO interference," Federal Communication Commission, Washington, DC, 2017.

[28] "European Communications Office," CEPT. [Online]. Available: https://www.cept.org/eco/. [Accessed: 15-Nov-2019].

[29] C. Johnson, Long Term Evolution IN BULLETS,, 2nd ed., CreateSpace Independent Publishing, 2012

[30] Department of Commerce, National Telecommunications and Information Agency, “CSMAC Working Groups List” July 21, 2012. [Online]. Available: https://www.ntia.doc.gov/files/ntia/publications/csmac_working_groups_list_07242012.pdf. [Accessed December 2018].

[31] Department of Commerce, National Telecommunications and Information Agency, “CSMAC Working Groups List” July 21, 2012. [Online]. Available: https://www.ntia.doc.gov/files/ntia/publications/csmac_working_groups_list_07242012.pdf . [Accessed December 2018].

[32] A. El-Rabbany, Introduction to GPS, The Global Positioning System, Norwood, MA: Artec House, Inc., 2002.

[33] Department of Commerce, National Telecommunications and Information Agency, "Assessment of compatibility between ultrawideband (UWB) systems and Global Positioning System (GPS) receivers," February 2001. [Online]. Available: https://www.ntia.doc.gov/legacy/osmhome/reports/UwbGps/NTIASP_01_45.pdf. [Accessed October 2018].

[34] Department of Commerce, National Telecommunications and Information Agency, "Assessment of compatibility between ultrawideband (UWB) systems and Global Positioning System (GPS) Receives (Report Addendum)," November 2001. [Online]. Available: http://www.ntia.doc.gov/osmhome/reports/sp0147/NTIA_Special_Publication_01_47_2.pdf. [Accessed October 2018].

[35] International Telecommunications Union, "Protection criteria for telemetry systems in the aeronautical mobile service and mitigation techniques to facilitate sharing with geostationary broadcasting-satellite and mobile-satellite services in the frequency bands 1 452-1 525 MHz and 2 310-2 360 MHz," 2000. [Online]. Available: https://www.itu.int/rec/R-REC-M.1459/en [Accessed 12 August 2019]

[36] K. Temple, "An initial look at adjacent band interference between aeronautical mobile telemetry and long-term evolution wireless service," 4 July 2016. [Online]. Available: https://apps.dtic.mil/dtic/tr/fulltext/u2/1012630.pdf. [Accessed 19 March 2019].

[37] National Advanced Spectrum and Communications Test Network, "Out-of-band emissions measurements of LTE devices operating in the AWS-3 band," January 2018. [Online]. Available: https://www.nist.gov/programs-projects/out-band-emissions-measurements-lte-devices-operating-aws-3-band. [Accessed January 2019].

[38] American National Standards Institute, "American national standard for evaluation of wireless coexistence," 11 May 2017. [Online]. Available: https://ieeexplore.ieee.org/document/7927764. [Accessed August 2018].

[39] Institute of Electrical and Electronics Engineers, "IEEE Recommended Practice for the Analysis of In-Band and Adjacent Band Interference and Coexistence Between Radio Systems," 29 July 2008. [Online]. Available: https://ieeexplore.ieee.org/stamp/stamp.jsp?tp=&arnumber=4584236. [Accessed October 2018].

[40] National Space-Based Positioning, Navigation, and Timing Systems Engineering Forum, "Follow-on Assessment of LightSquared Ancillary Terrestrial Component Effects on GPS Receivers," 19 January 2012. [Online]. Available: https://www.gps.gov/news/2012/02/lightsquared/NPEF-report.pdf. [Accessed October 2018].

[41] Lofquist, M., Jablonski, D., Cortes, A., Young, W., McGillivray, D., Midzor, M., Hartley, K., Stevens, I. “Advanced Wireless Service 3 (AWS-3) Long- Term Evolution (LTE) Impacts on Aeronautical Mobile Telemetry (AMT) Test and Metrology Test Plan.” National Advanced Spectrum and Communications Test Network (NASCTN) Plan [P-18-1]. Available at: https://www.nist.gov/sites/default/files/documents/2019/02/14/18.09.18_nasctn_lte_impacts_on_amt_testplanv2_master.pdf

[42] J. Andersen, T. Rappaport and S. Yoshida, "Propagation measurements and models for wireless communications hannels," January 1995. [Online]. Available: https://ieeexplore.ieee.org/document/339880/. [Accessed August 2018].

[43] National Institute of Standards and Technology, "NIST Technical Note 1954: '3.5 GHz radar waveform capture at Point Loma final test report'," May 2017. [Online]. Available: https://nvlpubs.nist.gov/nistpubs/TechnicalNotes/NIST.TN.1954.pdf. [Accessed 23 March 2019].

[44] U.S. Department of Standards National Bureau of Standards, Precision Measurement and Calibration Statistical Concepts and Procedures, Washington DC: U.S. Government Printing Office, 1969.

[45] M. J. Marcus, "Harmful Interference: The Definitional Challenge," IEEE Spectrum Policy and Regulatory, vol. 15, no. 3, June 2008.

[46] J. Carpenter, J. Johnson, M. Lofquist, K. Hartley, “Investigations and Analyses of LTE Network Cell Tower Deployments and Impact on Path Loss Calculations,” May 2019. [Online]. Available: https://apps.dtic.mil/docs/citations/AD1072846. [Accessed August 2019].

[47] International Telecommunications Union, "International Telecommunications Union, Radio Regulations Articles, Edition of 2016," 2016. [Online]. Available: http://search.itu.int/history/HistoryDigitalCollectionDocLibrary/1.43.48.en.101.pdf. [Accessed 4 April 2018].

[48] H. T. Friis, “A note on a simple transmission formula,” in Proceedings of the Institute of Radio Engineers, vol. 34, no. 5, 1946, pp. 254–256.

[49] Hata, M. "Empirical Formula for Propagation Loss in Land Mobile Radio Services", IEEE Transactions on Vehicular Technology, Vol VT-29, Num 3. Aug 1980. pp 317-325. DOI: 10.1109/T-VT.1980.23859

[50] Joint Committee for Guides in Metrology, "JCGM 100:2008, “Guide to the expression of uncertainty in measurement”," 2010. [Online]. Available: https://www.bipm.org/utils/common/documents/jcgm/JCGM_100_2008_E.pdf. [Accessed December 2018].

[51] W. K. Hastings, "Monte Carlo sampling methods using Markov chains and their applications," Biometrika, vol. 57, no. 1, pp. 97-109, April 1970.

[52] Philips, Caleb; Sicker, Douglas; Grunwald, Dirk; “A Survey of Wireless Path Loss Prediction and Coverage Mapping Methods” IEEE Communications Surveys & Tutorials, Vol. 15, No. 1, First Quarter 2013

[53] A. F. Molisch, Wireless Communications, Piscataway, NJ: Wiley-IEEE Press, 2010.

[54] T. W. Hazlett, The Political Spectrum, New Haven , CT: Yale University Press, 2017.

[55] National Telecommunications and Information Agency, "Manual of regulations and procedures for Federal radio frequency management," September 2017. [Online]. Available: https://www.ntia.doc.gov/files/ntia/publications/ntia_manual_september_2017_revision.pdf. [Accessed January 2019].

[56] Mobile Satellite Ventures and the U.S. GPS Industry Council, "Ex Parte Notice IB Docket No. 01-185 File No. SAT-ASG-20010302-00017," Federal Communications Commission, Washington, DC, 2002.

[57] Federal Communications Commission, "Flexibility for Delivery of Communications by Mobile Satellite Service Providers in the 2 GHz Band, the L-Band and the 1.6/2.4 GHz Bands. Second Order on Reconsideration," February 2005. [Online]. Available: https://docs.fcc.gov/public/attachments/FCC-05-30A1.pdf. [Accessed August 2018].

[58] Industry Canada, "Radio Standards Specification RSS-170, Issue 3, Mobile Earth Stations (MESs) and Ancillary Terrestrial Component (ATC) Equipment Operating in the Mobile-Satellite Service (MSS) Bands, replaces RSS-170, Issue 2, dated March 2011," July 2015. [Online]. Available: https://www.ic.gc.ca/eic/site/smt-gst.nsf/vwapj/rss-170-i3-e.pdf/$FILE/rss-170-i3-e.pdf. [Accessed August 2018].

[59] Satellite Industry Report, "State of the Satellite Industry Report, 2017," 2017. [Online]. Available: https://www.sia.org/wp-content/uploads/2017/07/SIA-SSIR-2017.pdf.

[60] Space-Based PNT Advisory Board Meeting, "DOT GPS Adjacent Band Compatibility (ABC) Assessment," Space-Based PNT Advisory Board, 2017.

[61] International Telecommunication Union, "Recommendation ITU-R M.1903, 'Characteristics and protection criteria for receiving Earth stations in the Radionavigation-Satellite Service (Space-to-Earth) and receivers in the Aeronautical Radionavigation Service operating in the band 1559-1610 MHz'," 2012. [Online]. Available: https://www.itu.int/dms_pubrec/itu-r/rec/m/R-REC-M.1903-0-201201-I!!MSW-E.docx. [Accessed 9 April 2018].

[62] GPS.GOV, "Use of a 1-dB Decrease in C/N0 as a GPS Protection Criterion," 2016. [Online]. Available: https://www.gps.gov/spectrum/ABC/1dB-background-paper.pdf. [Accessed January 2019].

[63] W. F. Young, A. Feldman, S. Genco, A. Kord, D. G. Kuester, J. Ladbury, D. A. McGillivray, A. K. Puls, A. Rosete, A. Wunderlich and W.-B. Yang, "NIST Technical Note 1952, LTE Impacts on GPS, Final Report," Department of Commerce, Boulder, 2017.

[64] A. F. Molisch, Wireless Communications, Piscataway, NJ: Wiley-IEEE Press, 2010.

[65] Department of Commerce, National Telecommunications and Information Agency, " EMC Measurements for Spectrum Sharing Between LTE Signals and Radar Receivers," July 2014. [Online]. Available: https://www.ntia.doc.gov/report/2014/emc-measurements-spectrum-sharing-between-lte-signals-and-radar-receivers. [Accessed October 2019].

[66] K. Borre, D. M. Akos, N. Bertelsen, P. Rinder and S. H. Jensen, A Software-Defined GPS and Galileo Receiver - A Single-Frequency Approach, Boston: Birkhauser, 2007.

[67] M. Petovello, "Inside GNSS," November/December 2010. [Online]. Available: http://insidegnss.com/auto/novdec10-Solutions.pdf. [Accessed October 2018].

[68] E. Jonietz, "Ultrawideband Squeezes In," MIT Technology Review, no. https://www.technologyreview.com/s/401641/ultrawideband-squeezes-in/, 1 September 2002.

[69] International Telecommunications Union Radiocommunication Study Groups, "Characteristics of UWB Devices - Wireless Communications & Signals," 23 January 2003. [Online]. Available: http://wcsp.eng.usf.edu/papers/UWBBasics.doc. [Accessed October 2018].

[70] Representatives of The U.S. GPS Industry Council, "Presentation on ET Docket 98-153," 28 September 2000. [Online]. Available: https://www.gps.gov/cgsic/international/2000/monaco/swiek.pdf. [Accessed October 2018].

[71] Federal Communications Commission, "Revision of Part 15 of the Commission's Rules Regarding Ultra-Wideband Transmission Systems," 11 August 2010. [Online]. Available: https://www.fcc.gov/document/revision-part-15-commissions-rules-regarding-ultra-wideband. [Accessed October 2018].

[72] Federal Communications Commision, "Revision of Part 15 of the Commission’s Rules Regarding Ultra-Wideband Transmission Systems," 22 April 2002. [Online]. Available: https://transition.fcc.gov/Bureaus/Engineering_Technology/Orders/2002/fcc02048.pdf. [Accessed October 2018].

[73] Department of Commerce, NTIA, "Testimony of Karl Nebbia at Hearing on Sustaining GPS for National Security," 15 September 2011. [Online]. Available: https://www.ntia.doc.gov/speechtestimony/2011/testimony-karl-nebbia-hearing-sustaining-gps-national-security-0. [Accessed October 2018].

[74] Department of Commerce, National Telecommunications and Information Agency, "Letter comments on FCC's Mobile Satellite Service (MSS) rulemaking," 24 January 2003. [Online]. Available: https://www.ntia.doc.gov/fcc-filing/2003/letter-comments-fccs-mobile-satellite-service-mss-rulemaking. [Accessed October 2018].

[75] Federal Communications Commission, " Flexibility for Delivery of Communications by Mobile Satellite Service Providers in the 2 GHz Band, the L-Band, and the 1.6/2.4 GHz Bands, IB Docket No. 01-185," 10 February 2003. [Online]. Available: https://docs.fcc.gov/public/attachments/FCC-03-15A1.pdf. [Accessed October 2019].

[76] Department of Transportation, "Global Positioning System (GPS) adjacent band compatibility assessment," April 2018. [Online]. Available: https://www.transportation.gov/pnt/global-positioning-systemgps-adjacent-band-compatibility-assessment. [Accessed October 2018].

Appendix A. HISTORY OF GPS SPECTRUM INTERFERENCE TESTING

This appendix provides a survey of GPS spectrum coexistence testing done in the past. This appendix is not an exhaustive reporting of the testing campaigns and does not report the conclusions drawn from the test results. Any testing results reported in this appendix are to illustrate differences in harmful interference determinations as different KPIs, waveforms, and definitions of harm are used. This survey of GPS spectrum coexistence testing shows that GPS harmful interference is a function of power level and waveform type and is subjective in nature. The subjectivity comes from how harmful is defined in the expression harmful interference. GPS testing has been done in the presence of x wireless system(s), where x = ultra-wideband, mobile satellite services, commercial mobile radio service, mobile broadband, etc.

A.1 GPS BACKGROUND

For decades, GPS navigation services operated with no concern for man-made harmful interference to its spectrum. There were no concerns about co-channel (defined as in-band) and adjacent band interference until UWB proposed operations across the L-Band spectrum. The GPS community proposed a 1 dB degradation of the C/N_0 as an IPC from an in-band protection scenario for GPS Assisted Devices, principally indoors from a UWB Local Area Network [70]. The MSS licensee adjacent to the GPS band proposed a strategy to improve its service by adding an ATC. The ATC would resemble cellular base stations offering MSS services to users that did not have line of sight view of the sky.

The GPS space segment consists of a 24-satellite constellation with the satellites distributed in six orbital planes at an approximate altitude of 20,000 km from Earth. The

orbits allow any spot of open sky on Earth to "see" 6–11 satellites simultaneously. The original GPS Block I satellite cluster launched February 22, 1978. The 50th Space Wing of the U.S. Air Force operates and maintains the GPS satellite constellation. For decades, GPS navigation services were concerned with only blockages to the RF channel, such as trees, extreme terrain, and urban canyons, all of which can compromise view of the GPS satellites. In the GPS L1 band, satellites transmit a spread spectrum signal using a multiple access capability known as code division multiple access (CDMA) centered on 1575.42 MHz where a C/A code is multiplexed with a quadrature-phase precision (P) code on the GPS L1 frequency. The C/A signal supports the standard positioning service, and the P signal supports the precise positioning service. A GPS receiver uses a correlator against a satellite code to extract signals that exist below the thermal noise floor. The noise floor is a function of temperature and radio frequency bandwidth and is present for all air channels used by spectrum dependent systems. Equation (44), from [66] shows the calculation for thermal noise power.

$$\begin{aligned} P_{thermal\ noise} &= kTB = 1.38e-23 \frac{\text{Joules}}{\text{Kelvin}} \cdot 290\ \text{Kelvin} \cdot 2e6\ \text{Hz} \\ &= 8.004 \cdot 10^{-15} \text{Watts}, or\ 10 \cdot log_{10}(8.004 \cdot 10^{-15}) \\ &= -140.97\ \text{dBW} = -110.97\ \text{dBm} \end{aligned} \tag{44}$$

The nominal GPS received signal power is –158.5 dBW (–128.5 dBm) [67], which is below the thermal noise floor.

A.2 UWB

Traditional spectrum licenses are for exclusive use, primary-coprimary, or primary-secondary licensees. Since the 1990s, consumer products such as cordless phones, baby

monitors, and Wi-Fi devices have made use of the industrial science, and medical unlicensed bands. The 900 MHz, 2400 MHz, and 5000 MHz bands were demonstrating value to consumers and technological breakthroughs for various industries. In an effort to increase unlicensed spectrum use, the concept of a UWB system was conceived. UWB was designed with sharing in mind; their emissions resemble random noise to other spectrum license holders [68]. UWB was intended to operate at a low power and span wide bandwidths of spectrum. Spectrum license holders across various industries[41] expressed early concerns that UWB would harm their ability to provide wireless services to their users (for example, Sprint PCS, XM Radio, and the GPS community). UWB proponents argued that because they are operating below the typical noise floor, its presence would not be seen as interference to those licensed users.

Because UWB is an unlicensed technology, there is no way to regulate user density. Expectations were that UWB unlicensed technologies would replace the universal serial bus (USB) connections. Aggregate interference levels were a concern and there were assertions of the aggregate interference levels rising to cause harmful interference to GPS receivers [69].

The GPS community feared that testing done on UWB across the L-Band could lead to misleading results because the test space would be overwhelmingly large.[42] Specifically, the UWB pulse train types have many variants and each pulse train would impact GPS differently—making a general solution impossible. Because each UWB pulse

[41] Such as cellular communications, satellite radio service providers, and radionavigation services.
[42] https://www.gps.gov/cgsic/international/2000/monaco/swiek.pdf

train must be tested independently the number of tests needed, and therefore the amount of time and money involved to arrive at a reliable answer, is large and unknown [70].

In 2000–2001, the Department of Defense and the NTIA launched simulation and test campaigns to calculate a maximum tolerable UWB power in the GPS band of spectrum. A partial list of testing and simulation reports released on GPS effects from the proposed UWB proposed deployments are given below [71]:

- NTIA Special Publication 01-45, Assessment of Compatibility between Ultrawideband (UWB) Systems and GPS Receivers, February 2001
- NTIA Special Publication 01-47, Assessment of Compatibility between Ultrawideband (UWB) Systems and GPS Receivers (Report Addendum), November 2001
- NTIA Report 01-383, The Temporal and Special Characteristics of Ultrawideband Signals, January 2001
- NTIA Report 01-384, Measurements to Determine Potential Interference to GPS Receivers from Ultrawideband Transmission Systems, February 2001
- NTIA Report 01-389, Addendum to NTIA Report 01-384: Measurements to Determine Potential Interference to GPS Receivers from Ultrawideband Transmission Systems, September 2001
- Final Report UWB-GPS Compatibility Analysis Project, 8 March 2001, Strategic Systems Department, The Johns Hopkins University/Applied Physics Laboratory
- Study submitted by NTIA on March 21, 2001, on behalf of the Department of Transportation regarding tests performed at Stanford University

IPC results summaries, as documented in the NTIA 01-45 test report, are listed in Table 12, where interference tolerance is dependent on (a) pulse repetition frequency (PRF), (b) indoor versus outdoor, and (c) narrow (carrier wave) versus wideband (noise-like) [68].

Table 12. IPC results summary from NTIA testing

UWB Device category	Noise-like interference (dBm/MHz)	Carrier wave-like interference (dBm)
Low PRF (100 kHz)	–61.0	N/A
High PRF (>100 kHz)	–65.3	–75.3
Vehicular	–69.3	–79.3
Indoor (to indoor GPS)	–69.3	–79.3

A key takeaway from these tests is that pulse rate and broadband waveforms affect GPS differently. This illustrates how each waveform type needs to be tested independently and generalizations are inappropriate. Spectrum use is described by three variable degrees of freedom: time, frequency, and power. Changing any one of these degrees of freedom affects GPS differently and results in a different level of UWB that affects GPS harmfully (according to the report).[43]

The NTIA UWB//GPS addendum, NTIA SP01-47 [34], adjusted the test space to include 32 UWB signal permutations to test their interference potential to GPS receivers. The signal permutations were chosen as representative for the various intended UWB applications. The UWB test space included four PRFs: 100 kHz, 1 MHz, 5 MHz, and 20 MHz; four modulation types; and two gating types.

[43] The International Telecommunication Union (ITU) IPC regarding UWB are more straightforward, recommending –75 dBW/MHz across the Radio Navigation-Satellite Service (RNSS) band for indoor and outdoor UWB devices [67, p. 12].

A.3 GPS KPIS FOR UWB TESTING

For GPS KPIs, the NTIA chose to use (a) "break-lock" and (b) "reacquisition." Break-lock refers to the loss of signal lock between the GPS receiver and a GPS satellite. Break-lock is described in NTIA SP01-47 as a condition where C/N_0 is high enough that the GPS receiver can no longer adequately determine the pseudo-range (the initial/uncorrected measure of distance from a single GPS satellite to a receiver) for the given satellite signal. The reacquisition threshold time is a measurement of the reacquisition time under various levels of UWB power level. Power levels that result in an abrupt increase in reacquisition time[44] are considered harmful interference. The NTIA testing included varying UWB emission power across a range of UWB waveform types and hop sequences.

A.4 SPECTRUM MASK FOR UWB

After analysis of the test results and rounds of comments, the FCC decided on a wideband spectrum mask for UWB emissions. A spectrum mask defines the emission of a spectrum-dependent system in dBm/MHz output power terms. The FCC modified the Part 15 unlicensed spectrum use ruling with UWB emission rules. The resulting UWB emissions masks has notches where GPS frequencies reside. Figure 50 is an example mask showing UWB emissions mask for indoor UWB emissions in dBm/MHz. For most higher frequencies (3.10 to 10.6 GHz), the UWB effective isotropic radiated powers (EIRP)

[44] This is the same KPI as was used by the NASCTN test and was labeled time to first reacquisition.

maximum limit is −41.3 dBm/MHz; in the GPS band the limit of − 75.3 dBm/MHz was imposed [72].

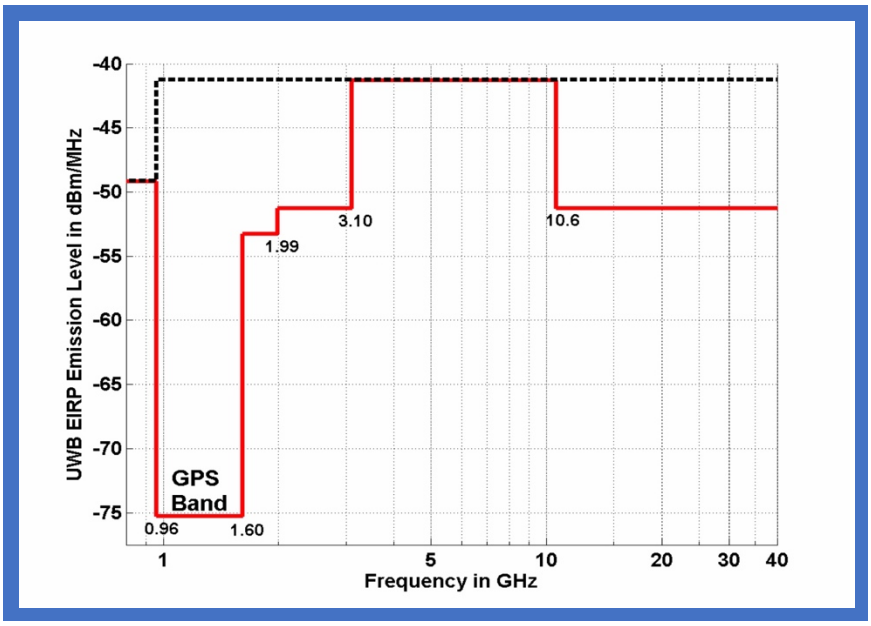

Figure 50. FCC spectrum emissions mask for indoor UWB devices

UWB did not gain the expected market share. Systems in the 2.4 GHz and 5 GHz industrial, scientific, and medical band continued to dominate the unlicensed space (using technologies such as Wi-Fi). UWB served as the first example of a wireless system threatening to encroach on GPS devices.

A.5 ATC IN THE MSS BAND

In 2003, the FCC granted MSS providers flexibility in how they could deliver their communications offerings by allowing them to integrate an ATC into their MSS networks. ATC deployments augment MSS by using terrestrial ground stations and mobile terminals that re-use frequencies assigned for satellite communications to enhance MSS coverage [73]. The FCC intended the ATC augmentation to offset the gaps in MSS coverage, making

spectrum more efficient in the L-Band. All other signals in this band and surrounding bands are low-wattage satellite downlinks; a terrestrial "cell tower" could be many times the power of the incumbent links. There was a concern from the GPS community that the ATC emissions could adversely affect GPS operations and spectrum coexistence testing was needed.

The NTIA launched a measurement campaign to test ATC adjacent band effects on GPS. Instead of using break-lock and reacquisition effects, the NTIA used the following expression to determine harmful interference: maximum allowable EIRP of the Mobile Terminal, EIRP_Max of –117 dBm/MHz (–147 dBW/MHz) was used. Equation (45) shows how the EIRP_Max was used to find minimum *D* (distance) separation:

$$-117\frac{dBm}{MHz} = 20 \cdot \log(F) + 20 \cdot \log(D) - 27.55 + G_r, \qquad (45)$$

Where F = Frequency, D = distance, and G_r = receiver antenna gain.

Equation (45) calculates EIRP values for different distance values. For example, according to this equation, for a GPS device 2 meters from an ATC, $D = 2$ meters, the max allowable ATC EIRP = –74.6 dBm/MHz [74], otherwise the GPS device will experience harmful interference. Note that for public safety spectrum users (such as early responders and law enforcement) operating at 700 MHz, the emission limits into the GPS band (of 1559 MHz to 1610 MHz) were calculated as –40 dBm/MHz. The public safety emission tolerance is 34.6 dB higher (which is more than 2,000 times more energy) than the ATC emission limit.

A.6 GPS KPIs FOR ATC TESTING

The NTIA ATC Impacts on GPS testing did not use KPIs of the GPS systems; it instead used a *GPS interference susceptibility level* of –117 dBm/MHz, called interference total, or I_t. The NTIA test documentation does not provide evidence of how –117 dBm/MHz was calculated, but it corresponds to the interference-to-noise ratio (INR) safety margin of 6 dB below the noise floor, shown in Equation (47).

$$I_t = P_{thermal\ noise} - 6\ \text{dB} = -111\ \frac{\text{dBm}}{\text{MHz}} - 6\ \text{dB} = -117\ \frac{\text{dBm}}{\text{MHz}}. \tag{46}$$

The I_t is the max EIRP of ATC emission as a function of distance. The maximum allowable out of band (OoB) emissions of an ATC terminal is plotted in Figure 51 and calculated using the following formula [74]:

$$\begin{aligned} &\text{Maximum allowable EIRP of the ATC Mobile Terminal (OOBE Level)} \\ &= \text{GPS Rx Interference Susceptibility Level} \\ &+ \text{Propagation Loss} + \text{GPS Rx Antenna Gain} \\ &= -117\ \frac{\text{dBm}}{\text{MHz}} \\ &+ [20 \cdot \log_{10}(1575.42) + 20 \cdot \log_{10}(\text{Distance}) - 27.55] \\ &+ G_r \end{aligned} \tag{47}$$

where D = minimum distance in meters that a GPS receiver can be from an ATC sector and G_r = gain of GPS receiving antenna, set to 0 dB for this analysis.

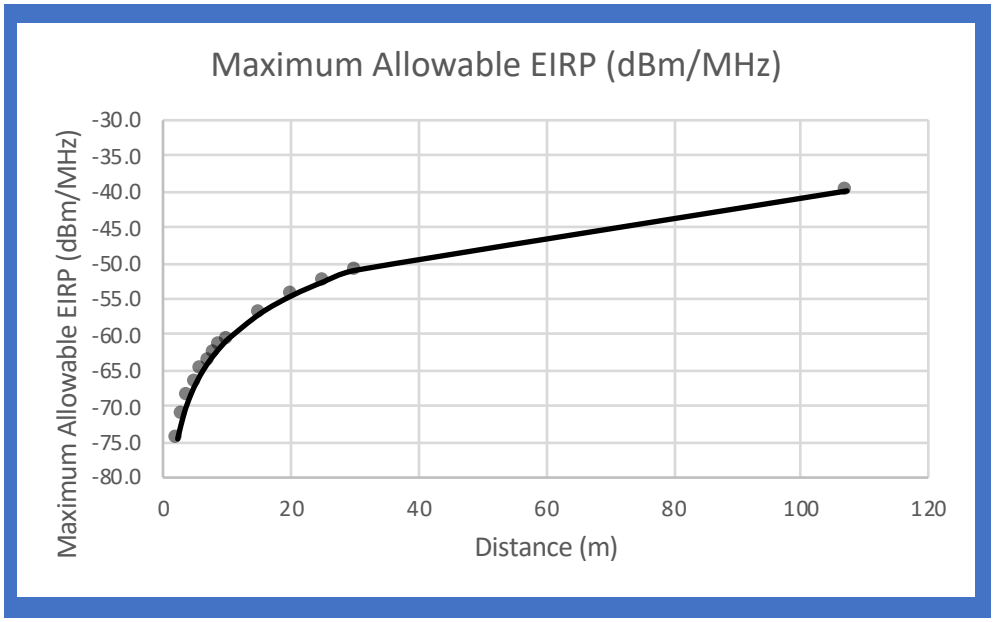

Figure 51. Maximum allowable ATC OOBE in the 1559–1610 MHz

According to Figure 51, if the OOBE of an ATC terminal in the 1559 MHz to 1610 MHz global navigation satellite systems (GNSS) band is approximately − 75 dBm/MHz, then a GPS receiver will need to be 2 meters or more away to avoid the INR of − 6 dB. If all GPS receivers could keep a distance of 20 meters (or greater) from an ATC terminal, then the OOBE of that terminal could be − 55 dBm/ MHz in the GNSS band.

A.7 SPECTRUM MASK FOR ATC

After NTIA testing GPS Industry Council and Mobile Satellite Ventures LP (MSV, the company that later became LightSquared) jointly submitted an ex parte agreement to the FCC specifying that the MSV ATC base stations will:

"[u]se filtering to achieve –100 dBW/MHz [–70 dBm/MHz], or lower emissions in the 1559–1605 MHz frequency band" [74].

A.8 LTE IN THE MSS BAND, LIGHTSQUARED/LIGADO NETWORKS

In November 2004, the FCC's International Bureau granted a predecessor company of LightSquared Subsidiary LLC (LightSquared) the authority to operate ATC facilities providing voice and data communication for users equipped with dual-mode MSS/ATC devices (i.e., handsets that could communicate both with orbiting satellites and terrestrial base stations). Additionally, in subsequent orders in 2005 and 2010, the FCC afforded LightSquared further flexibility for the technical design of its ATC network. The 1525 MHz to 1559 MHz band was allocated to MSS [45], and the GPS community agreed to the ATC deployments.

In 2012, Ligado (then LightSquared) submitted a request for modification to the ATC service rules to accommodate a stand-alone terrestrial frequency-duplexed network in the MSS bands it owned. The NPEF conducted an assessment of the effects of LightSquared's planned deployment of terrestrial broadband systems on GPS receivers [75].

Testing done to determine the effects of LTE in the MSS ATC band was performed by many parties, including the NPEF, the DoT [76], and the NASCTN, which is hosted by the NIST. The NPEF and DoT tests did not use the historical IPC definitions (e.g., break-lock, or –117 dBm/MHz measured at the GPS receiver); they chose to define harmful interference as a 1 dB degradation of the C/N_0 as reported by the GPS receiver. This is a risky measurand for the following reasons:

- C/N_0 it is not an absolute measure from test equipment that is traceable to a standard.

- In normal operating conditions, C/N_0 varies from $25 < \frac{C}{N_0} < 48$ dBHz [77].
- The C/N_0 algorithms are specific to the GPS receiver and proprietary to the GPS manufacturer. (This opacity makes it difficult to ascertain accuracy.)
- A 1 dB measurement is difficult to make because test sets, even over cables, can have error bars that span many dBs. For example, in NIST Technical Note 1952 the NASCTN test bed quantified measured and specified uncertainties of RF components in its measurement test bed and calculated 2.4 dB to 2.8 dB of expanded uncertainty. The DoT Adjacent Band Compatibility Test calculated a 2.8 dB uncertainty in its measurands.

A.9 INTERNATIONAL RECOMMENDATIONS ON GPS IPC

The international recommendation for GNSS (which includes GPS) interference is described in the International Telecommunications Union Recommendations, ITU-R M.1903 [61], which refers to ITU-R M.1318. In M.1903, interference levels are expressed in relative terms to the intended signal. For example, see Figure 1 from the M.1903, shown in this paper as Figure 52. For an interferer with a bandwidth of 100 kHz to 1 MHz, the relative interference level shall not exceed (relative to the GPS signal) 0 dB for tracking and -6 dB for acquisition in an L1 band C/A coded GPS signal. The exception to this relative measure was the assisted radionavigation satellite service (A-RNSS), which operates indoors or in highly stressed GPS signal environments where the GPS signal level is very low or hard to determine. In the case of the A-RNSS system, harmful interference is defined as a rising of the noise floor by 1 dB [61].

ITU-R M.1903 states that for aeronautical GNSS protection specifically for satellite-based augmentation systems used for aviation approach, the protection criterion is –140 dBW/MHz plus a 6 dB safety-of-life margin. This –146.5 dBW/MHz = –116.5 dBm/MHz and is likely how the NTIA's –117 dBm/MHz test criterion originated. The M.1903 recommendation rates interference into the 1559 MHz to 1610 MHz band as a

relative power. The dB offset to GPS signal power is given as signal power and interference relative, where 0 dB means interference power can equal GPS signal power. Figure 52 (reprinted from [61]) shows the relative interference tolerance versus band width of the interferer. A 1 MHz interferer can be the same power as the incoming GPS signal (0 dB) as shown by the red circle.

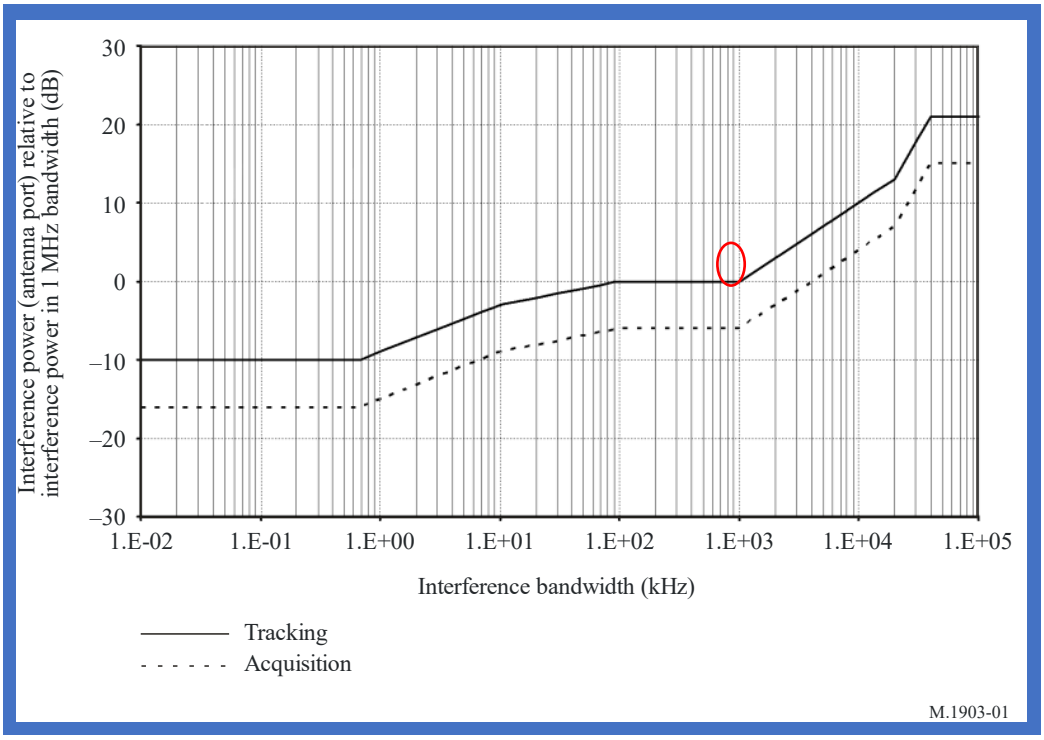

Figure 52. Relative tolerable interference into the 1559 MHz to 1610 MHz GNSS band

A.10 CONCLUSION

In defense of its operations, the GPS L1 band, coexistence studies were performed to protect its operations from harmful sources of interference. Potential interfering sources like Public Safety, UWB, MSS /ATC, and the proposed LTE from Ligado Networks' Mobile Broadband operations come with a risk of raising the *noise* floor (in the form of man-made noise). During each of these proposed entries to the neighboring spectrum (or

in the case of UWB, neighboring and co-channel spectrum), stakeholders have used different descriptions of harmful interference and different test methods to measure interference effects. Across the different test campaigns described in this paper, different GPS KPIs were used; for example, harmful interference was defined as:

- N_0 in the C/N_0 equation is raised to the point of "break-lock" where a receiver can no longer acquire pseudo-range.
- Time to first reacquisition was degraded.
- –117 dBm/MHz (equivalent to –6 dB INR) interference susceptibility level.
- 1 dB degradation of N_0 in the C/N_0 equation as reported by a GPS receiver.

Spectrum coexistence testing of UWB and GPS systems showed different powers of UWB affecting GPS as a function of UWB duty cycle and hop rates. Results show that differing types of waveforms affect GPS differently and should require differing operating rules to protect GPS. There is no single power level that can protect GPS L1 operations and allow for buildouts of other L-Band systems in a fair way. GPS testing used IPC that related to performance KPIs, but more recently have made attempts to create a general IPC that covers all potentially interfering signal types. This generalization leads to overly conservative stand-off distances and is not in keeping with maximizing spectrum use